[American Journal of Science, Vol. 321, June, 2021, P. 907–954, DOI 10.2475/06.2021.08]

RECONSTRUCTING LOST PLATES OF THE PANTHALASSA OCEAN THROUGH PALEOMAGNETIC DATA FROM CIRCUM-PACIFIC ACCRETIONARY OROGENS

LYDIAN M. BOSCHMAN*,**,†, DOUWE J.J. VAN HINSBERGEN*, COR G. LANGEREIS*, KENNET E. FLORES***, PETER J.J. KAMP§, DAVID L. KIMBROUGH§§, HAYATO UEDA§§§, SUZANNA H.A. VAN DE LAGEMAAT*, ERIK VAN DER WIEL*, and WIM SPAKMAN*

ABSTRACT. The Panthalassa Ocean, which surrounded the late Paleozoic-early Mesozoic Pangea supercontinent, was underlain by multiple tectonic plates that have since been lost to subduction. In this study, we develop an approach to reconstruct plate motions of this subducted lithosphere utilizing paleomagnetic data from accreted Ocean Plate Stratigraphy (OPS). We first establish the boundaries of the Panthalassa domain by using available Indo-Atlantic plate reconstructions and restorations of complex plate boundary deformation at circum-Panthalassa trenches. We reconstruct the Pacific Plate and its conjugates, the Farallon, Phoenix, and Izanagi plates, back to 190 Ma using marine magnetic anomaly records of the modern Pacific. Then, we present new and review published paleomagnetic data from OPS exposed in the accretionary complexes of Cedros Island (Mexico), the Santa Elena Peninsula (Costa Rica), the North Island of New Zealand, and Japan. These data provide paleolatitudinal plate motion components of the Farallon, Phoenix and Izanagi plates, and constrain the trajectories of these plates from their spreading ridges towards the trenches in which they subducted. For 83 to 150 Ma, we use two independent mantle frames to connect the Panthalassa plate system to the Indo-Atlantic plate system and test the feasibility of this approach with the paleomagnetic data. For times prior to 150 Ma, and as far back as Permian time, we reconstruct relative and absolute Panthalassa plate motions such that divergence is maintained between the Izanagi, Farallon and Phoenix plates, convergence is maintained with Pangean continental margins in Japan, Mexico and New Zealand, and paleomagnetic constraints are met. The reconstruction approach developed here enables data-based reconstruction of oceanic plates and plate boundaries in the absence of marine magnetic anomaly data or mantle reference frames, using Ocean Plate Stratigraphy, paleomagnetism, and constraints on the nature of circum-oceanic plate boundaries. Such an approach is a crucial next step towards quantitative reconstruction of the currently largely unknown tectonic evolution of the Earth's oceanic domains in deep geological time.

Key words: Panthalassa, plate reconstruction, paleomagnetism, Ocean Plate Stratigraphy, subduction, radiolarian chert, Farallon, Izanagi, Phoenix

* Department of Earth Sciences, Utrecht University, Princetonlaan 8a, 3584 CB, Utrecht, the Netherlands
** Now at Department of Environmental System Science, ETH Zurich, Universitätstrasse 16, 8092 Zurich, Switzerland
*** Department of Earth, Marine and Environmental Sciences, University of North Carolina at Chapel Hill 104 South Road, CB #3315, Chapel Hill, North Carolina, 27599-3315, United States
§ School of Science, University of Waikato, Hamilton 3240, New Zealand
§§ Department of Geological Sciences, San Diego State University, San Diego, California, USA
§§§ Department of Science, Niigata University, Niigata, Japan
† Corresponding author: lydian.boschman@usys.ethz.ch

INTRODUCTION

Understanding the dynamics of plate tectonics – the size and shapes of plates, their motions, and what is driving these motions – is cornerstone in understanding Earth's evolution and behavior. For mantle dynamics, the rate of motion of tectonic plates relative to the underlying mantle, as well as sudden changes in these motions, is of particular interest (Torsvik and others, 2010). Present-day plate motions can be obtained from earthquake focal mechanisms and GPS data, but for plate motion changes and evolution of mantle dynamics throughout Earth's history, we rely on plate reconstructions. Reconstructing tectonic plates requires knowledge on the past location and evolution of their plate boundaries – spreading ridges, transforms, and subduction zones, of which the vast majority is located within ocean basins. However, because oceanic lithosphere has a limited lifespan at the Earth's surface and is eventually lost to subduction, reconstructing plates and plate boundaries is increasingly challenging for deeper geological time: for the Jurassic, around 60% of the planet's surface consisted of lithosphere that is no longer present today, of which the vast majority was oceanic (Torsvik and others, 2010). Deep-time plate tectonic reconstructions rely therefore primarily on structural geological, paleontological, and paleomagnetic data from the continents. Such reconstructions (Stampfli and Borel, 2002; Torsvik, 2003; Scotese, 2004; Li and others, 2008, 2019; Nance and others, 2014; Pisarevsky and others, 2014) classically portray the distribution of continents through geological time and identify plate boundaries when they are located within or adjacent to continents. However, plates and plate boundaries within oceanic domains remain mostly unreconstructed, or are inferred only conceptually.

With the advent of free, user-friendly plate reconstruction software (particularly GPlates, www.gplates.org, Boyden and others, 2011; Gurnis and others, 2018; Müller and others, 2018), the last decade has seen a surge in deep-time dynamic plate motion models in which intra-oceanic plate boundaries and their evolution are portrayed in kinematically feasible, albeit still poorly constrained scenarios (Domeier and Torsvik, 2014, 2019; Domeier, 2016, 2018; Matthews and others, 2016; Merdith and others, 2017; Müller and others, 2019; Young and others, 2019). Such full-plate reconstructions are now available as input for numerical modeling studies and promise breakthroughs in our understanding of mantle dynamics and its evolution through time (Coltice and Shephard, 2018). However, it also makes the development of new data-based approaches to reconstruct lost oceanic plates and intra-oceanic plate boundaries particularly urgent.

Data on past tectonic motions of subducted oceanic plates may be collected from sparse remnants of these plates, preserved in accretionary orogens. Such remnants represent assemblages of rocks that once formed the upper part of oceanic [or (micro-)continental (van Hinsbergen and Shouten, 2021)] lithosphere that was scraped off and accreted during subduction. Records of these plates are preserved in rocks that are often fragmented, intensely deformed, metamorphosed, and highly incomplete, yet accretionary orogens preserve information on the tectonic history of oceanic plates from billions of years of Earth's history (Windley and others, 2007; Cawood and others, 2009, 2018; Xiao and others, 2009; Kusky and others, 2013). In this study, we aim to obtain quantitative data for kinematic reconstructions of lost oceanic plates and plate boundaries from such accretionary orogens. We hereby focus on the Panthalassa Ocean that in early Mesozoic time surrounded the supercontinent Pangea.

Marine magnetic anomalies of the Pacific Plate (fig. 1), which underlies the descendant of the Panthalassa Ocean, the Pacific Ocean, reveal that the Panthalassa Ocean was once underlain by at least three major oceanic plates – Farallon, Phoenix, and Izanagi. The Pacific Plate originated around 190 Ma at a triple junction between

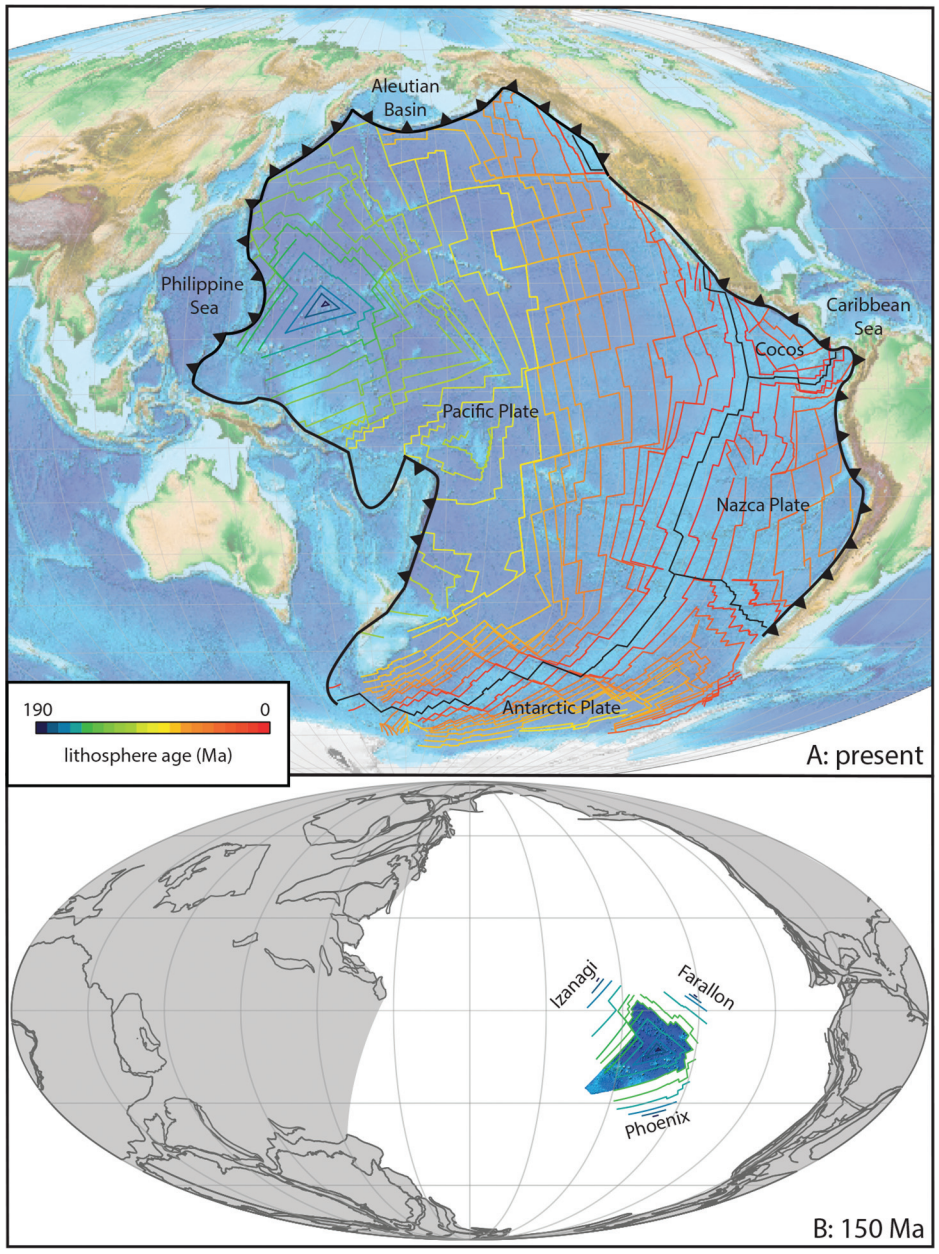

Fig. 1. (A) The Pacific Ocean, its modern plate configuration, and isochrons [from Wright and others (2016)]. (B) Latest Jurassic Panthalassa Ocean, including the young and growing Pacific Plate (in blue) and its conjugates, the Farallon, Izanagi, and Phoenix plates. Reconstruction of North/South America and Africa from Torsvik and others (2012); Europe/Asia from Müller and others (2016) and Domeier and Torsvik (2014).

these three plates, was surrounded by ridges, and grew upon the subduction and demise of Farallon, Phoenix and Izanagi (Larson and Chase, 1972; Larson and Pitman, 1972; Boschman and van Hinsbergen, 2016). Here, we aim to establish a data-based,

quantitative reconstruction of the plate tectonic evolution of the Panthalassa Ocean and estimate plate motions relative to the well-reconstructed Pangea plates. To this end, we use stratigraphic and geochemical data, as well as new and previously published paleomagnetic data, from Permian-Cretaceous rock assemblages that were scraped off the subducting Farallon, Phoenix, and Izanagi plates, and accreted in orogens exposed on Cedros Island (Baja California, Mexico), the Santa Elena Peninsula (Costa Rica), the North Island of New Zealand, and Japan.

RECONSTRUCTING PANTHALASSA PLATES: OUTSIDE-IN, INSIDE-OUT, BOTTOM-UP, AND FROM ACCRETED REMNANTS

Reconstruction of the lost plates of the Panthalassa Ocean is possible from four different angles: (1) Outside-in: Reconstructing the changes in the total area occupied by Panthalassa lithosphere follows from reconstructing Pangea break-up and preceding assembly. The estimate of net area change of the Panthalassa Ocean can further be refined by correcting for plate margin deformation. In most cases, such deformation is restricted to a few hundred kilometers (for example, extension in the North American Basin and Range province (McQuarrie and Wernicke, 2005), or shortening in the Andes (Eichelberger and McQuarrie, 2015; Schepers and others, 2017), and is thus only of secondary importance. In other cases, however, such deformation modified the area of the Panthalassa domain by many thousands of kilometers (for example, Cenozoic backarc extension in the southwest Pacific region (Seton and others, 2016; van de Lagemaat and others, 2018a) and is important to take into account.

(2) Inside-out: Formation of oceanic lithosphere at ridges within the Panthalassa domain is reconstructed from marine magnetic anomalies and fracture zones preserved on the Pacific Plate. These spreading records provide the detailed kinematic history of plate pairs whose ridges with the Pacific still exist (Juan de Fuca, Cocos, Nazca, West Antarctica, fig. 1A), and provide half-spreading records of plates that were conjugate to the Pacific Plate, but have now been subducted, including the conceptual Izanagi, Farallon and Phoenix plates (fig. 1B). The oldest Pacific ocean floor dates back to ~190 Ma (Lancelot and Larson, 1975; Hilde and others, 1977; Engebretson and others, 1985). The Pacific spreading records show that since ~83 Ma, the Pacific plate shared a ridge with the (West) Antarctic Plate, tying Pacific plate motions to the Indo-Atlantic plate circuit (Doubrovine and Tarduno, 2008; Doubrovine and others, 2012). Prior to 83 Ma, however, the Panthalassa plates were entirely separated from the Indo-Atlantic plate circuit by subduction zones. Nonetheless, some fragments of lithosphere that formed within the Panthalassa domain escaped subduction and are currently underlying the Caribbean, Aleutian, and Philippine Sea basins (fig. 1A). These lithospheric fragments provide geological and geophysical information on spreading history and post-spreading plate motion that may aid the inside-out reconstruction, but all of these fragments are Jurassic or younger in age (Pindell and Dewey, 1982; Hall, 2002; Boschman and others, 2014, 2019; Wu and others, 2016; Vaes and others, 2019).

In addition to spreading records that reveal relative plate motions, data on absolute plate motions of the Pacific Plate are available in the form of fixed hotspot reference frames. The latest version of these, by Torsvik and others (2019), estimates absolute plate motions of the Pacific Plate back to 150 Ma. Even though changes in inter-hotspot distances in the Pacific have been demonstrated (Wessel and Kroenke, 2009; Konrad and others, 2018), for pre-Late Cretaceous times, the Torsvik and others (2019) frame provides the best available constraint on absolute plate motions of the Panthalassa plate system. For times prior to 150 Ma, paleomagnetic data are available from ODP sites 801B and 801C (Leg 129), studied initially by Steiner and Wallick

(1992) and Wallick and Steiner (1992), and later by Fu and Kent (2018). These studies yielded paleolatitudes for the drill location (currently at 18.5°N) between 10°N and 20°S for Bathonian-Maastrichtian times. In our analysis, we use the data from Fu and Kent (2018), who analyzed samples from a middle Bathonian-late Valanginian (~167–133 Ma) sequence of red radiolarian chert, mudstone and basalt, dated by radiolarian biostratigraphy (Matsuoka, 1992, 1995), yielding southern hemispheric paleolatitudes between 0 to 20° for six ages (tables 1 and 2). Furthermore, based on consistent near-north declinations, Fu and Kent (2018) concluded that there has been no vertical axis rotation of the Pacific Plate since the middle Jurassic. The inside-out approach, including spreading records, mantle frames, and paleomagnetic data, provides data back to ~190 Ma.

(3) Bottom-up: Seismic tomographic images of the mantle reveal the presence of positive wave speed anomalies, which may be interpreted as subducted lithosphere. Systematic correlations have shown that deeper seismic wave speed anomalies correlate well with older geological records of subduction (van der Meer and others, 2010, 2018; Butterworth and others, 2014). Furthermore, although slabs may migrate forward, backward, or undergo trench-parallel drag over distances of >1000 km during active subduction (Schellart, 2017; van de Lagemaat and others, 2018a), there appears to be no systematic horizontal offset of slabs relative to one another after their break-off from surface plates (Domeier and others, 2016). Modern mantle structure may thus be used to determine the absolute location of past subduction zones, and this has in recent years become a tool to reconstruct the positions of former intra-oceanic subduction zones within the Panthalassa Ocean whose geological records have been significantly displaced after subduction termination (van der Meer and others, 2012; Sigloch and Mihalynuk, 2013; Wu and others, 2016; Domeier and others, 2017; Boschman and others, 2018b; Vaes and others, 2019; Clennett and others, 2020). The deepest slabs, located near the core-mantle boundary, correlate with subduction zones that were active up to ~250 Ma ago (van der Meer and others, 2010, 2018), implying that the bottom-up approach is restricted to Mesozoic and younger times.

(4) From accreted remnants: During subduction, rocks may get transferred from the subducting plate to the overriding plate, thereby preserving remnants of subducted plates. Such accreted rocks derived from oceanic lithosphere can be described as parts or entire sequences of 'Ocean Plate Stratigraphy' (OPS), a concept developed by the Japanese micropaleontologist Yukio Isozaki (Isozaki and others, 1990). Generally, OPS represents remnants of oceanic ridges, rises, seamounts, intra-oceanic arcs, and occasionally, the abyssal plain (Alvarez and others, 1980; Shibuya and Sasajima, 1986; Isozaki and others, 1990; Hagstrum and Sedlock, 1992; Hagstrum and Murchey, 1996; Oda and Suzuki, 2000; Ando and others, 2001; Kodama and others, 2007; Kasuya and others, 2012; Kirschvink and others, 2015). The preservation of OPS is rare; vast segments of the circum-Pacific subduction zones are devoid of accreted rock units. There are no accretionary records from Cenozoic subduction at the Aleutian, Kuriles, Izu-Bonin-Marianas, Tonga-Kermadec, Antarctic Peninsula, or (central-southern) Andean trenches. Moreover, where such accreted materials are present, such as in Japan, accretion events may be separated by extended periods of non-accretion or subduction erosion (Isozaki and others, 1990, 2010). Nevertheless, where present, OPS provides invaluable information on motions of partly or fully subducted plates.

Ocean Plate Stratigraphy consists, in its most complete form, of magmatic basement, cherts or limestones, hemipelagic sediments, and tuffaceous and turbiditic deposits. If the magmatic basement rocks have a MORB geochemical signature indicating formation at a mid-ocean ridge, the OPS sequence represents the full journey of oceanic lithosphere from a spreading ridge, through the open ocean (where cherts

TABLE 1

Parameters from all new and compiled paleomagnetic data

	Site	Ref.	Lat (°N)	Lon (°E)	Age	N	N45	D	ΔD_x	I	ΔI_x	k	α95	K	$A95_{min}$<A95<$A95_{max}$	λ*
Mexico	CC1-mt	1	28.055831	-115.227354		119	118	20.7	1.9	12.8	3.7	35	2.2	47		
	CC1-ht	1,2	28.055831	-115.227354	Late Triassic		**10**	**208.8**	**11.2**	**5.5**	**22.3**	**16.3**	**12.3**	**19.5**		**2.7**
	CC-mt	1	28.114172	-115.275147		30	27	22.8	7	29	11.1	12	8.4	18.1		
	CC2-ht	1	28.114172	-115.275147	uppermost Carnian to middle Norian	22	19	193.6	16.3	-65.4	8.3	21.1	7.5	10.4		
							22	**189.4**	**7**	**-10**	**13.6**	**17.1**	**7.7**	**20.9**	**3.5<7<11.7**	**5**
	CC1+CC2	1, 2			Late Triassic		**32**	**195.5**	**6.5**	**-52**	**12.9**	**13**	**7.3**	**16.3**	**3<6.5<9.2**	**2.6**
Costa Rica	SR1,3,4,10,11-mt	1	10.881325	-85.879024	~190-180 Ma	93	79	329.2	3.5	6.1	7	13.3	4.5	21.4		
	SR1,3,4,10,11-ht	1	10.881325	-85.879024	~190-180 Ma	14	14	1.7	10.4	-7.9	20.4	12	11.9	15.8		
							12	**350.1**	**9.5**	**-15.7**	**17.8**	**19.9**	**10**	**22.1**	**4.4<9.4<17.1**	**8**
	SR5-8	1	10.881389	-85.878912	~175 Ma	37	37	321.3	5.5	6.8	10.9	11.3	7.3	19.3		
	SR2	1	10.878507	-85.874661	~110 Ma	62	59	316.7	3.9	32.8	5.7	20	4.2	26.5		
							53	**45.7**	**4.3**	**24.9**	**7.3**	**22.1**	**4.3**	**22.9**	**2.5<4.2<6.7**	**13**
	BN	1	10.815429	-85.733133	124 ± 4.1 Ma	36	34	172.8	4.3	46.3	4.6	41.7	3.9	42.6		
							34	**213.8**	**3.6**	**36.6**	**5**	**41.7**	**3.9**	**53.3**	**2.9<3.4<8.9**	**20.4**
New Zealand	WB	1	-36.932241	175.19215		18	16	16.7	13.3	-71.3	4.8	73	4.3	25.8		
	TU	1	-35.618648	174.540604		15	14	22.1	34.7	-80.4	5.7	49.8	5.7	15.2		
	TP	1	-36.379692	174.81118		15	14	22.1	34.7	-80.4	5.7	49.8	5.7	15.2		
	TK	1	-37.736264	177.672451		54	52	45.9	6.9	-65.6	3.5	37.8	3.3	19.3		
	KB1	1	-34.997889	173.802669		14	11	7	14.9	-56.3	11.4	22.9	9.8	15.7		
	KB2	1	-34.997889	173.802669		13	11	24	15.6	-67	7.3	50.6	6.5	21.7		
	BI1	1	-35.250401	174.132982	Permian	18	14	43.6	14.9	30.9	22.9	7.2	15.9	8.7		
							15	**19.2**	**13.1**	**23.9**	**22.4**	**6.1**	**16.9**	**9.9**	**4.1<12.8<14.9**	**12.5**
	BI2	1	-35.250401	174.132982	Permian	12	12	161	11.4	18	21	8.8	15.5	15.7		
							12	**165.3**	**13**	**-27.3**	**21.1**	**11.3**	**15**	**15.8**	**4.8<12.5<19.2**	**14.5**
	BI3	1	-35.254136	174.132507	Permian	31	30	92.7	4.8	20.1	8.6	20.1	6	32.1		
	BI4	1	-35.254136	174.132507	Permian	7	7	21.4	15	-58.4	10.6	55	8.2	28		
	BI5	1	-35.257472	174.132507	Permian	7	5	323.9	9.2	7	18.1	60.5	9.9	70.6		
							5	**320.4**	**9.7**	**14**	**18.4**	**55.6**	**10.3**	**63.9**	**6.3<9.6<29.7**	**7.1**
	Waiheke Island	3	-38.6	174.9	Early Triassic	21		323		-1						
								349		**-53**		**5**	**17**			**-33.6**
Japan	ON4	1	42.673689	142.673946	Berriasian	25	25	299.4	8.4	37	11.5	13.7	8.1	14.5		
							24	**251.4**	**8**	**7.2**	**15.7**	**9.7**	**10**	**14.8**	**3.4<8<11.1**	**3.6**
	Inuyama	4	35.4	137	middle Triassic	**12**	**12**			**1.4**	**6.8**					**0.7 ± 3.4**
	Inuyama - C1	5	35.4	137	middle Anisian	32		270.9		-13.5						
								252.8		**-5.4**		**126.8**	**2.3**			**- 2.7**
	Inuyama - C2	5	35.4	137	upper Anisian	41		81		46.9						
								48		**10.9**		**26.8**	**4.4**			**- 5.5**

TABLE 1
(continued)

	Site	Ref.	Lat (°N)	Lon (°E)	Age	N	N45	D	ΔDx	I	ΔIx	k	α95	K	A95min<A95< A95max	λ*
Japan	Inuyama - N1	5	35.4	137	middle Carnian	36		176.5		23.7						
								339.4		**18.2**		**4.8**	**26.1**			**9.3**
	Inuyama - N3	5	35.4	137	lower Norian	23		163.9		35.8						
								218.7		**7.7**		**6.4**	**23.4**			**3.9**
	Inuyama - K1	5	35.4	137	upper Norian	9		352.2		16.6						
								320.8		**20**		**7.1**	**53.6**			**10.3**
	Inuyama - K4	5	35.4	137	lowermost Jurassic	17		185.5		72.9						
								234.2		**-7.2**		**5.5**	**43.7**			**3.6**
	Inuyama - UN1	6	35.4	137	Anisian	9		-124.8		-17.8		2.7	39.2			
								154.7		**12**		**3.2**	**34.3**			**6.7 ± 17.8****
	Inuyama - UN2	6	35.4	137	upper Norian	7		-39.3		-9.7		9.8	20.3			
								-88.8		**46.6**		**9.9**	**20.2**			**29.5 ± 17.4****
	Inuyama - KA1	6	35.4	137	Anisian	10		-35.1		8.2		4.2	26.8			
								111.9		**22.6**		**4.5**	**25.9**			**11.8 ± 14.6****
	Inuyama - KA2	6	35.4	137	lower Norian	9		-9.3		16.8		4.8	26.1			
								82.4		**39.4**		**8.1**	**19.3**			**23.5 ± 14.2****
	Inuyama - KA3	6	35.4	137	upper Norian-Rhaetian	7		4.4		-13.8		2.5	48.5			
								132.7		**16.5**		**2.9**	**43.3**			**9 ± 23.3****
	Inuyama - KA5	6	35.4	137	lower Ladinian	8		-32		17		8.8	19.8			
								94.5		**29.4**		**12.5**	**16.3**			**16.9 ± 10.2****
	Kamura	7	32.8	131.3	Upper Permian	150		149.6		-66.6		12.33	3.4			
								327.5		**-23.4**		**13.99**	**3.2**			**-12.2 ± 1.8**
Pacific Plate	OPD Site 801B	8	18.64199	156.35966	Upper Valanginian – LowerHauterivian	3										**-12.7 ± 1.8**
		8			Upper Tithonain – Lower Valanginian	11										**-7.7 ± 1.8**
		8			Lower Tithonian – Middle Tithonian	10										**-2.7 ± 1.3**
		8			Kimmeridgian	9										**-10.4 ± 3.8**
		8			middle Bathonian- Upper Callovian	10										**-4.5 ± 1.6**
		8			167.7 ± 1.4 Ma	11										**-4.4 ± 2.0**

N45: number of samples after 45° cut-off. Bold numbers are corrected for bedding tilt. *When not indicated, hemispheric origin unknown. **Palaolatitudes based on inclinations corrected for inclination shallowing. References: 1: this study; 2: Hagstrum and Sedlock 1992; 3: Kodama and others 2007; 4: Shibuya and Sasajima 1986; 5: Ando et al. 2001; 6: Oda & Suzuki 2000; 7: Kirschvink and others 2015; 8: Fu and Kent 2018.

TABLE 2

Estimates of age, paleolatitude and accretion age of OPS materials

	Location	*Site*	*Age (Ma)*	*λ*	*Uncertainty*	*ISC λ 0.7*	*Age in trench*	*Reconstructed at*	*Fit*
83-150 Ma	Costa Rica	SR2	110 (±2?)	±13	[9.0, 17.5]	18.3	100	13-14˚N	✓
	Costa Rica	BN	124 ± 4.1	±20.4	[17.1, 23.9]	-	100	8-12˚N	5 degrees too far south
	Pacific Plate	OPD Site 801B	Upper Valanginian - Lower Hauterivian (137.1 - 132.9 Ma)	-12.7	[-14.5, -10.9]	17.8	-	11˚S	✓
	Pacific Plate	OPD Site 801B	Upper Tithonian - Lower Valanginian (146.7 - 137.2 Ma)	-7.7	[-5.9, -9.5]	10.9	-	9-11˚S	✓
	Japan	ON4	Berriasian (145 - 139 Ma)	±3.6	[-4.3, 11.9]	5.1	100	1-5˚N	✓
	Pacific Plate	OPD Site 801B	Lower-middle Tithonian (152.1 - 146.7 Ma)	-2.7	[-4, -1.4]	3.9	-	9˚S	5 degrees too far south
150-190 Ma	Pacific Plate	OPD Site 801B	Kimmeridgian (157.3 - 152.1 Ma)	-10.4	[-14.2, -6.6]	14.7	-	9-10˚S	✓
	Pacific Plate	OPD Site 801B	Upper Bathonian - Lower Oxfordian (167.1 - 160.9 Ma)	-4.5	[-10.6, -2.9]	6.4	-	10-11˚S	✓
	Pacific Plate	OPD Site 801B	167.7 ± 1.4	-4.4	[-6.4, -2.4]	-	-	10˚S	4 degrees too far south
	Costa Rica	SR1,3,4,10,11-ht	190 - 180	±8	[-18.3, 1.1]	11.4	100	15-25˚S	✓
190-260 Ma	Japan	Inuyama cherts	215	20		27.5	170	20˚N	✓
	Mexico	CC1/CC2	Upper Triassic (uppermost Carnian to middle Norian)	±2.6	[-7.9, 5.2]	3.7	105	2.6˚S	✓
	Japan	Inuyama cherts	240	-5		7.1	170	5˚S	✓
	New Zealand	Waiheke Island	Lower Triassic (252 - 247 Ma)	-33.6	[-51.2, -20]	43.5	150	30-34˚S	✓
	New Zealand	BI1/BI2/BI5	Permian (299 - 252 Ma)	-11.4	[-24.9, -0.6]	16.1	150	22-32˚S	✓
	Japan	Kamura	Upper Permian (260 - 252 Ma)	-12.2	[-14, -10.4]	-	160	11-14˚S	✓

λ: paleolatitude, ISC λ: Inclination shallowing corrected paleolatitude using a flattening factor of 0.7.

are deposited), towards a trench (when first hemipelagic, and later turbiditic trench fill sediments are deposited). When OPS basement contains island arc, ocean island basalt, or large igneous province geochemical signatures, the age of the originally underlying magmatic basement may be considerably older, and the sequence reflects the journey from an intra-oceanic arc, seamount, or oceanic plateau towards a trench (Isozaki and others, 1990).

The aim of our study is to constrain past motions of the main lost plates of the Panthalassa Ocean. To do so, we focus on OPS sequences derived from the Farallon, Phoenix and Izanagi plates that formed at central Panthalassa spreading ridges, far from the continental margins. Previous geological and seismic tomographic studies have shown that large parts of the circum-Pacific accretionary orogens, for example in Canada, Alaska, and far-east Russia, did not form by simple oceanic subduction below the continental margins. Instead, these orogens contain remnants of multiple volcanic arcs and oceans that formed at simultaneously active Mesozoic subduction systems in the eastern and northern Panthalassa Ocean (Nokleberg and others, 2000; Johnston, 2001; Monger and Price, 2002; Sigloch and others, 2008; van der Meer and others, 2012; Sigloch and Mihalynuk, 2013; Domeier and others, 2017; Vaes and others, 2019). Discerning Izanagi- or Farallon-derived records from these orogens is challenging, and we therefore do not use OPS materials from these regions – we refer the reader to Nokleberg and others (2000), Monger and Price (2002), and Johnston (2008) for discussions on the tectonic history of these regions. Similarly, the region of intersection of the Tethys and Panthalassa domains in Southeast Asia has a complex subduction and accretion history and is outside of the scope of our current paper – we refer the reader to Hall (2002), Zahirovic and others (2014), Wu and others (2016), and Advokaat and others (2018) for a range of views on the tectonic evolution of this region.

In this study, we focus on Permian to Cretaceous OPS sequences that accreted during Jurassic and Cretaceous times to circum-Pacific continental margins on Cedros Island (Baja California, Mexico), the Santa Elena Peninsula (Costa Rica), the North Island of New Zealand, and Japan (fig. 2). Overriding plate deformation in these regions is reconstructed in previous studies: we use Boschman and others (2014, 2018a, 2018b) and McQuarrie and Wernicke (2005) for a reconstruction of the tectonic history of Mexico and Costa Rica, van de Lagemaat and others (2018a) for New Zealand, Vaes and others (2019) for Japan, and Matthews and others (2016) and Domeier and Torsvik (2014) for the China block motions (fig. 1B). To estimate paleolatitudes when using paleomagnetic data, we place the relative plate motion reconstructions in the paleomagnetic reference frame or Torsvik and others (2012).

TECTONIC SETTING, AVAILABLE PALEOMAGNETIC DATA, AND SAMPLING OF SELECTED CIRCUM-PACIFIC OPS

Eastern Panthalassa: Accreted Remnants of the Farallon Plate

Setting.—Relics of the Farallon Plate, which occupied the eastern Panthalassa Ocean, can in theory be expected along the western margin of the Americas. However, throughout the Mesozoic-Cenozoic, the South American margin experienced subduction erosion rather than accretion, and except for accreted oceanic fragments in the northernmost Andes of Colombia and Ecuador related to Late Cretaceous collision with the Caribbean Plate, no accretionary prism or subduction complex containing Farallon-derived material is present in South America (Kennan and Pindell, 2009; Horton, 2018; Montes and others, 2019). Moreover, as noted above, we do not consider the accretionary records related to the complex subduction history of the northeastern Panthalassa Ocean, that is, the records of the Canadian

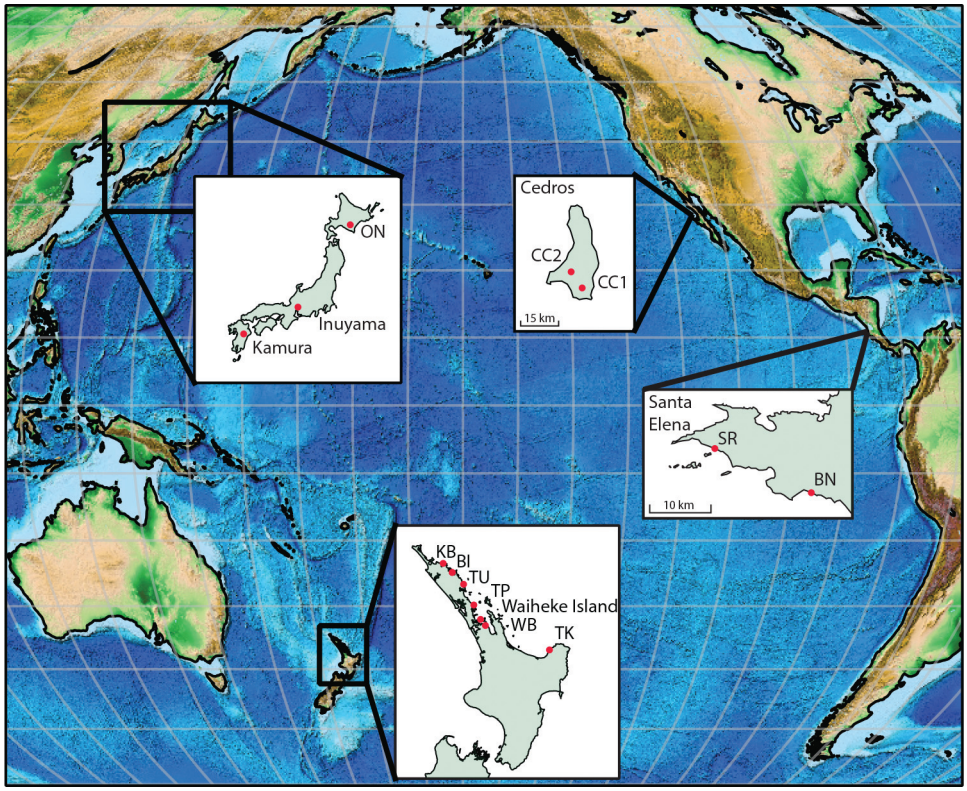

Fig. 2. Sampling locations from Kodama and others (2007) (Waiheke Island), Kirschvink and others (2015) (Kamura), Shibuya and Sasajima (1986), Ando and others (2001), Oda and Suzuki (2000) (Inuyama), and this study.

and US sectors of the North American Cordillera. Accreted Farallon records for which the tectonic history of the overriding plate is reasonably well known are exposed along the western margins of Mexico and Central America.

The geology of Mexico and northern Central America contains records of subduction spanning Triassic-present day times. The active Cenozoic volcanic arc is interpreted as a long-lived continental margin arc related to subduction of Farallon and its daughter plates (Cocos, Rivera) (Ferrari and others, 2007). Older records of Triassic-Cretaceous arc magmatism are exposed in the Guerrero terrane of mainland Mexico (Centeno-García and others, 2003, 2008; Talavera-Mendoza and others, 2007), in the Peninsular Ranges Batholith of Baja California (Johnson and others, 1999; Ortega Rivera, 2003), and in the Chortís and Mesquito terranes of northern Central America (Flores and Gazel, 2020). The Guerrero terrane is separated from mainland Mexico by the Guerrero terrane suture belt (GTSB), including sheared and folded meta-sedimentary rocks, Tithonian-Barremian felsic dikes and lavas, and Aptian-Cenomanian intraplate-like and mid-ocean-ridge basalts, interpreted as the remnants of the oceanic Arperos Basin (Martini and others, 2011, 2014). There is debate on the origin of the Arperos Basin: some authors argue that the basin represented a >1000 km wide ocean ('Mezcalera'), making the western terranes of Mexico exotic and potentially far-traveled to North America (Dickinson and Lawton, 2001; Hildebrand, 2013; Sigloch and Mihalynuk, 2013; Clennett and others, 2020). Detailed field geological studies of Mexican geology, however, showed that the Guerrero arc is built on a Triassic

accretionary prism and blueschist-bearing subduction complex (the Arteaga Complex), which contains detrital zircons matching the signature of mainland Mexico (Centeno-García and others, 2011), and that the Tithonian-Barremian felsic dikes and lavas of the GTSB contain Paleozoic and Precambrian inherited zircons (Martini and others, 2011). These studies thus rather indicate that the Guerrero terrane was located at the North American continental margin in Triassic times, and that the Arperos Basin opened and closed during the Late Jurassic to mid-Cretaceous as a narrow back-arc basin above a long-lived and continuous eastward-dipping subduction zone (Cabral-Cano and others, 2000; Elias-Herrera and others, 2000; Centeno-García and others, 2008, 2011; Martini and others, 2011; Fitz-Díaz and others, 2018). Subduction complex rock assemblages similar to those of the Arteaga complex (blueschists, serpentinites) are exposed in westernmost northern Central America reaching as far south as northern Costa Rica (Rogers and others, 2007; Baumgartner and others, 2008). Boschman and others (2018b) argued that seismic tomographic images revealing a continuous slab connected to the actively subducting Cocos Plate at the Middle America trench and reaching all the way to the lowermost mantle below the Atlantic (Grand and others, 1997; Bijwaard and others, 1998), are consistent with continuous subduction below the southern part of the North American continent since the Triassic. In addition, Boschman and others (2018a, 2018b) presented paleomagnetic data from the Guerrero terrane and from the Triassic Vizcaíno SSZ ophiolite and its Jurassic sedimentary cover exposed east of the Peninsular Ranges Batholith in Baja California, and showed that these western Mexican terranes have had a paleolatitudinal plate motion history equal to that of the North American Plate. As the paleolatitude of the Mesozoic overriding plate terranes below which the Farallon Plate subducted is therefore known, remnants of the subducted Farallon Plate accreted to this segment of the North American continental margin, such as exposed on Cedros Island (offshore of the Vizcaíno Peninsula of Baja California) and on the Santa Elena Peninsula of Costa Rica, are used in reconstructing plate motions of the Farallon Plate.

Previous paleomagnetic results, and sampling: Baja California and Costa Rica.—On Cedros Island (fig. 3), a blueschist-bearing serpentinite-matrix mélange is exposed that contains ~1 to 50 m scale blocks of (meta-) basalt, chert, limestone, and upper Lower Cretaceous (~105 Ma) turbiditic sedimentary rocks (Rangin, 1978; Sedlock, 1988). This mélange is part of an assemblage of Mesozoic subduction-related rocks, including a Triassic (~220 Ma) supra-subduction zone (SSZ) ophiolite, Jurassic arc magmatic rocks, and Cretaceous forearc deposits exposed throughout the Vizcaíno-Cedros region of central Baja California (Kimbrough and Moore, 2003). Boschman and others (2018b) recorded paleolatitudes from these SSZ ophiolitic and overlying sedimentary rocks.

Hagstrum and Sedlock (1990) sampled pillow basalts and chert beds from a continuous section of pillow basalts, ~40 m of red radiolarian ribbon cherts and ~250 m of thin-bedded turbidites exposed within the mélange on southeastern Cedros Island (fig. 3). Based on radiolarian biostratigraphy, the cherts were shown to represent a long, condensed stratigraphic section spanning the Upper Triassic to the Lower Cretaceous (Sedlock and Isozaki, 1990). Initially, Hagstrum and Sedlock (1990) concluded that these rocks were remagnetized, and that no original magnetic signal was present. However, later re-analyses of the chert samples (Hagstrum and Sedlock, 1992) yielded a stable high-temperature (600–680°C) component in 13 of 101 samples, including antipodal normal and reversed polarities, which they interpreted as the primary magnetization. The directions from these 13 samples suggest deposition of the cherts at equatorial latitudes ($2 \pm 3°$).

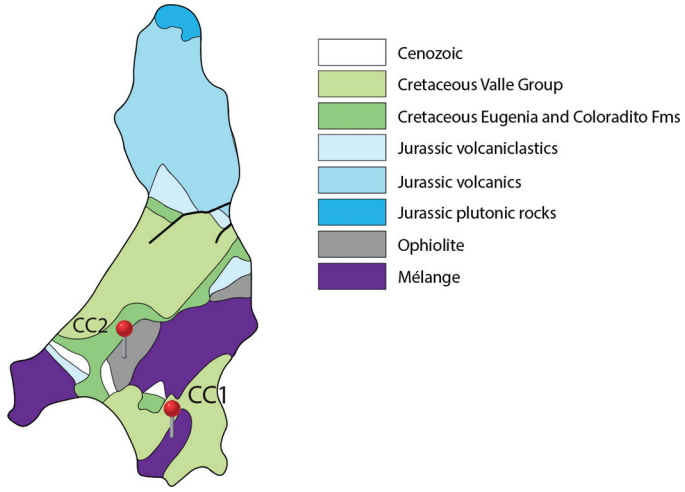

Fig. 3. Simplified geological map of Cedros Island, Mexico, including sampling locations of Hagstrum and Sedlock (1992) and this study. Based on Kimbrough and Moore (2003).

From the lower (Upper Triassic) part of the chert section sampled by Hagstrum and Sedlock (1990), we collected another 89 hand samples (CC1, figs. 2 and 3). Furthermore, we collected 16 hand samples from ~1.5 m of stratigraphy within a block of green chert exposed on southern central Cedros Island (CC2, figs. 2 and 3). Unlike CC1, this second block of chert is not in contact with its underlying magmatic basement. At the time of accretion (~105 Ma (Sedlock, 1988)) of these two chert sequences, Cedros Island was located at 32°N.

The Santa Elena Peninsula of northwestern Costa Rica exposes a peridotite nappe intruded by ~121 Ma diabase dikes overthrusting the Santa Rosa accretionary complex (SRAC, fig. 4). The SRAC contains sheared peridotites and megabreccias, an isolated block of layered gabbros, and volcano-sedimentary successions interpreted as the remnants of a seamount (Tournon, 1994; Baumgartner and Denyer, 2006; Gazel and others, 2006; Denyer and Gazel, 2009; Bandini and others, 2011; Buchs and others, 2013; Escuder-Viruete and Baumgartner, 2014; Madrigal and others, 2015). The seamount complex (sampling location SR, figs. 2 and 4) contains fault-bounded sequences of ~190 to 180 Ma red bedded cherts, ~175 Ma alkaline basalt sills and massive basalts, and ~110 Ma cherts, tuffaceous mudstones, turbiditic sedimentary rocks, and polymict breccias (Tournon, 1994; Baumgartner and Denyer, 2006; Bandini and others, 2011; Buchs and others, 2013). The layered gabbros, exposed at Bahia Nancite (sampling location BN, figs. 2 and 4) have been dated at 124 ± 4.1 Ma (^{40}Ar-^{39}Ar age, Hauff and others, 2000). The tectonic and magmatic origin of the Bahia Nancite gabbros and the Santa Elena ophiolite remain uncertain [see Madrigal and others (2015) for a discussion], but the position of the peridotite nappe in the hanging wall overthrusting the SRAC, which contains open-ocean derived material, indicates that the peridotite nappe must have been located at the westernmost boundary of the North American Plate, adjacent to a trench.

Accretion of the SRAC is dated by the youngest rocks (~110 Ma) of the seamount complex, in which the chert beds grade into muddy-sandy turbidites whereby amounts

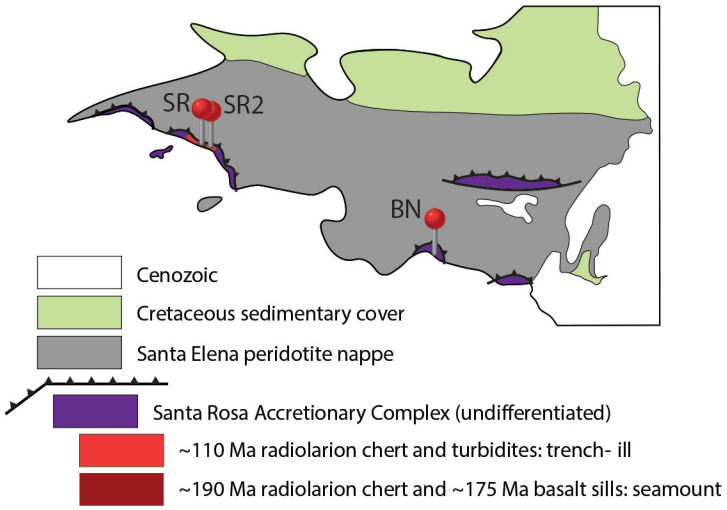

Fig. 4. Simplified geological map of the Santa Elena Peninsula, Costa Rica, including sampling locations. SR: sites SR1, 3, 4, 5-8, 10, 11. Based on Bandini and others (2011).

of tuffaceous material increase and are overlain by polymict breccia beds (Baumgartner and Denyer, 2006; Bandini and others, 2011; Buchs and others, 2013). This sequence is interpreted as (the transition to) trench-fill deposits, and radiolarians from the pelagic to hemipelagic facies dating the onset of distal detrital sedimentation have yielded a late early Albian to early middle Albian age (~110 Ma) (Bandini and others, 2011). From the top of this sequence, De Wever (1985) obtained a (less precise) Barremian-Cenomanian age. Buchs and others (2013) used the Albian (110 Ma) age of the chert at the base of the trench-fill sequence to interpret the seamount to have accreted at 110 Ma, but we argue that a considerable amount of time (and plate motion) must have passed between the deposition of the cherts and accumulation of the breccia beds, and interpret the age of accretion to be ~100 Ma, consistent with the younger end of the age spectrum for the top of the chert-to-breccia sequence. Accretion of SR and BN at 100 Ma postdated opening and subsequent closure of the Arperos backarc basin, which separated the continental margin from the main North American continent in latest Jurassic-mid Cretaceous times (Cabral-Cano and others, 2000; Centeno-García and others, 2011; Martini and others, 2011; Centeno- García, 2017; Boschman and others, 2018a). The Santa Elena Peninsula was located at the southwesternmost part of the North American Plate below which the Farallon Plate subducted. At 100 Ma, the Santa Elena Peninsula was located at 11°N.

From the SRAC, we collected 46 oriented hand samples from the ~190 to 180 Ma cherts (sites SR1,3,4,10,11), 30 hand samples from ~175 Ma basalt sills (sites SR5-9), and 20 hand samples from the ~110 Ma cherts (site SR2, fig. 4). Additionally, we collected 36 cores from the layered gabbros exposed at Bahia Nancite (site BN, fig. 4). Estimates of magmatic foliation in these gabbros were collected as a best (but uncertain) measure for the paleohorizontal.

Southern Panthalassa: Accreted Remnants of the Phoenix Plate

Setting.—Relicts of the Phoenix Plate are expected along the continental margins of the southern Panthalassa Ocean: in Antarctica, New Zealand, Australia, and Southeast Asia. Although accreted relics of Panthalassa plates are present in Southeast Asia (for example, Jasin and Tongkul, 2013), intense deformation of the accretionary

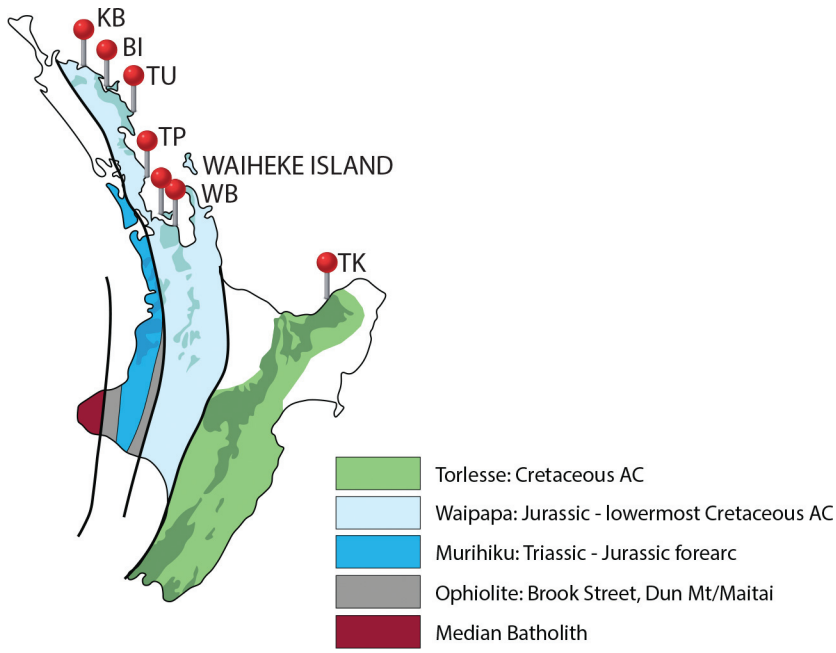

Fig. 5. Simplified geological map of the North Island of New Zealand, including sampling locations of Kodama and others (2007) and this study. AC: accretionary complex. Based on Mortimer (2014) and Price and others (2015).

orogens in the region of intersection of the Tethyan and Panthalassa plate systems makes interpretation of these records challenging, and we focus on remnants of the Phoenix Plate accreted at former Gondwana margins. Such accreted relics are well known from the North Island of New Zealand, where OPS is exposed in the Waipapa Terrane, a northwest-southeast trending accretionary complex belt (fig. 5). The Waipapa Terrane comprises pillow basalts, Permian-Lower Jurassic chert, limestone and argillite, and uppermost Jurassic - lowermost Cretaceous trench-fill deposits (Spörli and Grant-Mackie, 1976, Spörli and others, 1989; Kear and Mortimer, 2003; Adams and others, 2007, 2009, 2012; Mortimer and others, 2014). The maximum depositional age of the trench-fill sandstones is constrained through detrital zircon U-Pb ages of 141 ± 2 Ma (near Auckland) to 152 ± 1 Ma (in Northland) (Cawood and others, 1999; Adams and others, 2012). The Waipapa Terrane is part of New Zealand's Eastern Province that consists of volcanic arc, ocean floor preserved as ophiolite, an accretionary complex, and overlying deposits of the Murihiku forearc basin, which is collectively interpreted as an arc-trench system (Mortimer, 2004, fig. 5). This arc-trench system was separated from Gondwana-derived continental units exposed in western New Zealand by the Median Batholith, which represents a long-lived (~375–110 Ma) Gondwana margin arc (Mortimer, 2004). The tectonic origin of the Eastern Province has been subject to debate. Triassic plant fossils from the Murihiku forearc terrane and those recovered from rocks of the Gondwana continental margin are similar (Retallack, 1987), indicating that the Eastern Province was likely never separated from the Gondwana margin by a major ocean basin. Zircon provenance studies of Triassic rocks of the Murihiku terrane concluded a wide range of possible origins, from the northeastern margin of Australia, the New Zealand segment of the Median Batholith (that is, in its present position), or the Antarctic Peninsula (Adams and others, 2007; Campbell and others, 2020, and references therein). Sparse

paleomagnetic data from Murihiku forearc lavas and sedimentary rocks that escaped widespread Late Cretaceous remagnetization (Oliver, 1994; Haston and Luyendyk, 1991; Kodama and others, 2007; van de Lagemaat and others, 2018b) suggest Early Jurassic paleolatitudes of 66°S and 62.1 ± 12°S, respectively (Grindley and others, 1980; van de Lagemaat and others, 2018b). During the Early Jurassic, New Zealand's Gondwana margin was located at ~80°S. If the eastern Province indeed originated close to the Gondwana margin, a ~65°S paleolatitude would suggest that the Murihiku Terrane was derived from either the northeast Australian margin, or the Antarctic Peninsula (see Figure 11 in van de Lagemaat and others (2018b)). Regardless of the location of origin of the Eastern Province terranes, ages of conglomerate containing clasts derived from both Eastern and Western Province sources indicate that the two have been juxtaposed since the latest Jurassic (147 Ma) (Tulloch and others, 1999), implying that during the ~145 Ma accretion of OPS in the Waipapa Terrane, the Eastern Province was located in its modern position relative to Zealandia. During accretion, the Eastern Province (then Gondwana) margin, below which the Phoenix Plate subducted, was located at 80°S.

Previous paleomagnetic results, and sampling: New Zealand.—Kodama and others (2007) reported results from an extensive paleomagnetic sampling campaign on pre-Neogene rocks of New Zealand and demonstrated that the high unblocking temperature component of samples from a single Lower Triassic chert layer from the Waipapa OPS exposed on Waiheke Island (figs. 2 and 5) passes a reversal test and may thus be interpreted as primary. The directions from this chert layer indicate deposition at a paleolatitude of 33.6°S, that is, thousands of kilometers north of the Eastern Province margin.

From various locations within the Waipapa Terrane along the north coast of the North Island, we collected a total of 101 hand samples from 11 blocks of chert (sites TK, WB, TP, TU, BI1-5, KB1,2, figs. 2 and 5). Hand samples were typically collected from ~2 m of stratigraphy. Only the cherts from site WB1 were previously dated, yielding a radiolarian biostratigraphic age of Late Triassic - Early Jurassic (Spörli and others, 1989). The chert blocks from the Bay of Islands (BI1-5) are from a large (~200 m) coastal exposure including pillow basalts. We assume that the Waipapa Terrane encompasses a single disrupted sequence of OPS, and these cherts are therefore interpreted to represent the oldest (Permian) segment of the stratigraphy of the Waipapa Terrane.

Western Panthalassa: Accreted Remnants of the Izanagi Plate

Setting.—For remnants of the Izanagi Plate, we focus on the extensive accretionary record of Japan. The Japanese islands contain a ~500 Ma record of accretionary orogenesis related to long-lived subduction of Panthalassa lithosphere (Maruyama and Seno, 1986; Isozaki, 1996), first along the continental margin of the China blocks (part of Eurasia since the mid-Mesozoic), and since Oligo-Miocene opening of the Sea of Japan, at the Japanese island arc (Isozaki, 1996, 2000; Maruyama and others, 1997; Isozaki and others, 2010). This long-lived subduction resulted in the formation of two series of trenchward-younging accretionary complexes separated by the Median Tectonic Line (MTL) (Isozaki and others, 1990; Isozaki, 2000), fig. 6). The MTL is a major E-W striking, northward dipping fault, which is currently accommodating right-lateral strike-slip motion of about 5 to 10 mm/yr, interpreted as strain partitioning in the overriding plate resulting from oblique subduction at the Nankai Trough (Okada, 1973; Sugiyama, 1994). The MTL juxtaposes an outer (southern) accretionary orogen against an inner (northern) accretionary orogen. Similarities in (boreal) fauna between the inner zone and South Primorye (Far East Russia) indicate

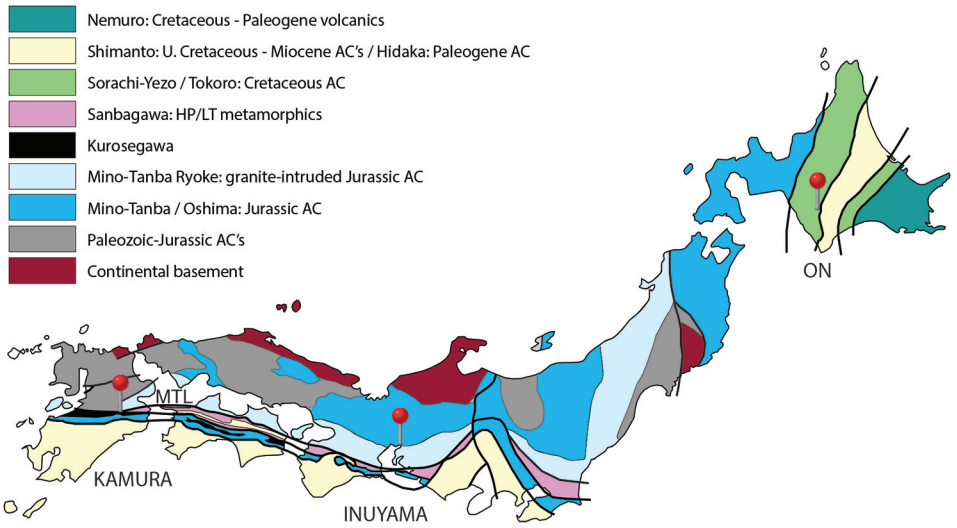

Fig. 6. Simplified geological map of Japan, including sampling locations from Kirschvink and others (2015), Shibuya and Sasajima (1986), Oda and Suzuki (2000), Ando and others (2001) and this study. MTL: Median Tectonic Line, AC: accretionary complex. Based on Isozaki and others (2010) and Ueda (2016).

that at least by Permian time, the inner zone was emplaced in its pre-Sea of Japan opening position adjacent to the Asian continent (Hayami, 1961; Sato, 1962; Kobayashi and Tamura, 1984; Tazawa, 2001). The outer zone, however, contains diverse Triassic - Jurassic faunal assemblages with a Tethyan affinity (Matsumoto, 1978; Hayami, 1984; Kobayashi and Tamura, 1984; Hallam, 1986). Sediment provenance studies have shown that Lower Cretaceous sedimentary rocks of the outer zone are related to the South China Block (Ikeda and others, 2016), and during the Late Cretaceous, a sinistral pull-apart basin formed along the MTL (the Izumi Group) (Ichikawa and others, 1979, 1981; Miyata, 1990; Noda and Toshimitsu, 2009; Noda and Sato, 2018). Following these observations, several authors have proposed a tectonic model in which the MTL accommodated large (>1000 km) left-lateral margin-parallel strike-slip motion, bringing the outer zone from a low-latitude position to its modern position juxtaposed against the inner zone during the Cretaceous (Taira and others, 1983; Yamakita and Otoh, 2000; Yao, 2000; Sakashima and others, 2003). However, a klippe of inner zone units has been identified overlying the outer zone, and geophysical data that show that the accretionary complexes of the outer zone are buried below the inner zone orogen far beyond the surface transect of the MTL, which has led others to argue that the inner and outer zones were juxtaposed by thrusting (Isozaki, 1988; Isozaki and Itaya, 1991; Sato and others, 2005, 2015; Ito and others, 2009). Boschman (ms, 2019) and Boschman and others (2021) illustrated through a reconstruction of intra-oceanic subduction at the Oku-Niikappu arc (see below) that in mid-Cretaceous time, the outer zone was likely separated from the Northeast Asian continental margin by a back-arc basin, and we follow its tectonic reconstruction in which the outer zone orogen rifted off the South China Block in the Jurassic, experienced ongoing accretion in Jurassic-Cretaceous time in an intra-oceanic position and accreted to the inner zone orogen in the Late Cretaceous. For the pre-Middle Jurassic position of the outer zone, this follows tectonic reconstructions of Ikeda and others (2016), Sakashima and others (2003), Tazawa (2002), and Uno and others (2011).

Hokkaido, the northern island of Japan, is interpreted to correlate to the outer zone (Ishiga and Ishiyama, 1987; Ueda, 2016). The pre-Neogene basement of Hokkaido is divided into five ~N-S trending tectonostratigraphic belts, containing accretionary complexes, overlain and intruded by magmatic arc and fore-arc assemblages (Kiminami, 1992; Ueda, 2016, fig. 6). Within the central Sorachi-Yezo Belt, Ueda and Miyashita (2005) identified a narrow (<2 km) serpentinite-bearing belt containing an aggregate of fault-bounded slices and blocks, which they named the Oku-Niikappu Complex. The Oku-Niikappu Complex consists of (1) massive and foliated serpentinite; (2) a sheeted dike complex containing andesitic, boninitic and MORB-like dykes; (3) (meta)volcanic rocks, volcaniclastic sedimentary rocks, conglomerates (containing clasts of volcanic rocks and serpentinite) and Lower Cretaceous (Berriasian and younger) red bedded chert; and (4) Albian-Cenomanian black mudstone and siliciclastic sandstone, partly containing meter-sized blocks of chert and (meta)volcanic rocks (Ueda, 2003; Ueda and Miyashita, 2003, 2005). Except for the MORB-like dikes, all igneous rocks from the Oku-Niikappu Complex show island arc geochemical characteristics (Ueda and Miyashita, 2005). Ueda and Miyashita (2005) interpreted the Oku-Niikappu complex as a latest Jurassic intra-oceanic island arc that went extinct while still in an intra-oceanic setting, was (hyper) extended and partly eroded, covered by cherts in a pelagic environment, and eventually, ~45 Ma after arc extinction, by Albian-Cenomanian trench-fill deposits. This remnant intra-oceanic arc indicates that at least during the Late Jurassic, the northwestern Panthalassa hosted not one (Izanagi), but at least two plates, whereby one oceanic plate subducted below the other (Ueda and Miyashita, 2005). We here follow the reconstruction of Boschman (ms, 2019) and Boschman and others (2021), who analyzed the stratigraphy and age relationships of all accretionary complexes exposing OPS sequences on Hokkaido, and reconstructed Jurassic intra-oceanic subduction of the Izanami Plate (located between the Izanagi and Pacific plates) below the Izanagi Plate. Boschman (ms, 2019) and Boschman and others (2021) illustrated that the Oku-Niikappu arc formed near the equator, above seismic tomographically imaged deeply subducted slab remnants below the central Pacific Ocean (van der Meer and others, 2012), and how the intra-oceanic Oku-Niikappu subduction zone likely went extinct as a result of ridge subduction, which is reflected in a change in marine magnetic anomaly and fracture zone orientations on the modern Pacific Plate (fig. 1).

Previous paleomagnetic results, and sampling: Japan.—The Inuyama region of the inner zone of central Japan (figs. 2 and 6), located within the Jurassic Mino-Tamba accretionary complex belt, contains the type locality of OPS (Isozaki and others, 1990, Matsuda and Isozaki, 1991; Isozaki, 2014), including a >80 m continuous section of chert beds spanning the Lower Triassic to Lower Jurassic (Yao and others, 1980; Matsuda and Isozaki, 1982; Isozaki, 2014). Paleomagnetic studies on the Inuyama cherts yielded positive fold tests, and indicate low-latitude depositional environments (between 15°S and 30°N, see table 1, fig. 7) (Shibuya and Sasajima, 1986; Oda and Suzuki, 2000; Ando and others, 2001). At the time of accretion of the Inuyama cherts (at ~170 Ma), the inner zone subduction system was located at ~52°N.

In the Kamura region of the outer zone of southwestern Japan (figs. 2 and 6), located in the Jurassic accretionary complex of the Chichibu belt, Permian-Triassic limestone is exposed, interpreted to have formed in the atoll of a mid-oceanic seamount (Sano and Nakashima, 1997; Isozaki and Ota, 2001; Ota and Isozaki, 2006; Kasuya and others, 2012; Kirschvink and others, 2015). Kirschvink and others (2015) presented paleomagnetic data from these limestones, yielding a positive reversal test, and a paleolatitude of 12.2°S for the Permian, whereby the southern hemispheric origin is concluded based on correlation of the polarity pattern with the

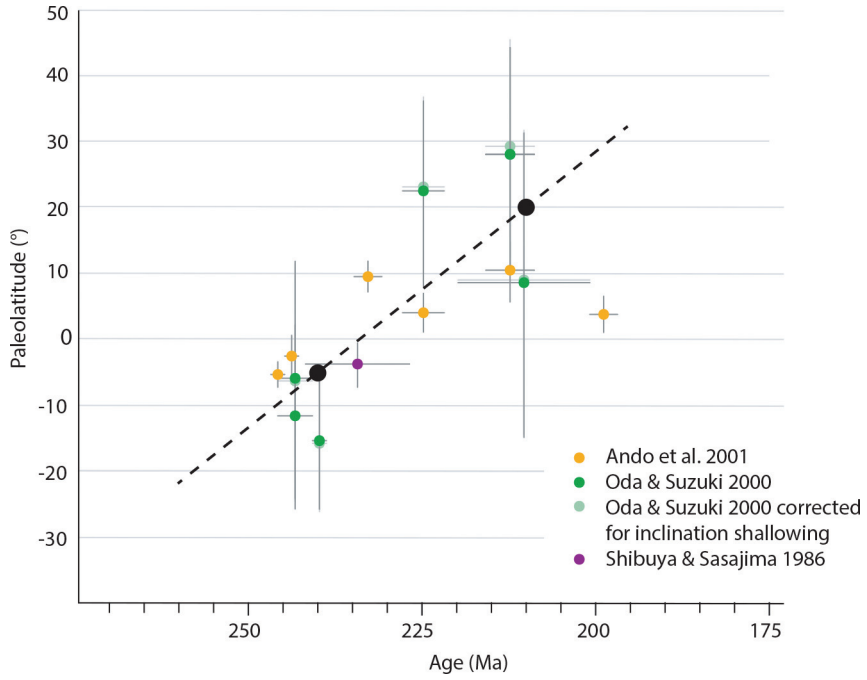

Fig. 7. Compilation of paleolatitudes derived from paleomagnetic data from the Inuyama cherts. The black dashed line represents the inferred paleolatitudinal motion of the Inuyama OPS (5°S at 240 Ma, 20° N at 215 Ma) used in the reconstruction.

magnetostratigraphic timescale. At the time of accretion of the Kamura limestones (at ~160 Ma), the outer zone subduction system was located at ~34°N.

From the Oku-Niikappu Complex of Hokkaido, we sampled 4 sites: ON1 consists of pillow basalts (45 cores, one sample per pillow, ON1.34–1.45 are from a single(?) andesitic lava). At site ON2 (55 cores), we sampled through a ~50 m section of dykes, containing approximately 27 dikes. ON3 and ON4 (12 and 10 hand samples) were sampled in red bedded chert stratigraphically overlying the pillow basalts of ON1. At the location of ON3 (which is the base of the chert section), radiolarian biostratigraphy yielded a Berriasian age (Ueda and Miyashita, 2005). ON4 is located up section relative to ON3 and is therefore slightly younger; the basaltic rocks of ON1 are underlying the chert section and are therefore inferred to be earliest Cretaceous in age or older. We assume that the paleo-horizontal of the basalts of ON1 is the same as the average bedding orientation of ON3 and 4.

METHODS

Anticipating the extreme durability of radiolarian cherts, we collected hand samples, from which we drilled typical 25 mm diameter paleomagnetic cores in the paleomagnetic laboratory Fort Hoofddijk (Utrecht University, the Netherlands) using a drill press. Hand samples yielded between one and six cores, which were subsequently cut into specimens of maximum 22 mm length. We determined core orientations by measuring planes on the hand samples in the field (generally bedding planes), and drilling perpendicular to those planes. Based on the red color of the cherts that may indicate the presence of hematite, most red chert samples were subjected to thermal demagnetization only; other lithologies (black/gray chert, basalt) were subjected to both thermal and alternating field demagnetization up to 680° or 100 mT. The samples were measured on a 2G DC SQUID cryogenic magnetometer. Interpretation of

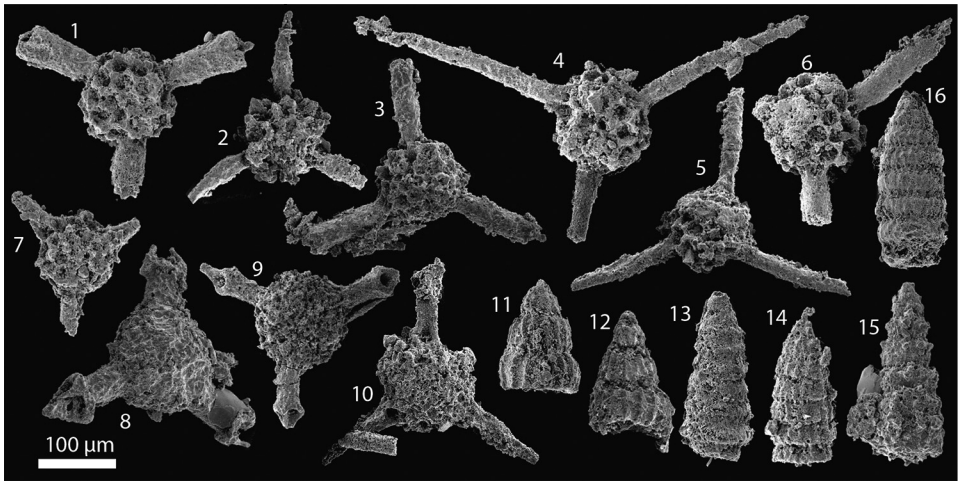

Fig. 8. SEM photographs of representative radiolarians from sample CC2. 1: *Canoptum anapetes* (De Wever) (De Wever and others, 2002); 2: *Capnodoce crystallina* (Pessagno) 3: *Capnodoce* sp., 4&5: *Capnodoce fragilis* (Blome), 6: *Capnodoce* cf. *extenta* (Blome), 7: *Justium* sp., 8: *Capnuchosphaera* cf. *theloides* (De Wever), 9: *Capnuchosphaera* sp., 10: *Sarla?* sp. 11&12: *Xipha* cf. *pessagnoi* (Nakaseko and Nishimura), 13: *Canoptum* sp. 14: *Corum?* sp., 15: *Pachus* sp., and 16: *Latium?* sp.

the demagnetization diagrams [plotted in Zijderveld (2013) diagrams] and associated statistical analyses (following procedure described in Deenen and others (2011) were performed using the online portal Paleomagnetism.org (Koymans and others, 2016, 2020). We used the principal component analysis of Kirschvink (1980) to interpret demagnetization diagrams, determined great circle solutions using the method of McFadden and McElhinny (1988), calculated site mean directions using Fisher (1953) statistics applied on VGP's, calculated declination and inclination errors ΔD_x and ΔI_x following Butler (1992), and applied 45° cut-offs per sampling location (Johnson and others, 2008). We assess whether sampling collections have a scatter that may represent paleosecular variation (PSV) of the geomagnetic field following Deenen and others (2011). For sampling locations in which the stratigraphic younging direction was not determined (all New Zealand sites and Cedros site CC2), we corrected the interpreted directions for both the normal facing (<90° tilting) and overturned (>90° tilting) option. When possible, we sampled through various bedding orientations within a block, and when applicable, we used the fold test of Tauxe and Watson (1994). To test for common true mean directions, we used the bootstrapped coordinate test of Tauxe (2010).

RESULTS

Radiolarian Biostratigraphy Cedros Island

From Cedros Island, we analyzed chert samples from the CC2 sampling location. These yielded abundant but poorly preserved radiolarian fossils consisting dominantly of genus *Capnodoce, Capnuchosphaera, and Canoptum*, as well as occurrences of other genera such as *Justium*, *Sarla?* and *Xipha* (fig. 8). According to Pessagno and others (1979) and Blome (1984), the genus *Capnodoce* is the primary marker of the *Capnodoce* Zone, which ranges from latest Carnian to middle Norian. Occurrence of the genus *Xipha* compare *pessagnoi* suggests the *Xipha striata* Subzone in the *Capnodoce* Zone (Blome 1984), which was assigned to approximately early Norian (De Wever and others, 2002). Therefore, the age of CC2 is Late Triassic [full possible range latest Carnian to middle Norian, probably restricted to the early Norian (~225 Ma)].

Paleomagnetism

Mexico.—Specimens of the Upper Triassic chert samples of site CC1 (N=131) did not (or barely) demagnetize in alternating fields up to 100 mT, indicating that hematite is the primary carrier of the magnetization in these cherts. Thermal demagnetization yielded a northward-directed low-temperature (20–100°C) component in most samples, and a stable, consistent medium-temperature (~200–600°C) component (fig. 9A). This medium-temperature component has a mean direction of D $\pm$ ΔD_x = 20.7 $\pm$ 1.9°, I $\pm$ ΔI_x = 12.8 $\pm$ 3.7° (fig. 9B), and yielded a clearly negative fold test (best clustering between -13 and 4% unfolding, Appendix fig. A1). We interpret this medium-temperature component as a post-folding overprint. Thermal demagnetization did not yield the stable high temperature (600–680°C) component reported by Hagstrum and Sedlock (1992), except for in a single sample (CC1.82, fig. 9D). However, we determined great circles encompassing the transition between a medium (300–600°C) and a high (>600°C) temperature component (figs. 9E and 9F). These great circles pass through and thus confirm the high-temperature ChRM directions interpreted by Hagstrum and Sedlock (1992) (figs. 9G and 9H), and we use their result (tables 1 and 2) to estimate of paleolatitude during deposition of the Upper Triassic CC1 cherts.

Demagnetization (both thermal and alternating field) of specimens of the Upper Triassic CC2 cherts yielded again a stable, consistent medium-temperature (~200–450°C) or 12 to 40 mT component (fig. 9I). Although statistically not distinguishable, this component is very similar to the medium-temperature component of CC1, with a mean direction of D $\pm$ ΔD_x = 22.8 $\pm$ 7.0°, I $\pm$ ΔI_x = 29.0 $\pm$ 11.1° (fig. 9J). Variations in bedding orientations within CC2 are too small to allow for a meaningful fold test, but based on the similarity with the medium-temperature component of CC1, we interpret the CC2 medium-temperature component as the same, post-folding overprint. Demagnetization of CC2 also yielded a second stable, higher temperature component, in the range of 450 to 550°C or 16-60 mT (figs. 9L and 9M), yielding a mean direction of D $\pm$ ΔD_x = 189.4 $\pm$ 7.0°, I $\pm$ ΔI_x =−10.0 $\pm$ 13.6° after correcting for bedding tilt (fig. 9O). This direction is (both with and without correcting for bedding tilt) significantly different from the Geocentric Axial Dipole (GAD) field (fig. 9O), significantly different from the recorded post-folding overprint, and satisfies the quality criteria of representing paleosecular variation (A95min = 3.5° < A95 = 7° < A95max = 11.7°, table 1), and we identify it as likely primary. The mean high-temperature direction corresponds to a paleolatitude of $\pm$ 5° [−1.8°, 12.3°], consistent with the result from CC1. Stratigraphic younging directions are not determined, but when assuming overturned strata in the CC2 chert block, the degree of clustering and the mean inclination remain unchanged, albeit positive (I $\pm$ ΔI_x = 10.0 $\pm$ 13.8°).

Costa Rica.—Demagnetization behavior of the ~190 to 180 Ma red chert samples collected at sites SR1,3,4,10,11 shows that Curie temperatures are generally around 580 to 600°C (Appendix fig. A2), indicating that these cherts contain magnetite as the dominant carrier. Twenty-one out of the total of 105 measured samples also contain a high-temperature component, likely carried by hematite, which differs from the medium and low temperature components and is best preserved in SR11 (Appendix fig. A2). We interpreted a medium-temperature component (~430–580°C or ~25–60 mT, figs. 10A and 10B), which yields a negative fold test (best clustering between -7 and 20% unfolding, Appendix fig. A1C), indicating that this component reflects a secondary, post-folding magnetization. Furthermore, we interpret a high-temperature component (540–680°C, figs. 10G and 10 H). A fold test on the set of high-temperature directions is indeterminate (Appendix fig. A1D). If primary, the mean direction of SR1,3,4,10,11-ht (N=12,

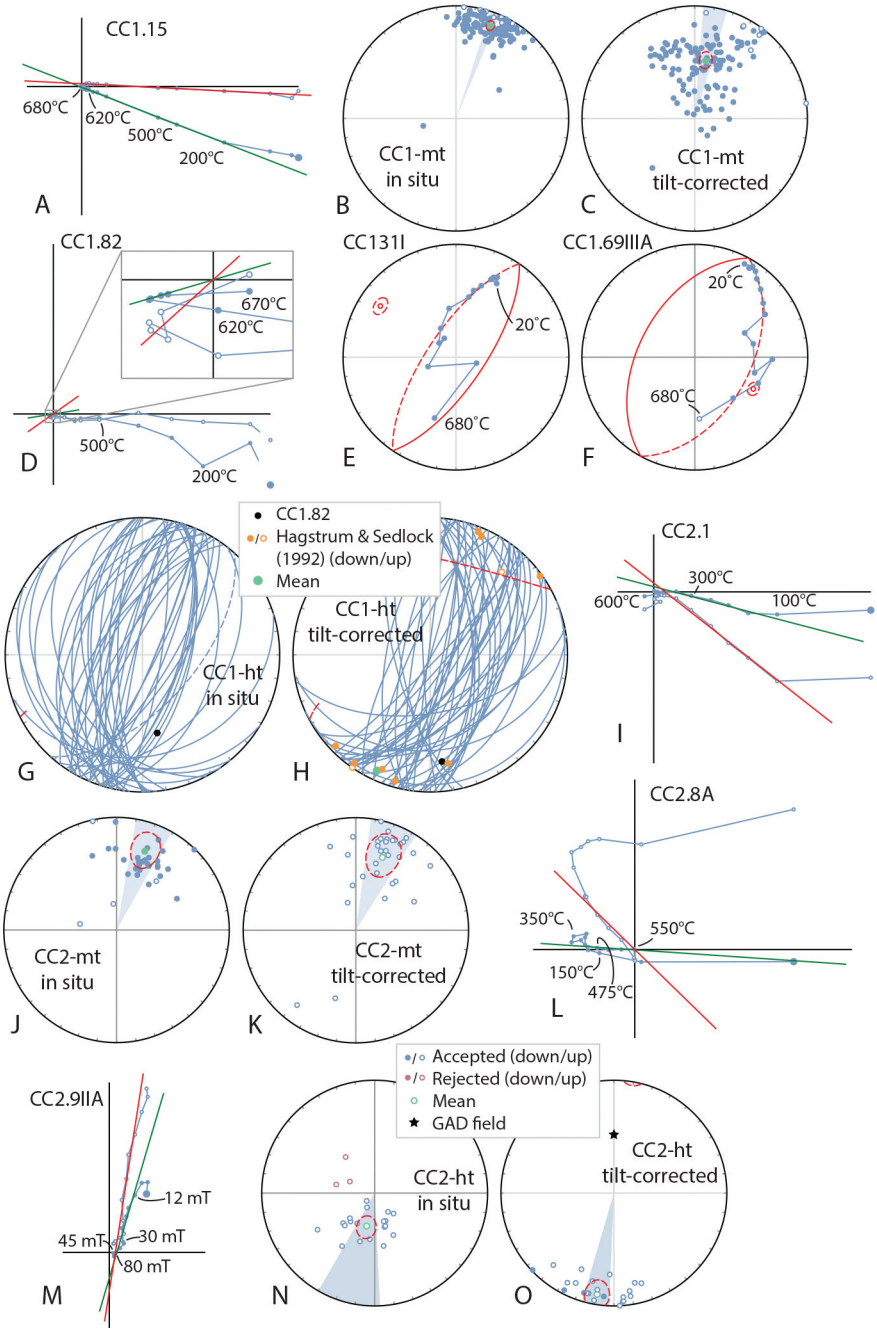

Fig. 9. Orthogonal vector (A, D, I, L, M) and equal area (E, F) diagrams of representative samples of sites CC1 and CC2 from Cedros Island, in geographic coordinates (not corrected for bedding tilt), closed (open) symbol for declination (inclination), up/west projection. Great circles of CC1 and interpreted directions from Hagstrum and Sedlock (1992) (G and H) and interpreted directions from CC1 and CC2 (E, F, J, K, N, O).

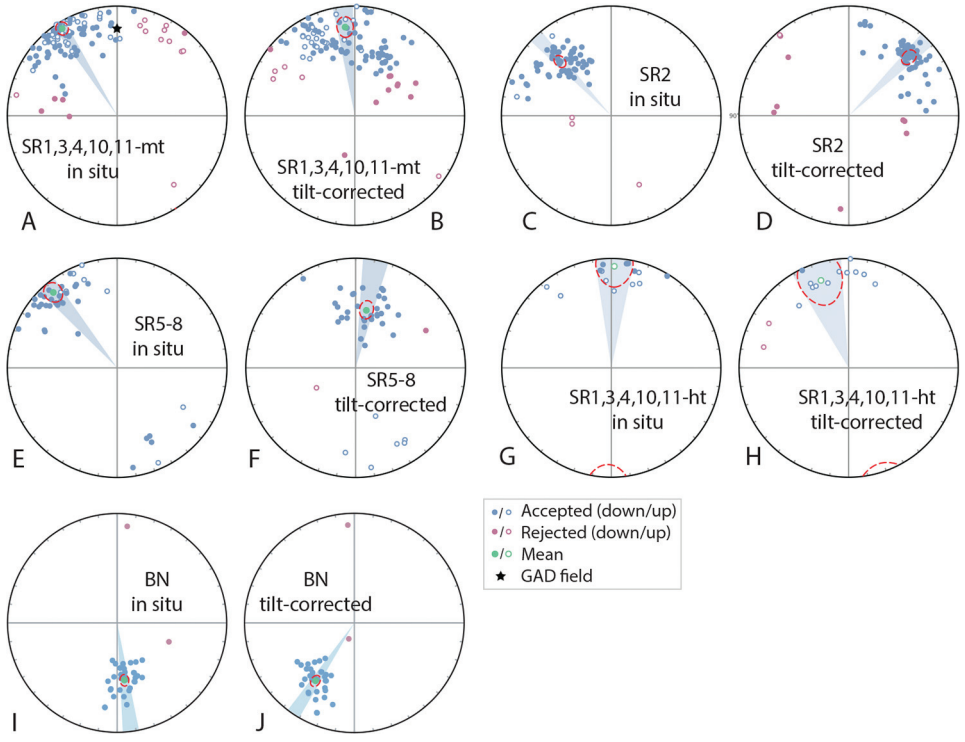

Fig. 10. Interpreted directions from localities SR and BN (Costa Rica).

Dec $\pm$ ΔD_x = 350.1 $\pm$ 9.5°, Inc $\pm$ ΔI_x = −15.7 $\pm$ 17.8°, corrected for bedding tilt) indicates a depositional latitude of 8.0° [−18.3°, 1.1°].

ChRMs from the bedding-parallel basaltic sills sampled at sites SR5-9 were interpreted in the 16–45 mT or 360 to 520°C ranges (Appendix fig. A2). Site SR9 was excluded from further analysis due to high dispersion (K=2.0 before 45° cut-off). Assuming pre-tilt, bedding parallel intrusion, the paleohorizontal of these sills was determined from bedding measurements of the surrounding chert layers; variations in these measurements are too small to yield conclusive results of a fold test. SR6 and SR7 yielded both normal and reversed directions, but a reversal test is negative. The directions recovered from the sills are similar to the medium temperature directions determined from the SR1,3,4,10,11cherts (figs. 10A and 10E) and we therefore interpret these samples to have recorded the same remagnetization.

Demagnetization behavior of the ~110 Ma red chert samples collected at site SR2 is similar to that of sites SR1,3,4,10,11; ChRMs are interpreted at 20 to 50 mT or 300 to 500°C (Appendix fig. A2). Correcting for bedding tilt yields an enigmatic result. The bulk of the directions cluster significantly better after tilt correction, but the number of outliers is increased (figs. 10C and 10D). We interpret this pattern to be the result of partial remagnetization and the tight cluster (fig. 10D) to represent a pre-folding, and thus likely, pre-accretion, magnetization. The mean (D $\pm$ ΔD_x = 45.7 $\pm$ 4.3°, I $\pm$ ΔI_x = 24.9 $\pm$ 7.3°) indicates deposition at a latitude of 13.0° [9.0°, 17.5°].

Demagnetization of the BN gabbros yielded very stable, single component directions (fig. A2). ChRM's are typically interpreted between 390 to 560°C or 35 to 70 mT (fig. A2). The mean (tilt corrected) ChRM direction is D $\pm$ ΔD_x = 213.8 $\pm$ 3.6°, I $\pm$

ΔI_x = 36.6 ± 5.0° (fig. 10J), which corresponds to a latitude of formation of 20.4° [17.1°, 23.9°], assuming that the magmatic foliation represents the paleohorizontal.

New Zealand.—Demagnetization behavior of specimens from the ten blocks of chert from the Waipapa Terrane varies strongly. From BI1, BI2, BI3 and BI5, some specimens yielded erratic results (mostly when demagnetized with alternating fields), but in others, a single component could be interpreted (Appendix figs. A3A–A3D and A3F). Thermal demagnetization of BI4 and TP yielded consistent single component behavior except for a northward-directed overprint in the lowest (20–100°C) temperature steps (figs. A3E and A3J), and BI4 samples did not (or only barely) demagnetize in alternating fields up to 100 mT. Samples from KB1 and TK also did not or only partly demagnetize in alternating fields (figs. A3G and A3I), and thermal demagnetization yielded two-component behavior. We interpreted the higher temperature component, together with the partial alternating field component as the ChRM. KB2, TU and WB showed very consistent, single component behavior (figs. A3H, A3K and A3L). From the total of ten blocks of chert, six blocks (TK, TU, TP, WB, KB1,2, BI4) yielded mean directions (not corrected for bedding tilt) similar to the Late Cretaceous remagnetization direction documented by van de Lagemaat and others (2018b) (fig. 11A). Overall, demagnetization behavior from these six blocks was consistent, and mostly only a single component could be interpreted. Four blocks (BI1, BI2, BI3 and BI5) yielded different results (fig. 11B), indicating the possibility of a primary magnetization. In BI3 only, variations in bedding were sufficient to allow for a statistically meaningful fold test, which is negative (best clustering between -17 and 17% unfolding, fig. A1H). The magnetizations of BI1, BI2 and BI5 cannot be confirmed as primary based on field tests, but the mean directions are statistically different from the GAD field (fig. 11B) and from the two recorded post-folding overprints, and satisfy the quality criteria of representing paleosecular variation (A95min < A95 < A95max, table 1). The mean ChRM directions (corrected for bedding tilt) from BI1, BI2 and BI5 are D ± ΔD_x = 19.2 ± 13.1°, I ± ΔI_x = 23.9 ± 22.4°, D ± ΔD_x = 165.3 ± 13.0°, I ± ΔI_x = −27.3 ± 21.1°, and D ± ΔD_x = 320.4 ± 9.7°, I ± ΔI_x = 14.0 ± 18.4° (fig. 11F, H, L), corresponding to paleolatitudes of 12.5° [0.8°, 27.6°], 14.5° [3.1°, 29.4°], and 7.1° [−2.2°, 17.6°], respectively. When corrected for bedding assuming overturned strata, ChRM directions cluster significantly less for all three sites.

Japan.—Demagnetization behavior of specimens from ON1 is highly variable; most samples contain single components trending towards the origin (for example ON1.7, Appendix fig. A4B), but some contain overlapping components (for example ON1.3, fig. A4A) that do not reach the origin. Dispersion of the interpreted directions is high (K=5.4) and especially inclinations vary substantially (between -70 and +70°, fig. 12A), hampering calculation of a meaningful mean direction of this site. Demagnetizations from ON2 are straightforward directions trending towards the origin (figs. A4C and A4D), but dispersion of the interpreted directions is essentially random (K = 1.9) and at least a third of the directions (interpreted in relatively low demagnetization steps, for example ON2.14) scatter around the GAD field (fig. 12B). ON3 and ON4 are demagnetized thermally only. ON3 yielded consistent, single components, in the range of ~450 to 640°C (figs. A4E and A4F). A fold test on these directions is negative (best clustering between −42 and 3% unfolding, figs. 12E, 12F, A1J). From ON4, two components are interpreted: a medium-temperature component (420-560°C) and a high-temperature-component (620–680°C, figs. A4G–A4J). The medium-temperature component from ON4 is very similar to that of ON3 (figs. 12C–12F), and although they do not share a common mean, we interpreted both these directions as a shared post-tilting magnetization. The high-temperature component (figs. 12G and 12H) may represent a primary magnetic signal, although no field tests

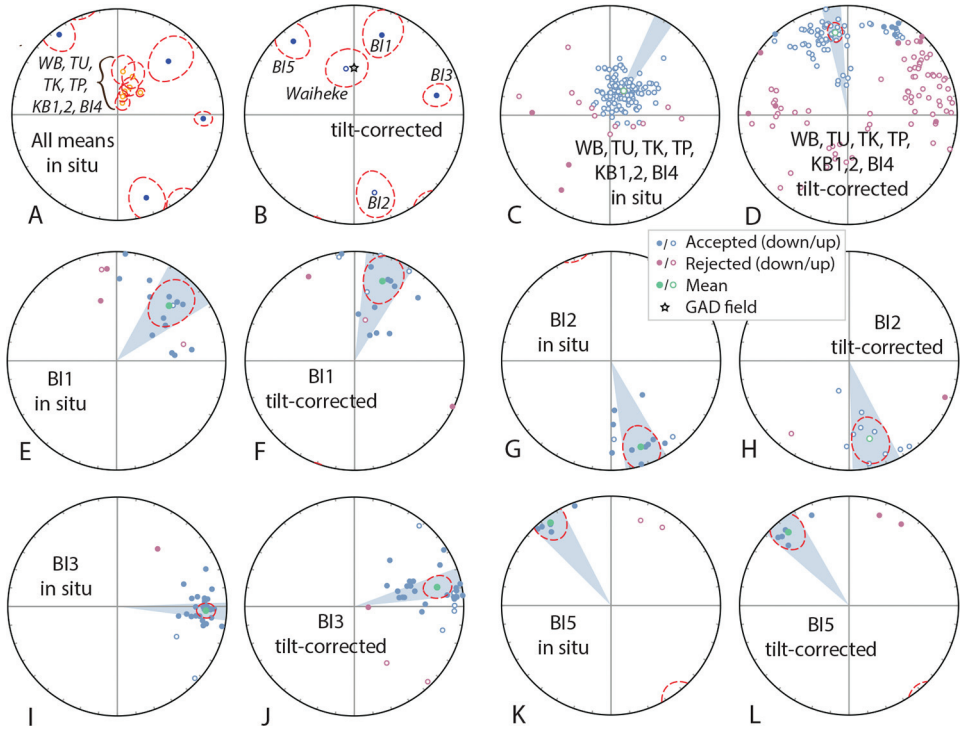

Fig. 11. Interpreted directions from sites in New Zealand, including results from Kodama and others (2007).

can be performed to confirm this, as no reversals were recorded and within-site variations in bedding orientation were not large enough to allow for a statistically meaningful fold test. Nonetheless, the ON4-ht component yields directions (not corrected for bedding tilt) significantly different from the GAD field (fig. 12B) and from the recorded post-folding magnetization. Furthermore, the magnetization is carried by hematite with very high (620–680°C) unblocking temperatures, and satisfies the quality criteria of representing paleosecular variation (A95min = 3.4° < A95 = 8° < A95max = 11.1°, table 1). For these reasons, we argue that a primary nature of this magnetization is likely. The mean direction (after tilt-correction) from ON4-ht is: Dec $\pm$ ΔD_x = 251.4 $\pm$ 8.0°, Inc $\pm$ ΔI_x = 7.2 $\pm$ 15.7° (fig. 12H), corresponding to a paleolatitude of 3.6° [-4.3°, 11.9°].

INTERPRETATION OF PALEOMAGNETIC RESULTS

Potential Inclination Error

Radiolarian chert is in principle suitable for obtaining depositional latitudes through paleomagnetic analysis because it preserves well-developed bedding planes necessary to restore the paleomagnetic vector to its original direction, can be dated with biostratigraphy, and generally contains sufficient magnetic carrier minerals. A possible problem of using chert, however, is that little is known about its compaction behavior. Compaction of sediments after deposition has been shown to significantly alter the inclination of primary magnetizations, which may lead to significant underestimation of paleolatitude (Collombat and others, 1993; Torsvik and Van der Voo, 2002; Kent and Tauxe, 2005; Krijgsman and Tauxe, 2006). Two general methods have

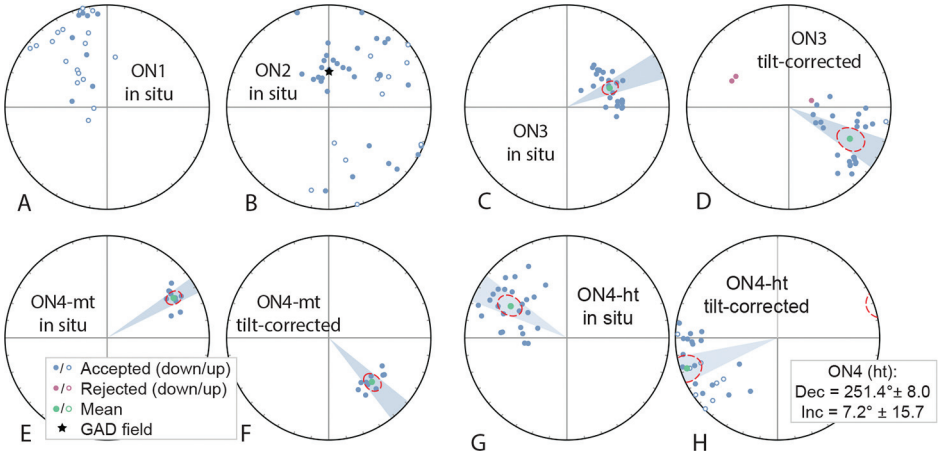

Fig. 12. Interpreted directions from sites in Hokkaido (Japan).

been developed to account for inclination shallowing, either using magnetic fabrics (Jackson and others, 1991; Kodama, 2009), or using the relationship between elongation of typical paleomagnetic direction scatters induced by paleosecular variation of the geomagnetic field, and inclination (Tauxe and Kent, 2004). Alternatively, a typical compaction factor may be inferred (for example 0.6 used by Torsvik and others, 2012), although compaction varies strongly between and even within sediment types (Vaes and others, 2021). It is unclear, however, what compaction factor may be appropriate for radiolarian chert, and our datasets are not large enough to attempt estimating compaction with the E/I method of Tauxe and Kent (2004).

Previous estimates on inclination shallowing in chert vary. Huang and others (2015) collected large paleomagnetic sample sets from two sections of Lower Cretaceous (~130–120 Ma) radiolarian chert and a section of time-equivalent sandstone, both deposited on the Indus-Yarlung ophiolites of southern Tibet. They demonstrated through detrital zircon analysis that these sandstones were derived from the Tibetan Plateau, which during the Early Cretaceous was located at a latitude of ~15°N (Ma and others, 2014; Yang and others, 2015; van Hinsbergen and others, 2019). Inclinations of the sandstones and cherts were similar, and correcting for inclination shallowing in the sandstone samples by both the E/I and the magnetic fabric method yielded a corrected paleolatitude estimate of ~16°N, consistent with the latitude of the Tibetan Plateau (Huang and others, 2015). Correcting the inclinations of the chert data to match the sandstone paleolatitude would require a compaction factor for the cherts of ~0.7 to 0.8. Iijima and others (1989) estimated much higher compaction in Triassic chert from central Honshu (Japan): 60 to 80% (which corresponds to a compaction factor of 0.2–0.4), based on the bending of sedimentary laminae around a fragment of silicified wood. Oda and Suzuki (2000) on the other hand, applied the relationship between ARM anisotropy and inclination shallowing of Jackson and others (1991) to IRM anisotropy and concluded that this correction method changed their obtained inclinations by a maximum of 2° only (corresponding to flattening factors of 0.9–1.0, fig. 3). Radiolaria are commonly preserved unflattened, suggesting that compaction in chert is generally rather minor (Ando and others, 2001), or, that compaction strain is fully accommodated in the matrix hosting the radiolaria.

Due to the lack of control on the amount of compaction in chert and the absence of data to apply a correction method, we use uncorrected values of inclination, which correspond to minimum estimates of depositional paleolatitude. As a result of the

non-linear relationship between inclination and latitude, the effect of compaction on inclination is largest around ~50°N/S and considerably smaller around the poles and the equator (Tauxe and Kent, 2004). The highest latitudes from cherts used in this study were obtained from New Zealand (33°, for Triassic cherts sampled by Kodama and others (2007), and using the compaction factor of 0.7 as estimated by Huang and others (2015), not taking inclination shallowing into account would underestimate the paleolatitude by 10° (table 2). All other paleolatitudes, being closer to the equator, would be underestimated by smaller amounts.

Hemispheric Origin

Because major rotation of rock units in accretionary complexes is probable, it is difficult to determine the magnetic polarity and hemispheric origin. Based on a correlation with the global magnetostratigraphic timescale, Kirschvink and others (2015) and Ando and others (2001) argued for a southern hemispheric origin of the Permian Kamura limestone and Anisian chert of the Inuyama region of Japan. For all other obtained paleolatitudes from OPS materials, however, hemispheric origin is unknown. In our reconstruction, we generally assume minimum plate motions, implying that we assume a northern hemisphere origin for the post-Anisian rocks accreted in Japan (fig. 7) and a southern hemisphere origin for the rocks accreted in New Zealand. For a discussion of hemispheric origin of the rocks accreted in Costa Rica and Mexico, see below.

Summary of Paleomagnetic Constraints on Farallon, Phoenix, and Izanagi Plate Motion

Our compilation of previously published and newly collected paleomagnetic data from OPS derived from the Farallon, Phoenix, and Izanagi plates provides direct control on latitudinal motion components of these plates between the time of formation of the OPS and subsequent accretion in the circum-Panthalassa trenches. The paleolatitudinal path of the Farallon Plate is constrained by the Late Triassic paleolatitude of CC1/CC2 combined (2.6°N/S [−7.9°, 5.2°]) from Cedros Island, which accreted at 105 Ma at 32° N. Furthermore, the 190 to 180 Ma SR cherts (paleolatitude of 8.0°N/S [−18.3°, 1.1°]), the 124 Ma BN gabbros (paleolatitude of 20.4°N/S [17.1°, 23.9°]), and the 110 Ma SR2 cherts (paleolatitude of 13.0°N/S [−9.0°, 17.5°]) from the Santa Elena Peninsula of Costa Rica accreted at 100 Ma at 11° N. Phoenix plate motion is constrained by the paleolatitudes of the upper Permian BI cherts (11.4°S [−0.6°, −24.9°]) and the Lower Triassic Waiheke Island cherts (33.6°S [−51.2°, −20°]), which accreted at the Eastern Province trench of New Zealand at 150 Ma at ~80°S. Lastly, Izanagi plate motion is constrained by the paleolatitude of the upper Permian Kamura limestone (12.2°S [−14°, −10.4°]), data from the Inuyama cherts, here summarized as having a 240 Ma paleolatitude of 5°S and a 215 Ma paleolatitude of 20°N (fig. 7, table 2), and the paleolatitude of the Berriasian ON cherts (3.6°N/S [−4.3°, 11.9°]). The Inuyama cherts accreted at the inner zone subduction system of Japan at 170 Ma at 52°N, and the Kamura limestones and ON cherts accreted at 160 Ma and 100 Ma at the outer zone subduction system of Japan at 34°N and 54°N respectively. The SR cherts, the Kamura limestones, and the ON cherts were all formed in an intra-plate setting (the SR cherts and the Kamura limestones at a seamount, the Berriasian ON cherts at a then extinct island arc), indicating deposition at an unknown distance away from the spreading ridge at which the underlying basement formed. From all the other compiled and new datasets of OPS sequences, the origin of the underlying magmatic basement in unknown.

RECONSTRUCTION: RELATIVE PLATE MOTION, MANTLE REFERENCE FRAMES, AND PALEOMAGNETIC DATA

0 to 150 Ma

For 0 to 83 Ma, we use the reconstruction of the Pacific Plate and its conjugates, linked to the Indo-Atlantic plate system through marine spreading records of the

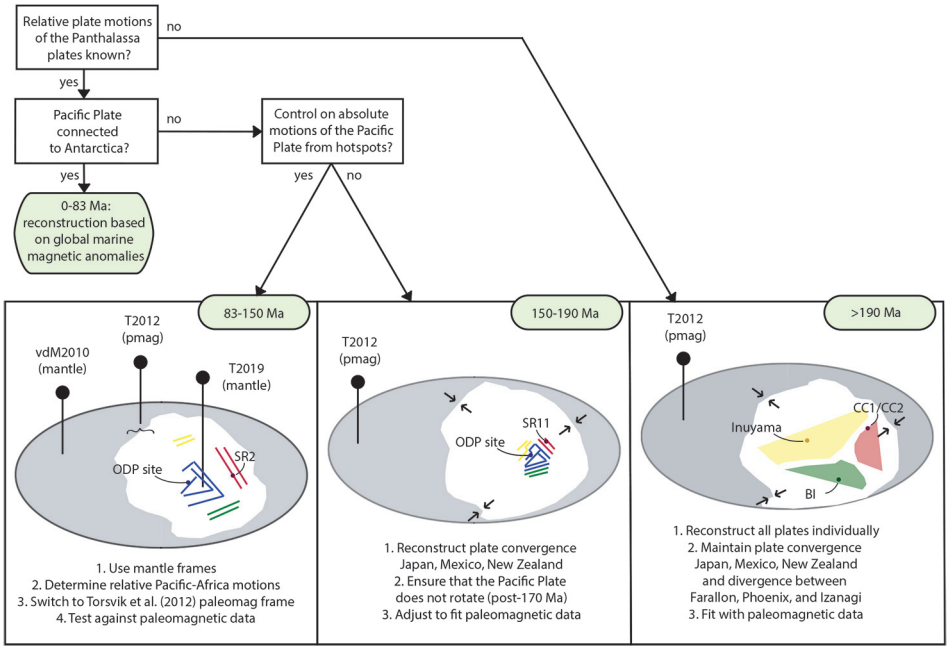

Fig. 13. Flowchart illustrating the adopted reconstruction approach to reconstruct the plates of the Panthalassa Ocean and link the tectonic history of those plates to the global plate circuit.

Antarctic-Pacific ridge, from Wright and others (2016). Prior to 83 Ma, when no ridge was present connecting the Panthalassa and Indo-Atlantic plate systems, relative plate motions of the two systems cannot be constrained from marine geophysical data and we determine relative motions between these systems by placing both in independent mantle reference frames, following Boschman and others (2019, fig. 13). We use the Pacific hotspot frame of Torsvik and others (2019) for the Panthalassa plate system, and the slab-fitted frame of van der Meer and others (2010) for the Indo-Atlantic plate system. We subsequently place the global plate circuit in the paleomagnetic reference frame of Torsvik and others (2012). We test the resulting 83 to 150 Ma reconstruction with post-150 Ma paleomagnetic data of the Pacific Plate (Riisager and others, 2003; Fu and Kent, 2018), from OPS from Costa Rica (SR2 and BN) and from Japan (ON4). To do so, we take the following steps: we first reconstruct Farallon, Phoenix, and Izanagi plate motion by mirroring marine magnetic anomalies preserved on the Pacific Plate, assuming symmetric spreading parallel to transform faults. Second, we add marking points representing the SR2, BN and ON4 rocks that are located at the Santa Elena and Hokkaido trenches at the age of their accretion (100 Ma), and attach these to the Farallon and Izanagi plates before these times (following the cross-over reconstruction approach of (van Hinsbergen and Schmid, 2012). The 83 to 150 Ma reconstruction (140 Ma shown in fig. 14A) is fully consistent with the paleolatitudinal estimates from SR2 (110 Ma), ON4 (145 Ma) and the youngest two estimates from ODP Site 801B (135 and 142 Ma), and within 5° from the 149.4 Ma estimate from ODP site 801B, and BN (124 Ma) (table 2). The connection of the two plate circuits through mantle reference frames thus successfully predicts paleolatitudes of the Panthalassa plates, and establishes an accurate global plate circuit back to 150 Ma. Furthermore, the Farallon, Phoenix and Izanagi plates are now reconstructed from

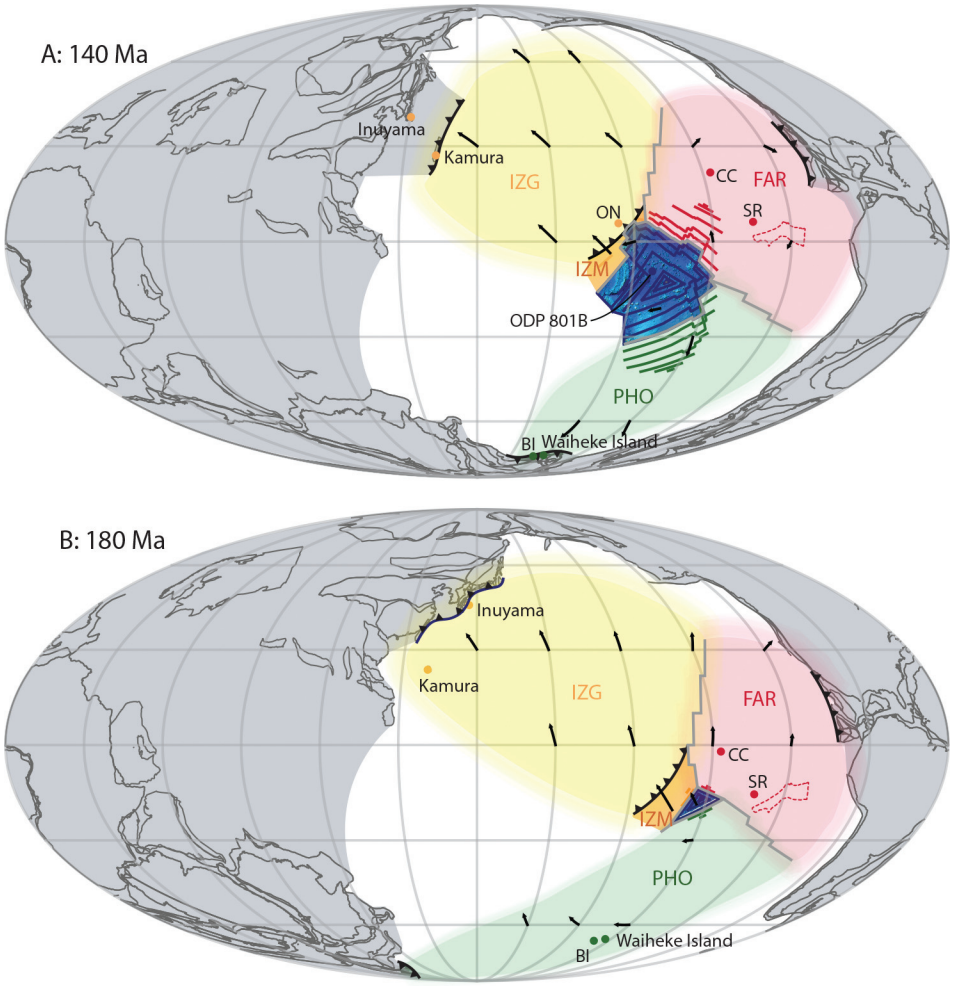

Fig. 14. Reconstruction of the Izanagi (IZG), Izanami (IZM), Farallon (FAR) and Phoenix (PHO) plates of the Panthalassa Ocean (Reconstruction poles in Supplementary data 3, http://earth.geology.yale.edu/%7eajs/SupplementaryData/2021/Boschman) at (A) 140 Ma, (B) 180 Ma, (C) 220 Ma, and (D) 260 Ma. Outline of the lithospheric basement of the future Caribbean Plate (red dashed line in Farallon Plate) for reference. Reconstruction of North/South America and Africa from Torsvik and others (2012); Europe/Asia from Müller and others (2016) and Domeier and Torsvik (2014).

their spreading ridge (relative to the Pacific Plate) to the subduction zones in which they subducted during the Cretaceous (relative to the circum-Panthalassa trenches).

150 to 190 Ma

The geological records of Mexico, New Zealand, and Japan contain evidence of subduction since at least 220 Ma, 375 Ma, and 500 Ma, respectively (Maruyama and Seno, 1986; Isozaki, 1996; Mortimer, 2004; Boschman and others, 2018b). These geological records (arc volcanic rocks, accretionary complexes, forearc sequences, *et cetera*) are far from continuous, and temporal interruptions in subduction or episodes of trench migration can thus not be excluded. Nonetheless, overall, they testify to hundreds of millions of years of overall plate convergence between the Panthalassa and Indo-Atlantic plate systems. Furthermore, the continuous Cocos slab, connected

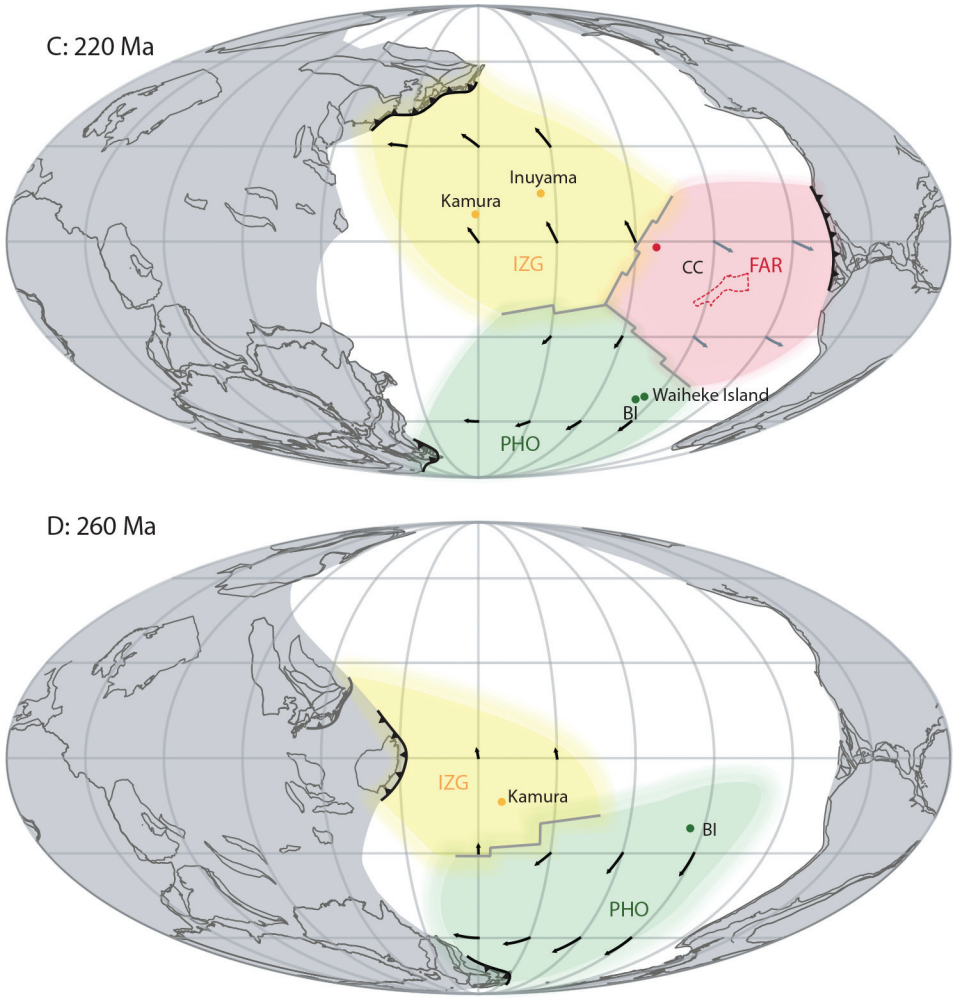

Fig. 14. Continued

to the actively subducting Cocos Plate and reaching into the lowermost mantle below the Atlantic indicates that subduction below the Mexican margin was uninterrupted since probably 220 Ma (Boschman and others, 2018b). We therefore determine 150 to 190 Ma plate motions of the Panthalassa plate system based on the inferred convergence between Izanagi and Japan, Farallon and Mexico, and Phoenix and New Zealand, and on paleomagnetic data from the Pacific Plate and SR (Costa Rica). Furthermore, for the northwestern Panthalassa domain, we incorporate subduction in the near-equatorial intra-oceanic Oku-Niikappu trench (figs. 14A and 14B) as reconstructed in Boschman (ms, 2019) and Boschman and others (2021). The rate of subduction at this trench, where the Izanami Plate subducts below the Izanagi Plate, is slightly larger than the half-spreading rate of the Izanami-Pacific ridge, which means that the Izanami Plate decreases in size, resulting in ridge subduction in Berriasian time (fig. 14A). The age of initiation of intra-oceanic subduction at the Oku-Niikappu trench is unknown; in our reconstruction, subduction starts at 185 Ma.

We add a marking point for the 190 Ma SR cherts on the Farallon Plate. We reconstruct the Panthalassa plate system back to 190 Ma (by moving the Pacific Plate, which is the base of the Panthalassa plate system) such that (1) preceding (130–150 Ma) convergence directions between Farallon and Mexico/Costa Rica and Izanagi and Japan are maintained as much as possible, and (2) there is no significant vertical axis rotation of the Pacific Plate, as concluded by Fu and Kent (2018). Next, we adjust the reconstruction to place the marking points of the ODP site 801B and SR within the uncertainty limit of the obtained paleolatitudes. For SR, there are two hemispheric options. Placing SR at the northern hemisphere would place the ODP site 801B (from which southern hemispheric latitudes are obtained) at the northern hemisphere as well, and furthermore, would predict southeastward motion of the Farallon Plate relative to North America (sub-parallel to the continental margin). To comply with convergence and a southern hemispheric origin for the OPD site 801B sedimentary rocks, we thus place SR at the southern hemisphere (fig. 14B), yielding a reconstruction without major relative plate motion changes. The resulting 190 to 150 Ma reconstruction upholds the relative plate motions of the Panthalassa plate system from marine magnetic anomaly data and fits all paleomagnetic data within a few (<4) degrees (table 2).

This new reconstruction (fig. 14B) does not agree with the 190 Ma possible positions of the (birthplace of the) Pacific Plate suggested by Boschman and van Hinsbergen (2016). Boschman and van Hinsbergen (2016) illustrated that the birth of the Pacific Plate may be explained by cessation of an intra-oceanic subduction system between the Farallon and Izanagi plates, and suggested that the location of the early Pacific Plate may be inferred from fitting the ~190 Ma Izanagi-Farallon-Phoenix triple junction on a lower mantle slab remnant of this subduction. Fitting the 190 Ma Izanagi-Farallon-Phoenix triple junction on the Trans-Americas slab (which is the preferred scenario in Boschman and van Hinsbergen (2016)) yields divergence between Farallon and North America between 190 to 150 Ma and is thus not likely. Similarly, fitting the triple junction on a Telkhinia slab (van der Meer and others, 2012) yields phases of divergence between the Izanagi Plate and Japan. Assuming continuous subduction around the Pacific, the 190 Ma absolute location of the Izanagi-Farallon-Phoenix triple junction was most likely located somewhere between the Trans-Americas and the Telkhinia slab. This region is associated with very low resolution in mantle tomography (fig. 4 in Boschman and van Hinsbergen, 2016) and slabs may exist within this domain, but cannot be used for a slab-fitting approach.

190 to 260 Ma

Reconstructing pre-190 Ma motions of the Izanagi, Farallon and Phoenix plates, or any older ocean, requires a different approach, as there is no control on relative plate motions from marine geophysical data. As a consequence, a 'plate system' is no longer available, but needs to be inferred from motions of individually reconstructed plates (fig. 13). Boschman and van Hinsbergen (2016) discussed how the birth of the Pacific Plate followed upon reorganization at an unstable triple junction that was generated upon cessation of a subduction zone between the Farallon and Izanagi plates. Even though no data are available that recorded the events leading up to the 190 Ma birth of the Pacific, simple rules of plate kinematics (Cox and Hart, 1986) allow us to hypothesize the situation that preceded the plate reorganization. The orientation of the pre-190 Ma Farallon-Izanagi subduction segment (fig. 15C) is not straightforwardly explained in a Farallon-Izanagi spreading context, but instead, is equal to the orientation of Izanagi-Phoenix transforms. We therefore suggest that initiation of the subduction that culminated in the birth of the Pacific plate may have followed upon capture of a fragment of Phoenix lithosphere by the Farallon Plate (fig. 15B). Plate capture may have been preceded by reorganization of the original Izanagi-Farallon-Phoenix

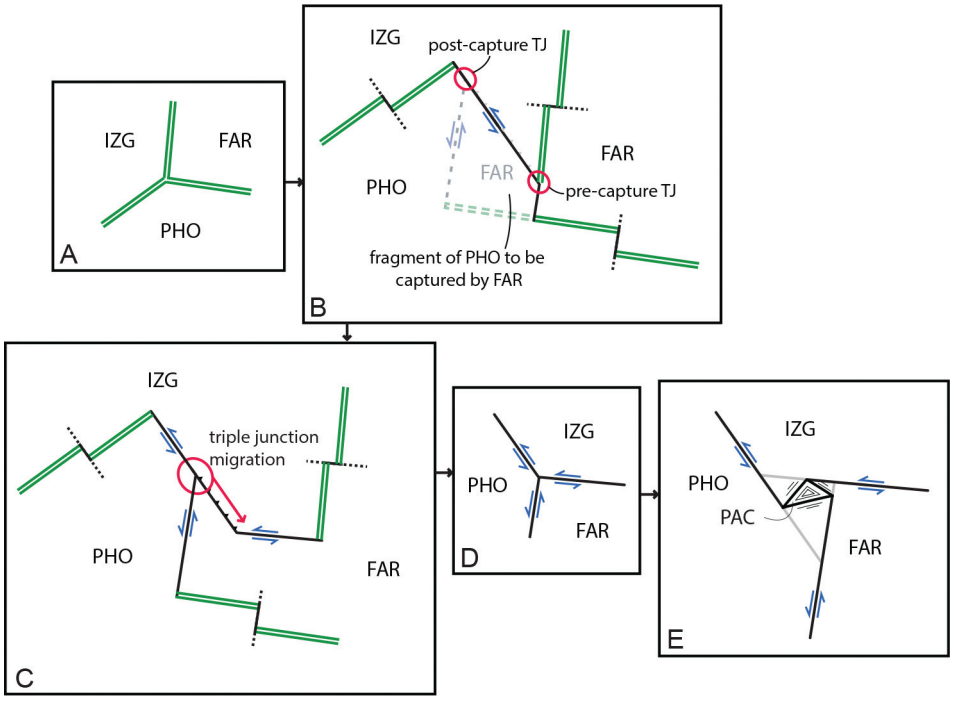

Fig. 15. Schematic representation of ~190 Ma tectonic events that may have led to the birth of the Pacific Plate. (A) Pre-plate reorganization, long-lived Izanagi–Farallon–Phoenix triple junction. (B) Capture of a fragment of Phoenix lithosphere by the Farallon Plate, resulting in a triple junction jump. (C) Migration of the newly formed trench-transform-transform triple junction migration until arrival at the kink in the Farallon-Izanagi plate boundary. (D) 190 Ma: formation of an instable transform-transform-transform triple junction. E) Birth of the Pacific Plate.

ridge-ridge-ridge triple junction into a ridge-transform-transform or ridge-ridge-transform triple junction, which has been documented for RRR triple junctions (Kleinrock and Morgan, 1988, Viso and others, 2005). The duration of subduction depends on the length of the transform segment along which the triple junction migrated from the moment of plate capture until formation of the unstable transform-transform-transform triple junction (fig. 15D) and may have been in the order of only a few to ten million years. Before that time, we assume that the Izanagi, Farallon and Phoenix plates were joined in a long-lived stable RRR triple junction (fig. 15A).

To reconstruct pre-190 Ma plate motions, we add additional marking points: the Permian BI1/BI2/BI5 and Lower Triassic Waiheke Island cherts from New Zealand, the 215 Ma and 240 Ma Inuyama cherts, the upper Permian Kamura limestone from Japan, and the CC1/CC2 cherts from Cedros Island, Mexico. Next, we reconstruct Farallon, Izanagi and Phoenix plate motion, whereby we accommodate (1) the paleomagnetic data; (2) minimal relative plate motion changes; (3) continuous convergence between Izanagi and Japan, Farallon and Mexico, and Phoenix and New Zealand; and (4) continuous divergence between Izanagi, Farallon and Phoenix. Through these latter two restrictions on plate motions, the hemispheric origin of the paleomagnetic sites for which this was unknown is determined: both the CC1/CC2 cherts from Cedros island and the BI and Waiheke Island cherts from New Zealand are derived from the southern hemisphere (figs. 14C and 14D). Restricted by the age of the oldest rocks from which paleolatitudes are obtained, the Farallon Plate is reconstructed back to 220 M and the Izanagi and Phoenix plates to 260 Ma (figs. 14C and 14D).

DISCUSSION: FUTURE IMPROVEMENTS IN RECONSTRUCTING LOST OCEANIC PLATES

In multiple field campaigns of sampling geological records of ancient subduction processes in accretionary orogens around the Pacific, we collected a total of 674 hand samples from OPS. From those, 106 (16%) yielded paleomagnetic directions that we interpreted as (potentially) primary. Despite being high risk, this project illustrates that reconstructing lost oceanic plates from paleomagnetic data of OPS rocks is possible, and that attempting to do so is worthwhile. Even though the pre-190 Ma reconstruction of the Panthalassa Ocean developed in this study is still associated with considerable uncertainties from paleomagnetic data, plate geometries, plate rotations and longitudinal plate motion rates, it does comply with all currently available geological, paleomagnetic, and marine geophysical data of the Pacific and Mexico, Costa Rica, New Zealand and Japan. This study illustrates that even with limited data, it is possible to integrate geological records from accretionary orogens with paleomagnetic datasets from OPS, and quantitatively reconstruct the kinematic evolution of plates that are (almost) entirely lost to subduction.

In the reconstruction presented in this study, the reconstructed sampling sites are at all times within 5° of the paleomagnetically determined paleolatitudes. Compilations of paleomagnetic data from the Indo-Atlantic plate system, however, illustrate that individual paleomagnetic poles scatter considerably around Apparent Polar Wander Paths (Torsvik and others, 2008, 2012). Tectonic reconstructions of large plates from paleomagnetic data thus improve when larger datasets including multiple poles per time period are used. Currently, available paleomagnetic data from OPS from circum-Pacific accretionary orogens is still limited, and as a result, the reconstruction displayed in figure 15 is preliminary and may change with growing datasets.

In this study, we have deliberately not included reconstructions of the continental margins in the northern Panthalassa realm (the Russian northeast and Alaskan-Canadian Cordillera) and of Southeast Asia. These orogens contain remnants of multiple volcanic arcs that formed at synchronous Mesozoic subduction systems, and reconstructions either do not exist or are controversial, which means that correlating OPS exposed in these orogens to oceanic plates is not straightforward. As a result, the presented here Panthalassa reconstruction is incomplete, and further development requires progress in the development of kinematic reconstructions of the remaining segments of Mesozoic circum-Panthalassa trenches, and the incorporation of newly collected or already published paleomagnetic data from OPS rocks accreted in these segments [for example, Cretaceous limestones from the Franciscan complex (Tarduno and others, 1986)]. Nonetheless, our partial reconstruction does already shed some light on the tectonic history of the northern and western Panthalassa Ocean. The OPS that are currently exposed in Japan, New Zealand and Central America were all formed in the central Panthalassa Ocean, at low latitudes. This implies that, except for the Oku-Niikappu subduction zone, there were no plate boundaries between the central Panthalassa Ocean and the continental margins of these three regions. From this observation, we can conclude that intra-oceanic arcs accreted to the northern and western continental margins cannot have traveled extensively throughout the Panthalassa Ocean and were most likely fringing arc systems; their pre-accretion motion was restricted to the northern and western Panthalassa Ocean, respectively. Following progress in the reconstruction of the here-excluded regions, plate rotations (or a lack thereof) of the Izanagi, Farallon and Phoenix plates can be determined when paleomagnetic data are available from age-equivalent OPS rocks derived from accretionary complexes far apart (for example for Farallon, from Mexico and from accretionary complexes of the Canadian Cordillera). Additionally, geochemical analyses on magmatic basement sections may provide information on the nature of the oceanic basement of the OPS (MORB, IAT, OIB). In cases of MORB

basement, ridge segments can be reconstructed, thereby gradually generating a picture of the geometry of the Panthalassa plates.

Continuing the reconstruction further back into the Paleozoic requires data collection from accretionary orogens that formed during older subduction of the Panthalassa plates, such as the New England orogen of eastern Australia (Cawood and others, 2011), the Beishan orogen in China (Xiao and others, 2010b), or the orogen in central Mongolia that formed at the expense of the Mongol-Okhotsk Ocean (Tomurtogoo and others, 2005). Similar approaches may be feasible for other lost Paleozoic oceans such as the Rheic Ocean that closed during construction of much of Europe (Nance and others, 2010; Domeier, 2016; Franke and others, 2017), the Iapetus Ocean that closed during the Caledonian orogeny (Torsvik and others, 1996; Domeier, 2016), the oceans that formed the Central Asian Orogenic Belt (Windley and others, 2007, Xiao and others, 2010a; Domeier, 2018), or even Neoproterozoic to Cambrian ocean floor of which OPS remnants are found in the Bohemian Massif (Ackerman and others, 2019).

CONCLUSIONS

We presented a quantitative kinematic reconstruction of subducted plates of the Panthalassa Ocean, based on (1) relative plate motions derived from marine magnetic anomaly and fracture zone data; (2) absolute plate motions from hotspot tracks; and (3) paleomagnetic data from OPS accreted in the circum-Pacific accretionary orogens and the Pacific Plate. We showed that determining relative plate motions between the Panthalassa and Indo-Atlantic plate system through the use of two independent mantle reference frames is in line with paleomagnetic data. Furthermore, in the absence of absolute plate motion control, we reconstructed plate motions of the Izanagi, Farallon and Phoenix plates such that divergence between the three major oceanic plates is maintained, convergence with the continental margins of Japan, Mexico and New Zealand is maintained, and paleomagnetic constraints are met. The reconstruction approach developed in this study illustrates that in the absence of marine magnetic anomaly data and mantle reference frames, deep-time plate circuits of supercontinents and superoceans may be reconstructed using OPS sequences, paleomagnetism, and constraints on the nature of circum-oceanic plate boundaries.

ACKNOWLEDGMENTS

This work was funded by Netherlands Organization for Scientific Research (NWO) grant 824.01.004; D.J.J.vH acknowledges NWO Vidi grant 864.11.004. We thank Stephen Johnston and Camilo Montes for constructive reviews. Logistics for the fieldwork in Costa Rica were supported by the Universidad de Costa Rica with project 830-B0-242 and ED-2700 to Percy Denyer. We thank M. M. Chavarria and R. Blanco of the Área de Conservación Guanacaste for their valuable support during fieldwork in the Santa Rosa National Park, and M. Salazar Alvarado and I. Boschini López of the Dirección de Geología y Minas for their support in exporting the samples. Supplementary materials S2 contains paleomagnetic data files that can be viewed in paleomagnetism.org and http://earth.geology.yale.edu/%7eajs/SupplementaryData/2021/Boschman

APPENDIX

Supplementary materials S2 (http://earth.geology.yale.edu/%7eajs/SupplementaryData/2021/Boschman).

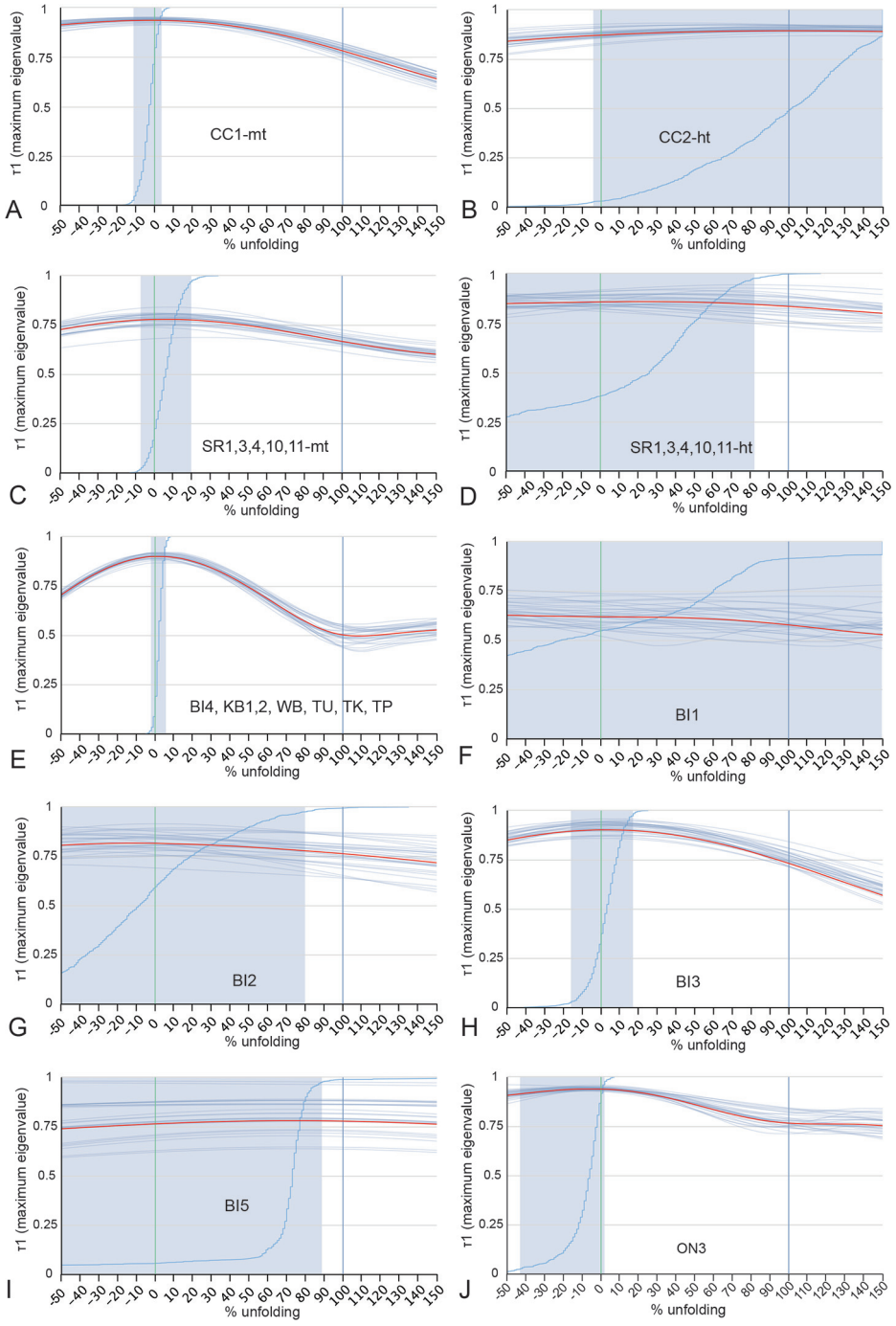

Fig. A1. Orthogonal vector diagrams of representative samples of localities SR and BN (Costa Rica) in geographic coordinates (not corrected for bedding tilt), closed (open) symbol for declination (inclination), up/west projection.

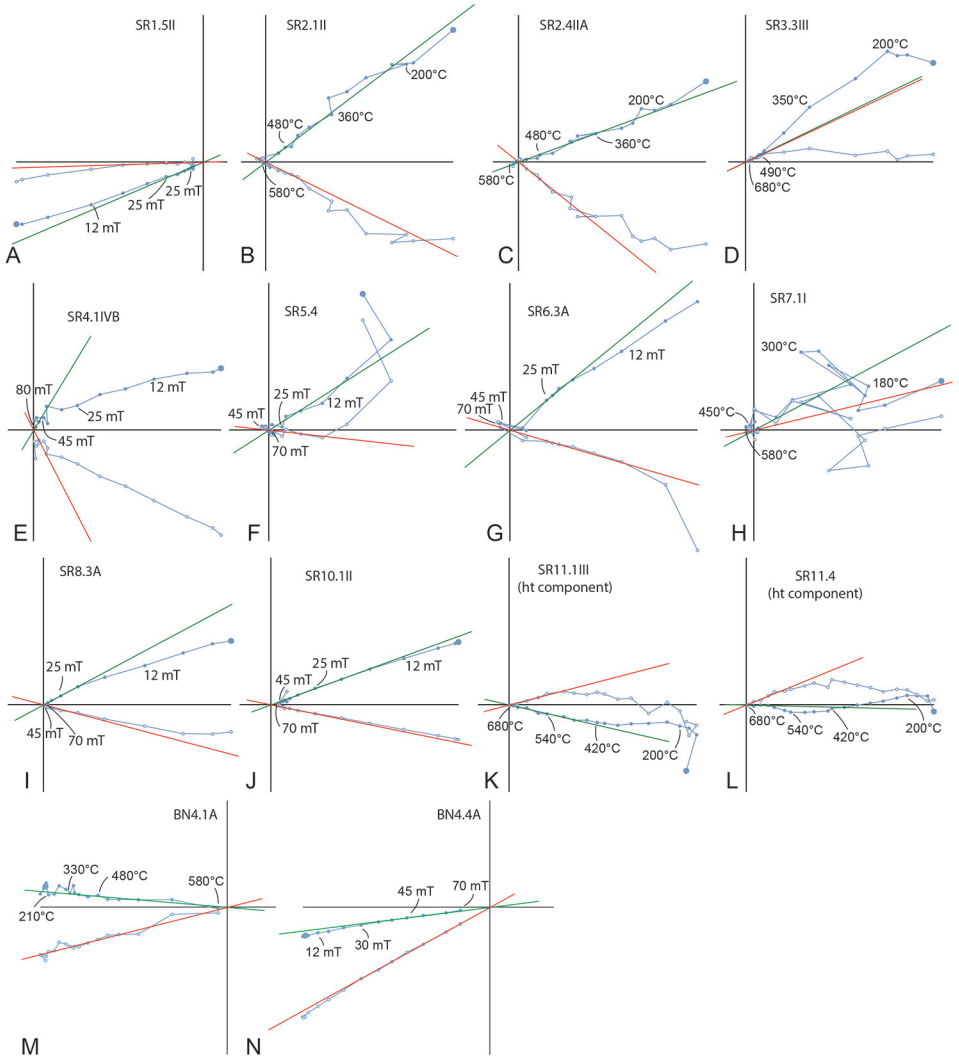

Fig. A2. Orthogonal vector diagrams of representative samples from New Zealand in geographic coordinates (not corrected for bedding tilt), closed (open) symbol for declination (inclination), up/west projection.

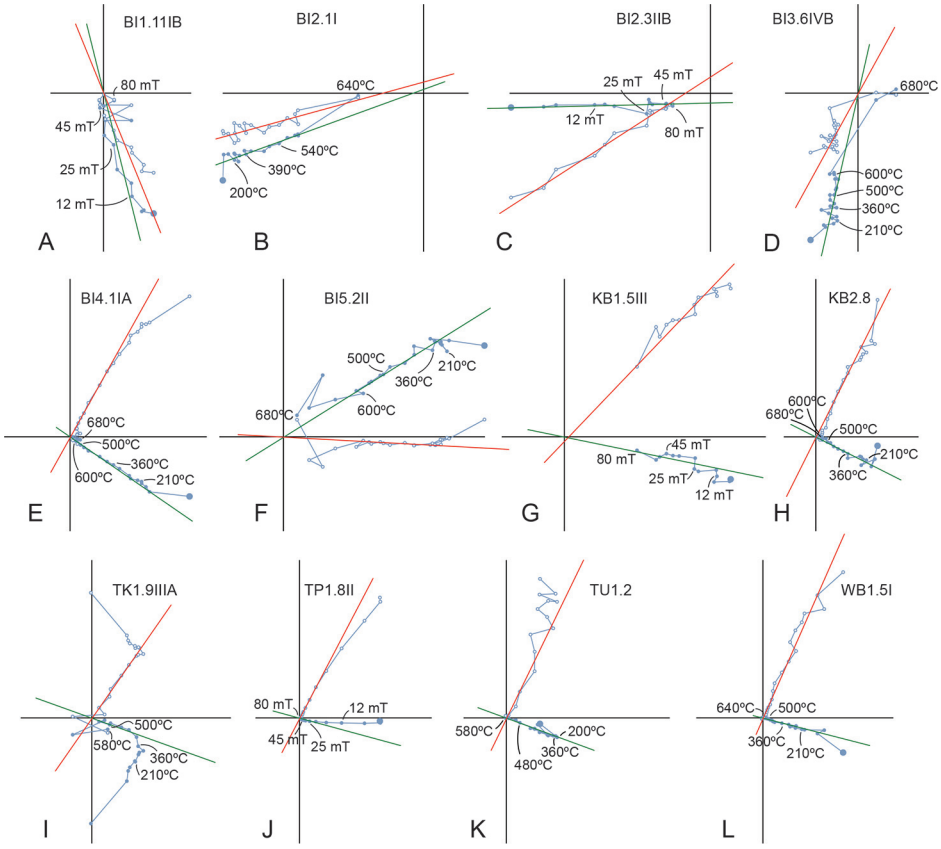

Fig. A3. Orthogonal vector and equal area diagrams of representative samples from Japan in geographic coordinates (not corrected for bedding tilt), closed (open) symbol for declination (inclination), up/west projection.

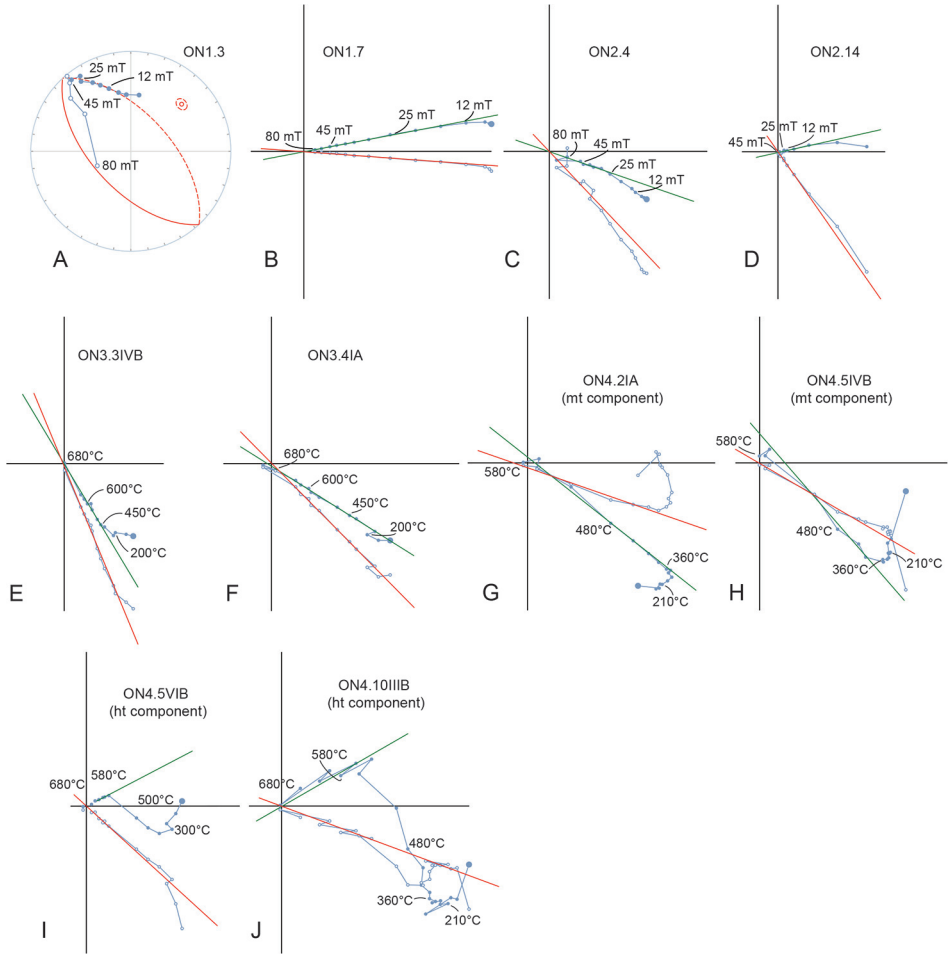

Fig. A4. Bootstrapped fold tests on directions from sites from Cedros Island (CC1, CC2), Costa Rica (SR1,3,4,10,11-mt and SR1,3,4,10,11-ht), New Zealand (BI4, KB1,2, WB, TU, TK, TP, BI1, BI2, BI3, and BI5), and Japan (ON3). Cumulative distribution function (with confidence interval in light blue) based on 1000 bootstraps (average of bootstraps in red).

TABLE A1

List of radiolarians from CC2

Capnococe anaptes (De Wever)
Capnodoce crystallina (Pessagno)
Capnodoce crystallina (Pessagno)
Capnodoce cf. *fragilis* (Blome)
Capnodoce spp.
Justium spp.
Betraccium? sp.
Triactoma spp.
Sarla? spp.
Capnuchosphaera cf. *theloides* (De Wever)
Capnuchosphaera spp.
Paronaella sp.
Ferresium? sp.
Xipha cf. *pessagnoi* (Nakaseko and Nishimura)
Canoptum spp.
Pachus sp.
Corum? spp.
Latium ? sp.

REFERENCES

Ackerman, L., Hajná, J., Žák, J., Erban, V., Sláma, J., Polák, L., Kachlík, V., Strnad, L., and Trubač, J., 2019, Architecture and composition of ocean floor subducted beneath northern Gondwana during Neoproterozoic to Cambrian: A palinspastic reconstruction based on Ocean Plate Stratigraphy (OPS): Gondwana Research, v. 76, p. 77–97, https://doi.org/10.1016/j.gr.2019.07.001

Adams, C. J., Campbell, H. J., and Griffin, W. L., 2007, Provenance comparisons of Permian to Jurassic tectonostratigraphic terranes in New Zealand: Perspectives from detrital zircon age patterns: Geological Magazine, v. 144, n. 4, https://doi.org/10.1017/S0016756807003469

Adams, C. J., Mortimer, N., Campbell, H. J., and Griffin, W. L., 2009, Age and isotopic characterisation of metasedimentary rocks from the Torlesse Supergroup and Waipapa Group in the central North Island, New Zealand: New Zealand Journal of Geology and Geophysics, v. 52, n. 2, p. 149–170, https://doi.org/10.1080/00288300909509883

Adams, C. J., Mortimer, N., Campbell, H. J., and Griffin, W. L., 2012, Detrital zircon geochronology and sandstone provenance of basement Waipapa Terrane (Triassic–Cretaceous) and Cretaceous cover rocks (Northland Allochthon and Houhora Complex) in northern North Island, New Zealand: Geological Magazine, v. 150, p. 89–109, https://doi.org/10.1017/S0016756812000258

Advokaat, E. L., Marshall, N. T., Li, S., Spakman, W., Krijgsman, W., and van Hinsbergen, D. J. J., 2018, Cenozoic rotation history of Borneo and Sundaland, SE Asia revealed by paleomagnetism, seismic tomography, and kinematic reconstruction: Tectonics, v. 37, n. 8, p. 2486–2512, https://doi.org/10.1029/2018TC005010

Alvarez, W., Kent, D. V., Premoli Silva, I., Schweickert, R. A., and Larson, R. A., 1980, Franciscan Complex limestone deposited at 17 south paleolatitude: GSA Bulletin, v. 91, n. 8, p. 476–484, https://doi.org/10.1130/0016-7606(1980)91<476:FCLDAS>2.0.CO;2

Ando, A., Kodama, K., and Kojima, S., 2001, Low-latitude and Southern Hemisphere origin of Anisian (Triassic) bedded chert in the Inuyama area, Mino terrane, central Japan: Journal of Geophysical Research: Solid Earth, v. 106, n. B6, p. 1973–1986, https://doi.org/10.1029/2000JB900305

Bandini, A. N., Baumgartner, P. O., Flores, K., Dumitrica, P., and Jackett, S. J., 2011, Early Jurassic to Early Late Cretaceous Radiolarians from the Santa Rosa Accretionary Complex (Northwestern Costa Rica): Ofioliti, v. 36, n. 1, p. 1–35, https://doi.org/10.4454/ofioliti.v36i1.392

Baumgartner, P. O., and Denyer, P., 2006, Evidence for middle Cretaceous accretion at Santa Elena Peninsul a (Santa Rosa Accretionary Complex), Costa Rica: Geologica Acta, v. 4, n. 1–2, p. 179–191.

Baumgartner, P. O., Flores, K., Bandini, A. N., Girault, F., and Cruz, D., 2008, Upper Triassic to Cretaceous radiolaria from Nicaragua and Northern Costa Rica – The Mesquito Composite Oceanic Terrane: Ofioliti, v. 33, n. 1, p. 1–19, https://doi.org/10.4454/ofioliti.v33i1.356

Bijwaard, H., Spakman, W., and Engdahl, E. R., 1998, Closing the gap between regional and global travel time tomography: Journal of Geophysical Research: Solid Earth, v. 103, n. B12, p. 30055–30078, https://doi.org/10.1029/98JB02467

Blome, C. D., 1984, Upper Triassic Radiolaria and radiolarian zonation from western North America: Bulletin of American Paleontology, v. 85, p. 1–88.

Boschman, L., ms, 2019, Reconstructing lost plates of the Panthalassa Ocean: Utrecht, The Netherlands, Ph. D. thesis, 311 p.

Boschman, L. M., and van Hinsbergen, D. J. J., 2016, On the enigmatic birth of the Pacific Plate within the Panthalassa Ocean: Science Advances, v. 2, n. 7, e1600022, https://doi.org/10.1126/sciadv.1600022

Boschman, L. M., van Hinsbergen, D. J. J., Torsvik, T. H., Spakman, W., and Pindell, J. L., 2014, Kinematic reconstruction of the Caribbean region since the Early Jurassic: Earth-Science Reviews, v. 138, p. 102–136, https://doi.org/10.1016/j.earscirev.2014.08.007

Boschman, L. M., Garza, R. S. M., Langereis, C. G., and van Hinsbergen, D. J. J., 2018a, Paleomagnetic constraints on the kinematic relationship between the Guerrero terrane (Mexico) and North America since Early Cretaceous time: GSA Bulletin, v. 130, n. 7–8, p. 1131–1142, https://doi.org/10.1130/B31916.1

Boschman, L. M., van Hinsbergen, D. J. J., Kimbrough, D. L., Langereis, C. G., and Spakman, W., 2018b, The dynamic history of 220 million years of subduction below Mexico: A correlation between slab geometry and overriding plate deformation based on geology, paleomagnetism, and seismic tomography: Geochemistry, Geophysics, Geosystems, v. 19, n. 12, p. 4649–4672, https://doi.org/10.1029/2018GC007739

Boschman, L. M., van der Wiel, E., Flores, K. E., Langereis, C., and van Hinsbergen, D. J. J., 2019, The Caribbean and Farallon plates connected: Constraints from stratigraphy and paleomagnetism of the Nicoya Peninsula, Costa Rica: Journal of Geophysical Research: Solid Earth, v. 124, n. 7, p. 6243–6266, https://doi.org/10.1029/2018JB016369

Boschman, L. M., van Hinsbergen, D. J. J., and Spakman, W., 2021, Reconstructing Jurassic-Cretaceous intra-oceanic subduction evolution in the northwestern Panthalassa Ocean using Ocean Plate Stratigraphy from Hokkaido, Japan: Tectonics, v. 40, n. 8, e2019TC005673, https://doi.org/10.1029/2019TC005673

Boyden, J., Müller, R. D., Gurnis, M., Torsvik, T., Clark, J. A., Turner, M., Ivey-Law, H., Watson, R. J., and Cannon, J. S., 2011, Next-generation plate-tectonic reconstructions using GPlates: Geoinformatics: Cyberinfrastructure for the Solid Earth Sciences: Cambridge, England, Cambridge University Press, p. 95–114, https://doi.org/10.1017/CBO9780511976308.008

Buchs, D. M., Pilet, S., Cosca, M., Flores, K. E., Bandini, A. N., and Baumgartner, P. O., 2013, Low-volume intraplate volcanism in the Early/Middle Jurassic Pacific basin documented by accreted sequences in Costa Rica: Geochemistry, Geophysics, Geosystems, v. 14, n. 5, p. 1552–1568, https://doi.org/10.1002/ggge.20084

Butler, R. F., 1992, Paleomagnetism: magnetic domains to geologic terranes: Boston, Massachusetts, Blackwell Scientific Publications, v. 319, 336 p.

Butterworth, N. P., Talsma, A. S., Müller, R. D., Seton, M., Bunge, H.-P., Schuberth, B. S. A., Shephard, G. E., and Heine, C., 2014, Geological, tomographic, kinematic and geodynamic constraints on the dynamics of sinking slabs: Journal of Geodynamics, v. 73, p. 1–13, https://doi.org/10.1016/j.jog.2013.10.006

Cabral-Cano, E., Lang, H. R., and Harrison, C. G. A., 2000, Stratigraphic assessment of the Arcelia-Teloloapan area, southern Mexico: Implications for southern Mexico's post-Neocomian tectonic evolution: Journal of South American Earth Sciences, v. 13, n. 4–5, p. 443–457, https://doi.org/10.1016/S0895-9811(00)00035-3

Campbell, M. J., Rosenbaum, G., Allen, C. M., Mortimer, N., and Shaanan, U., 2020, Episodic behavior of the eastern Gondwanan margin: Insights from detrital zircon petrochronology from the Murihiku Terrane, New Zealand: Lithos, v. 356–357, p. 105367, https://doi.org/10.1016/j.lithos.2020.105367

Cawood, P. A., Nemchin, A. A., Leverenz, A., Saeed, A., and Balance, P. F., 1999, U/Pb dating of detrital zircons: Implications for the provenance record of Gondwana margin terranes: GSA Bulletin, v. 111, n. 8, p. 1107–1119, https://doi.org/10.1130/0016-7606(1999)111<1107:UPDODZ>2.3.CO;2

Cawood, P. A., Kröner, A., Collins, W. J., Kusky, T. M., Mooney, W. D., and Windley, B. F., 2009, Accretionary orogens through Earth history: Geological Society, London, Special Publications, v. 318, p. 1–36, https://doi.org/10.1144/SP318.1

Cawood, P. A., Pisarevsky, S. A., and Leitch, E. C., 2011, Unraveling the New England orocline, east Gondwana accretionary margin: Tectonics, v. 30, n. 5, https://doi.org/10.1029/2011TC002864

Cawood, P. A., Hawkesworth, C. J., Pisarevsky, S. A., Dhuime, B., Capitanio, F. A., and Nebel, O., 2018, Geological archive of the onset of plate tectonics: Philosophical Transactions of the Royal Society A: Mathematical, Physical and Engineering Sciences, v. 376, issue 2132, p. 20170405, https://doi.org/10.1098/rsta.2017.0405

Centeno-García, E., Corona-Chávez, P., Talavera-Mendoza, O., and Iriondo, A., 2003, Geologic and tectonic evolution of the western Guerrero terrane—A transect from Puerto Vallarta to Zihuatanejo, Mexico,

Geologic transects across Cordilleran Mexico: Puerto Vallarta, Jalisco, Mexico Guidebook for the field trips of the 99th Geological Society of America Cordilleran section annual meeting, p. 4–7.
Centeno-García, E., Guerrero-Suastegui, M., and Talavera-Mendoza, O., 2008, The Guerrero Composite Terrane of western Mexico: Collision and subsequent rifting in a supra-subduction zone, *in* Draut, A. E., Clift, P. D., and Scholl, D. W., editors, Formation and Applications of the Sedimentary Record in Arc Collision Zones: Geological Society of America Special Paper 436, p. 279–308, https://doi.org/10.1130/2008.2436(13)
Centeno-García, E., Busby, C., Busby, M., and Gehrels, G., 2011, Evolution of the Guerrero composite terrane along the Mexican margin, from extensional fringing arc to contractional continental arc: GSA Bulletin, v. 123, n. 9–10, p. 1776–1797, https://doi.org/10.1130/B30057.1
Centeno-García, E., 2017, Mesozoic tectono-magmatic evolution of Mexico: An overview: Ore Geology Reviews, v. 81, Part 3, p. 1035–1052, https://doi.org/10.1016/j.oregeorev.2016.10.010
Clennett, E. J., Sigloch, K., Mihalynuk, M. G., Seton, M., Henderson, M. A., Hosseini, K., Mohammadzaheri, A., Johnston, S. T., and Müller, R. D., 2020, A Quantitative Tomotectonic Plate Reconstruction of Western North America and the Eastern Pacific Basin: Geochemistry, Geophysics, Geosystems, v. 21, n. 8, p. e2020GC009117, https://doi.org/10.1029/2020GC009117
Collombat, H., Rochette, P., and Kent, D. V., 1993, Detection and correction of inclination shallowing in deep-sea sediments using the anisotropy of anhysteretic remanence: Bulletin de la Société Géologique de France, v. 164, p. 103–111.
Coltice, N., and Shephard, G. E., 2018, Tectonic predictions with mantle convection models: Geophysical Journal International, v. 213, n. 1, p. 16–29, https://doi.org/10.1093/gji/ggx531
Cox, A., and Hart, R. B., 1986, Plate Tectonics - How it works: Palo Alto, California, Blackwell Scientific Publications, 392 p.
De Wever, P., 1985, Découverte de materiel océanique du Lias-Dogger inférieur dans la peninsula de Santa Elena (Costa Rica, Amerique Centrale): Comptes Rendus de l'Academie des Sciences de Paris Serie II, v. 15, p. 759–764.
De Wever, P., Dumitrica, P., Caulet, J. P., Nigrini, C., and Caridroit, M., 2002, Radiolarians in the sedimentary record: Boca Raton, Florida, CRC Press, 533 p., https://doi.org/10.1201/9781482283181
Deenen, M. H. L., Langereis, C. G., van Hinsbergen, D. J. J., and Biggin, A. J., 2011, Geomagnetic secular variation and the statistics of palaeomagnetic directions: Geophysical Journal International, v. 186, n. 2, p. 509–520, https://doi.org/10.1111/j.1365-246X.2011.05050.x
Denyer, P., and Gazel, E., 2009, The Costa Rican Jurassic to Miocene oceanic complexes: Origin, tectonics and relations: Journal of South American Earth Sciences, v. 28, n. 4, p. 429–442, https://doi.org/10.1016/j.jsames.2009.04.010
Dickinson, W. R., and Lawton, T. F., 2001, Carboniferous to Cretaceous assembly and fragmentation of Mexico: GSA Bulletin, v. 113, n. 9, p. 1142–1160, https://doi.org/10.1130/0016-7606(2001)113<1142:CTCAAF>2.0.CO;2
Domeier, M., 2016, A plate tectonic scenario for the Iapetus and Rheic oceans: Gondwana Research, v. 36, p. 275–295, https://doi.org/10.1016/j.gr.2015.08.003
Domeier, M., 2018, Early Paleozoic tectonics of Asia: Towards a full-plate model: Geoscience Frontiers, v. 9, n. 3, p. 789–862, https://doi.org/10.1016/j.gsf.2017.11.012
Domeier, M., and Torsvik, T. H., 2014, Plate tectonics in the late Paleozoic: Geoscience Frontiers, v. 5, n. 3, p. 303–350, https://doi.org/10.1016/j.gsf.2014.01.002
Domeier, M., and Torsvik, T. H., 2019, Full-plate modelling in pre-Jurassic time: Geological Magazine, v. 156, n. 2, p. 261–280, https://doi.org/10.1017/S0016756817001005
Domeier, M., Doubrovine, P. V., Torsvik, T. H., Spakman, W., and Bull, A. L., 2016, Global correlation of lower mantle structure and past subduction: Geophysical Research Letters, v. 43, n. 10, p. 4945–4953, https://doi.org/10.1002/2016GL068827
Domeier, M., Shephard, G. E., Jakob, J., Gaina, C., Doubrovine, P. V., and Torsvik, T. H., 2017, Intraoceanic subduction spanned the Pacific in the Late Cretaceous–Paleocene: Science Advances, v. 3, n. 11, https://doi.org/10.1126/sciadv.aao2303
Doubrovine, P. V., and Tarduno, J. A., 2008, A revised kinematic model for the relative motion between Pacific oceanic plates and North America since the Late Cretaceous: Journal of Geophysical Research, v. 113, n. B12, https://doi.org/10.1029/2008JB005585
Doubrovine, P. V., Steinberger, B., and Torsvik, T. H., 2012, Absolute plate motions in a reference frame defined by moving hot spots in the Pacific, Atlantic, and Indian oceans: Journal of Geophysical Research: Solid Earth, v. 117, n. B9, https://doi.org/10.1029/2011JB009072
Eichelberger, N., and McQuarrie, N., 2015, Kinematic reconstruction of the Bolivian orocline: Geosphere, v. 11, n. 2, p. 445–462, https://doi.org/10.1130/GES01064.1
Elias-Herrera, M., Sánchez-Zavala, J. L., and Macias-Romo, C., 2000, Geologic and geochronologic data from the Guerrero terrane in the Tejupilco area, southern Mexico: New constraints on its tectonic interpretation: Journal of South American Earth Sciences, v. 13, n. 4–5, p. 355–375, https://doi.org/10.1016/S0895-9811(00)00029-8
Engebretson, D. C., Cox, A., and Gordon, R. G., 1985, Relative Motions Between Oceanic and Continental Plates in the Pacific Basin: Geological Society of America Special Papers, v. 206, https://doi.org/10.1130/SPE206-p1
Escuder-Viruete, J., and Baumgartner, P. O., 2014, Structural evolution and deformation kinematics of a subduction-related serpentinite-matrix mélange, Santa Elena peninsula, northwest Costa Rica: Journal of Structural Geology, v. 66, p. 356–381, https://doi.org/10.1016/j.jsg.2014.06.003
Ferrari, L., Valencia-Moreno, M., and Bryan, S., 2007, Magmatism and tectonics of the Sierra Madre Occidental and its relation with the evolution of the western margin of North America, *in* Alaniz-Alvarez, S. A., and Nieto-Samaniego, A. F., editors, Geology of México: Celebrating the Centenary of

the Geological Society of México: Geological Society of America Special Paper, v. 422, p. 1–39, https://doi.org/10.1130/2007.2422(01)
Fisher, R. A., 1953, Dispersion on a Sphere: Proceedings of the Royal Society A: Mathematical, Physical and Engineering Sciences, v. 217, n. 1130, p. 295–305, https://doi.org/10.1098/rspa.1953.0064
Fitz-Díaz, E., Lawton, T. F., Juárez-Arriaga, E., and Chávez-Cabello, G., 2018, The Cretaceous-Paleogene Mexican orogen: Structure, basin development, magmatism and tectonics: Earth-Science Reviews, v. 183, p. 56–84, https://doi.org/10.1016/j.earscirev.2017.03.002
Flores, K. E., and Gazel, E., 2020, A 100 m.y. record of volcanic arc evolution in Nicaragua: Island Arc, v. 29, n. 1, p. e12346, https://doi.org/10.1111/iar.12346
Franke, W., Cocks, L. R. M., and Torsvik, T. H., 2017, The Palaeozoic Variscan oceans revisited: Gondwana Research, v. 48, p. 257–284, https://doi.org/10.1016/j.gr.2017.03.005
Fu, R. R., and Kent, D. V., 2018, Anomalous Late Jurassic motion of the Pacific Plate with implications for true polar wander: Earth and Planetary Science Letters, v. 490, p. 20–30, https://doi.org/10.1016/j.epsl.2018.02.034
Gazel, E., Denyer, P., and Baumgartner, P. O., 2006, Magmatic and geotectonic significance of Santa Elena Peninsula, Costa Rica: Geologica Acta, v. 4, p. 193–202.
Grand, S. P., van der Hilst, R. D., and Widiyantoro, S., 1997, Global Seismic Tomography: A Snapshot of Convection in the Earth: GSA Today, v. 7, p. 1–7.
Grindley, G., Oliver, P., and Sukroo, J., 1980, Lower Mesozoic position of southern New Zealand determined from paleomagnetism of the Glenham Porphyry, Murihiku Terrane, eastern Southland: Wellington, New Zealand, Gondwana Five, p. 319–326.
Gurnis, M., Yang, T., Cannon, J., Turner, M., Williams, S., Flament, N., and Müller, R. D., 2018, Global tectonic reconstructions with continuously deforming and evolving rigid plates: Computers & Geosciences, v. 116, p. 32–41, https://doi.org/10.1016/j.cageo.2018.04.007
Hagstrum, J. T., and Murchey, B. L., 1996, Paleomagnetism of Jurassic radiolarian chert above the Coast Range ophiolite at Stanley Mountain, California, and implications for its paleogeographic origins: Geological Society of America Bulletin, v. 108, n. 6, p. 643–652, https://doi.org/10.1130/0016-7606(1996)108<0643:POJRCA>2.3.CO;2
Hagstrum, J. T., and Sedlock, R. L., 1990, Remagnetization and northward translation of Mesozoic red chert from Cedros Island and the San Benito Islands, Baja California, Mexico: Geological Society of America Bulletin, v. 102, n. 7, p. 983–991, https://doi.org/10.1130/0016-7606(1990)102<0983:RANTOM>2.3.CO;2
Hagstrum, J. T., and Sedlock, R. L., 1992, Paleomagnetism of Mesozoic Red Chert from Cedros Island and the San-Benito Islands, Baja-California, Mexico Revisited: Geophysical Research Letters, v. 19, n. 3, p. 329–332, https://doi.org/10.1029/91GL02692
Hall, R., 2002, Cenozoic geological and plate tectonic evolution of SE Asia and the SW Pacific: Computer-based reconstructions, model and animations: Journal of Asian Earth Sciences, v. 20, n. 4, p. 353–431, https://doi.org/10.1016/S1367-9120(01)00069-4
Hallam, A., 1986, Evidence of displaced terranes from Permian to Jurassic faunas around the Pacific margins: Journal of the Geological Society, v. 143, p. 209–216, https://doi.org/10.1144/gsjgs.143.1.0209
Haston, R. B., and Luyendyk, B. P., 1991, Paleomagnetic Results from the Waipapa Terrane, Northland Peninsula, North Island, New-Zealand - Tectonic Implications from Widespread Remagnetizations: Tectonics, v. 10, n. 5, p. 986–994, https://doi.org/10.1029/91TC00861
Hauff, F., Hoernle, K., van den Bogaard, P., Alvarado, G., and Garbe-Schönberg, D., 2000, Age and geochemistry of basaltic complexes in western Costa Rica: Contributions to the geotectonic evolution of Central America. Geochemistry, Geophysics, Geosystems, v. 1, n. 5, https://doi.org/10.1029/1999GC000020
Hayami, I., 1961, On the Jurassic pelecypod faunas in Japan: University of Tokyo, Journal of the Faculty of Science University of Tokyo, v. 13, n. 2, p. 243–343.
Hayami, I., 1984, Jurassic marine bivalve faunas and biogeography in Southeast Asia: University of Tokyo, Geology and Palaeontology of Southeast Asia, v. 25, p. 229–237.
Hilde, T. W. C., Uyeda, S., and Kroenke, L., 1977, Evolution of the western Pacific and its margin: Tectonophysics, v. 38, n. 1–2, p. 145–165, https://doi.org/10.1016/0040-1951(77)90205-0
Hildebrand, R. S., 2013, Mesozoic assembly of the North American Cordillera: Geological Society of America Special Paper 495, 169 p., https://doi.org/10.1130/SPE495
Horton, B. K., 2018, Sedimentary record of Andean mountain building: Earth-Science Reviews, v. 178, p. 279–309, https://doi.org/10.1016/j.earscirev.2017.11.025
Huang, W., Van Hinsbergen, D. J. J., Maffione, M., Orme, D. A., Dupont-Nivet, G., Guilmette, C., Ding, L., Guo, Z., and Kapp, P., 2015, Lower Cretaceous Xigaze ophiolites formed in the Gangdese forearc: Evidence from paleomagnetism, sediment provenance, and stratigraphy: Earth and Planetary Science Letters, v. 415, p. 142–153, https://doi.org/10.1016/j.epsl.2015.01.032
Ichikawa, K., Shinohara, M., and Miyata, T., 1979, Stratigraphy of the Izumi Group in Izumi Mountains, in Proceedings of the Kansai Branch, Geological Society of Japan: Geological Society of Japan, v. 85, p. 10–11.
Ichikawa, K., Miyata, T., and Shinohara, M., 1981, Eastward stepwise shift of the Izumi sedimentary basin with reference to the movement picture of the Median Tectonic Line: Proceedings of the Kansai Branch, Geological Society of Japan: Geological Society of Japan, v. 89, p. 11–12.
Iijima, A., Kakuwa, Y., and Matsuda, H., 1989, Silicified wood from the Adoyama chert, Kuzuh, Central Honshu, and its bearing on compaction and depositional environment of radiolarian bedded chert, *in* Hein, J. R., and Obradović, J., editors, Siliceous deposits of the Tethys and Pacific Regions: Berlin, Springer, p. 151–168, https://doi.org/10.1007/978-1-4612-3494-4_11

Ikeda, T., Harada, T., Kouchi, Y., Morita, S., Yokogawa, M., Yamamoto, K., and Otoh, S., 2016, Provenance analysis based on detrital-zircon-age spectra of the Lower Cretaceous formations in the Ryoseki–Monobe area, Outer Zone of Southwest Japan: Memoir of the Fukui Prefectural Dinosaur Museum, v. 15, p. 33–84.

Ishiga, H., and Ishiyama, D., 1987, Jurassic accretionary complex in Kaminokuni terrane, southwestern Hokkaido, Japan: Mining Geology, v. 37, p. 381–394.

Isozaki, Y., 1988, Sanbagawa metamorphism and the formation of the Sanbosan-Shimanto belt: Earth Monthly, v. 10, p. 367–371.

Isozaki, Y., 1996, Anatomy and genesis of a subduction-related orogen: A new view of geotectonic subdivision and evolution of the Japanese Islands: Island Arc, v. 5, n. 3, p. 289–320, https://doi.org/10.1111/j.1440-1738.1996.tb00033.x

Isozaki, Y. 2000, The Japanese Islands: Its origin, evolution, and future: Science Journal Kagaku, v. 70, p. 133–145.

Isozaki, Y., 2014, Memories of Pre-Jurassic Lost Oceans: How To Retrieve Them From Extant Lands: Geoscience Canada, v. 41, n. 3, p. 283–311, https://doi.org/10.12789/geocanj.2014.41.050

Isozaki, Y., and Itaya, T., 1991, Pre-Jurassic klippe in northern Chichibu Belt in west-central Shikoku, Southwest Japan-Kurosegawa terrrane as a tectonic outlier of the pre-Jurassic rocks of the Inner zone: Journal of the Geological Society of Japan, v. 97, n. 6, p. 431–450, https://doi.org/10.5575/geosoc.97.431

Isozaki, Y., and Ota, A., 2001, Middle-Upper Permian (Maokouan-Wuchiapingian) boundary in mid-oceanic paleo-atoll limestone of Kamura and Akasaka, Japan: Proceedings of the Japan Academy, Series B, v. 77, n. 6, p. 104–109, https://doi.org/10.2183/pjab.77.104

Isozaki, Y., Maruyama, S., and Furuoka, F., 1990, Accreted Oceanic Materials in Japan: Tectonophysics, v. 181, n. 1–4, p. 179–205, https://doi.org/10.1016/0040-1951(90)90016-2

Isozaki, Y., Aoki, K., Nakama, T., and Yanai, S., 2010, New insight into a subduction-related orogen: A reappraisal of the geotectonic framework and evolution of the Japanese Islands: Gondwana Research, v. 18, n. 1, p. 82–105, https://doi.org/10.1016/j.gr.2010.02.015

Ito, T., Kojima, Y., Kodaira, S., Sato, H., Kaneda, Y., Iwasaki, T., Kurashimo, E., Tsumura, N., Fujiwara, A., Miyauchi, T., Hirata, N., Harder, S., Miller, K., Murata, A., Yamakita, S., Onishi, M., Abe, S., Sato, T., and Ikawa, T., 2009, Crustal structure of southwest Japan, revealed by the integrated seismic experiment Southwest Japan 2002: Tectonophysics, v. 472, n. 1–4, p. 124–134, https://doi.org/10.1016/j.tecto.2008.05.013

Jackson, M. J., Banerjee, S. K., Marvin, J. A., Lu, R., and Gruber, W., 1991, Detrital remanence, inclination errors, and anhysteretic remanence anisotropy: Quantitative model and experimental results: Geophysical Journal International, v. 104, n. 1, p. 95–103, https://doi.org/10.1111/j.1365-246X.1991.tb02496.x

Jasin, B., and Tongkul, F., 2013, Cretaceous radiolarians from Baliojong ophiolite sequence, Sabah, Malaysia: Journal of Asian Earth Sciences, v. 76, p. 258–265, https://doi.org/10.1016/j.jseaes.2012.10.038

Johnson, C. L., Constable, C. G., Tauxe, L., Barendregt, R., Brown, L. L., Coe, R. S., Layer, P., Mejia, V., Opdyke, N. D., Singer, B. S., Staudigel, H., and Stone, D. B., 2008, Recent investigations of the 0-5 Ma geomagnetic field recorded by lava flows: Geochemistry, Geophysics, Geosystems, v. 9, n. 4, p. Q04032, https://doi.org/10.1029/2007GC001696

Johnson, S. E., Tate, M. C., and Fanning, C. M., 1999, New geologic mapping and SHRIMP U-Pb zircon data in the Peninsular Ranges batholith, Baja California, Mexico: Evidence for a suture?: Geology, v. 27, n. 8, p. 743–746, https://doi.org/10.1130/0091-7613(1999)027<0743:NGMASU>2.3.CO;2

Johnston, S. T., 2001, The Great Alaskan Terrane Wreck: Reconciliation of paleomagnetic and geological data in the northern Cordillera: Earth and Planetary Science Letters, v. 193, n. 3–4, p. 259–272, https://doi.org/10.1016/S0012-821X(01)00516-7

Johnston, S. T., 2008, The cordilleran ribbon continent of North America: Annual Review of Earth and Planetsry Sciences, v. 36, p. 495–530, https://doi.org/10.1146/annurev.earth.36.031207.124331

Kasuya, A., Isozaki, Y., and Igo, H., 2012, Constraining paleo-latitude of a biogeographic boundary in mid-Panthalassa: Fusuline province shift on the Late Guadalupian (Permian) migrating seamount: Gondwana Research, v. 21, n. 2–3, p. 611–623, https://doi.org/10.1016/j.gr.2011.06.001

Kear, D., and Mortimer, N., 2003, Waipa Supergroup, New Zealand: A proposal: Journal of the Royal Society of New Zealand, v. 33, n. 1, p. 149–163, https://doi.org/10.1080/03014223.2003.9517725

Kennan, L., and Pindell, J. L., 2009, Dextral shear, terrane accretion and basin formation in the Northern Andes: Best explained by interaction with a Pacific-derived Caribbean Plate?: Geological Society, London, Special Publications, v. 328, p. 487–531, https://doi.org/10.1144/SP328.20

Kent, D. V., and Tauxe, L., 2005, Corrected Late Triassic latitudes for continents adjacent to the North Atlantic: Science, v. 307, n. 5707, p. 240–244, https://doi.org/10.1126/science.1105826

Kimbrough, D. L., and Moore, T. E., 2003, Ophiolite and volcanic arc assemblages on the Vizcaino Peninsula and Cedros Island, Baja California Sur, México: Mesozoic forearc lithosphere of the Cordilleran magmatic arc, *in* Johnson, S. E., Paterson, S. R., Fletcher, J. M., Girty, G. H., Kimbrough, D. A., and Martin-Barajas, A., editors, Tectonic evolution of northwestern Mexico and the southwestern USA: Geological Society of America Special Paper, v. 374, p. 43–71, https://doi.org/10.1130/0-8137-2374-4.43

Kiminami, K., 1992, Cretaceous-Paleogene arc-trench systems in Hokkaido, Paleozoic and Mesozoic terranes: basement of the Japanese Island arcs : 29th IGC field trip guidebook, v. 1, p. 1–43.

Kirschvink, J. L., 1980, The least-squares line and plane and the analysis of palaeomagnetic data: Geophysical Journal International, v. 62, n. 3, p. 699–718, https://doi.org/10.1111/j.1365-246X.1980.tb02601.x

Kirschvink, J. L., Isozaki, Y., Shibuya, H., Otofuji, Y.-i., Raub, T. D., Hilburn, I. A., Kasuya, T., Yokoyama, M., and Bonifacie, M., 2015, Challenging the sensitivity limits of paleomagnetism: Magnetostratigraphy of weakly magnetized Guadalupian–Lopingian (Permian) limestone from Kyushu, Japan: Palaeogeography, Palaeoclimatology, Palaeoecology, v. 418, p. 75–89, https://doi.org/10.1016/j.palaeo.2014.10.037

Kleinrock, M. C., and Morgan, J. P., 1988, Triple junction reorganization: Journal of Geophysical Research: Solid Earth, v. 93. n. B4, p. 2981–2996, https://doi.org/10.1029/JB093iB04p02981

Kobayashi, T., and Tamura, M., 1984, The Triassic bivalvia of Malaysia, Thailand and adjacent areas: Geology and Palaeontology of Southeast Asia, v. 25, p. 201–228.

Kodama, K. P., 2009, Simplification of the anisotropy-based inclination correction technique for magnetite- and haematite-bearing rocks: A case study for the Carboniferous Glenshaw and Mauch Chunk Formations, North America: Geophysical Journal International, v. 176, n. 2, p. 467–77, https://doi.org/10.1111/j.1365-246X.2008.04013.x

Kodama, K., Fukuoka, M., Aita, Y., Sakai, T., Hori, R. S., Takemura, A., Campbell, H. J., Hollis, C., Grant-Mackie, J. A., and Spörli, K. B., 2007, Paleomagnetic results from Arrow Rocks in the framework of paleomagnetism in pre-Neogene rocks from New Zealand, *in* SpörliTakemura, A., and Hori, R. S., editors, The Oceanic Permian/Triassic Boundary Sequence at Arrow Rocks (Oruatemanu), Northland, New Zealand: Lower Hutt, New Zealand: Geological and Nuclear Science Monograph, v. 24, p. 177–196.

Konrad, K., Koppers, A. A. P., Steinberger, B., Finlayson, V. A., Konter, J. G., and Jackson, M. G., 2018, On the relative motions of long-lived Pacific mantle plumes: Nature Communications, v. 9, article number, 854, https://doi.org/10.1038/s41467-018-03277-x

Koymans, M. R., Langereis, C. G., Pastor-Galán, D., and van Hinsbergen, D. J. J., 2016, Paleomagnetism.org: An online multi-platform open source environment for paleomagnetic data analysis: Computers & Geosciences, v. 93, p. 127–137, https://doi.org/10.1016/j.cageo.2016.05.007

Koymans, M. R., van Hinsbergen, D. J. J., Pastor-Galán, D., Vaes, B., and Langereis, C. G., 2020, Towards FAIR paleomagnetic data management through Paleomagnetism. org 2.0: Geochemistry, Geophysics, Geosystems, v. 21, n. 2, p. e2019GC008838, https://doi.org/10.1029/2019GC008838

Krijgsman, W., and Tauxe, L., 2006, E/I corrected paleolatitudes for the sedimentary rocks of the Baja British Columbia hypothesis: Earth and Planetary Science Letters, v. 242, n. 1–2, p. 205–216, https://doi.org/10.1016/j.epsl.2005.11.052

Kusky, T. M., Windley, B. F., Safonova, I., Wakita, K., Wakabayashi, J., Polat, A., and Santosh, M., 2013, Recognition of ocean plate stratigraphy in accretionary orogens through Earth history: A record of 3.8 billion years of sea floor spreading, subduction, and accretion: Gondwana Research, v. 24, n. 2, p. 501–547, https://doi.org/10.1016/j.gr.2013.01.004

Lancelot, Y., and Larson, R., 1975, Sedimentary and tectonic evolution of the northwestern Pacific: Initial Reports Deep Sea Drilling Reports and Publications, v. 32, p. 925–939, https://doi.org/10.2973/dsdp.proc.32.138.1975

Larson, R. L., and Chase, C., G., 1972, Late Mesozoic Evolution of the Western Pacific Ocean: GSA Bulletin, v. 83, n. 12, p. 3627–3644, https://doi.org/10.1130/0016-7606(1972)83[3627:LMEOTW]2.0.CO;2

Larson, R. L., and Pitman, W. C. III, , 1972, World-Wide Correlation of Mesozoic Magnetic Anomalies, and Its Implications: GSA Bulletin, v. 83, n. 12, p. 3645–3662, https://doi.org/10.1130/0016-7606(1972)83[3645:WCOMMA]2.0.CO;2

Li, Z.-X., Bogdanova, S. V., Collins, A. S., Davidson, A., De Waele, B., Ernst, R. E., Fitzsimons, I. C. W., Fuck, R. A., Gladkochub, D. P., Jacobs, J., Karlstrom, K. E., Lu, S., Natapov, L. M., Pease, V., Pisarevsky, S. A., Thrane, K., and Vernikovsky, V., 2008, Assembly, configuration, and break-up history of Rodinia: A synthesis: Precambrian Research, v. 160, n. 1–2, p. 179–210, https://doi.org/10.1016/j.precamres.2007.04.021

Li, Z. X., Mitchell, R. N., Spencer, C. J., Ernst, R., Pisarevsky, S., Kirscher, U., and Murphy, J. B., 2019, Decoding Earth's rhythms: Modulation of supercontinent cycles by longer superocean episodes: Precambrian Research, v. 323, p. 1–5, https://doi.org/10.1016/j.precamres.2019.01.009

Ma, Y., Yang, T., Yang, Z., Zhang, S., Wu, H., Li, H., Li, H., Chen, W., Zhang, J., and Ding, J., 2014, Paleomagnetism and U-Pb zircon geochronology of Lower Cretaceous lava flows from the western Lhasa terrane: New constraints on the India-Asia collision process and intracontinental deformation within Asia: Journal of Geophysical Research: Solid Earth, v. 119, n. 10, p. 7404–7424, https://doi.org/10.1002/2014JB011362

Madrigal, P., Gazel, E., Denyer, P., Smith, I., Jicha, B., Flores, K. E., Coleman, D., and Snow, J., 2015, A melt-focusing zone in the lithospheric mantle preserved in the Santa Elena Ophiolite, Costa Rica: Lithos, v. 230, p. 189–205, https://doi.org/10.1016/j.lithos.2015.04.015

Martini, M., Mori, L., Solari, L., and Centeno-García, E., 2011, Sandstone Provenance of the Arperos Basin (Sierra de Guanajuato, Central Mexico): Late Jurassic–Early Cretaceous Back-Arc Spreading as the Foundation of the Guerrero Terrane: The Journal of Geology, v. 119, n. 6, p. 597–617, https://doi.org/10.1086/661989

Martini, M., Solari, L., and López-Martínez, M., 2014, Correlating the Arperos Basin from Guanajuato, central Mexico, to Santo Tomás, southern Mexico: Implications for the paleogeography and origin of the Guerrero terrane: Geosphere, v. 10, n. 6, p. 1385–1401, https://doi.org/10.1130/GES01055.1

Maruyama, S., and Seno, T., 1986, Orogeny and relative plate motions: Example of the Japanese Islands: Tectonophysics, v. 127, n. 3–4, p. 305–329, https://doi.org/10.1016/0040-1951(86)90067-3

Maruyama, S., Isozaki, Y., Kimura, G., and Terabayashi, M., 1997, Paleogeographic maps of the Japanese Islands: plate tectonic synthesis from 750 Ma to the present: Island Arc, v. 6, n. 1, p. 121–142, https://doi.org/10.1111/j.1440-1738.1997.tb00043.x

Matsuda, T., and Isozaki, Y., 1982, Radiolarians around the Triassic-Jurassic boundary from the bedded chert in the Kamiaso area, Southwest Japan. Appendix:" Anisian Radiolarians": News of Osaka Micropaleontoly, Special Volume, v. 5, p. 93–101.

Matsuda, T., and Isozaki, Y., 1991, Well-Documented Travel History of Mesozoic Pelagic Chert in Japan - from Remote Ocean to Subduction Zone: Tectonics, v. 10, n. 2, p. 475–499, https://doi.org/10.1029/90TC02134

Matsumoto, T., 1978, Japan and adjoining areas: Mesozoic A, p. 79–144.

Matsuoka, A., 1992, Jurassic and Early Cretaceous radiolarians from ODP Leg 129, Sites 800 and 801, western Pacific ocean: College Station, Texas, USA, Proceedings of the Ocean Drilling Program, Scientific results, v. 129, p. 203–220, https://doi.org/10.2973/odp.proc.sr.129.121.1992

Matsuoka, A., 1995, Jurassic and Lower Cretaceous radiolarian zonation in Japan and in the western Pacific: Island Arc, v. 4, n. 2, p. 140–153, https://doi.org/10.1111/j.1440-1738.1995.tb00138.x

Matthews, K. J., Maloney, K. T., Zahirovic, S., Williams, S. E., Seton, M., and Müller, R. D., 2016, Global plate boundary evolution and kinematics since the late Paleozoic: Global and Planetary Change, v. 146, p. 226–250, https://doi.org/10.1016/j.gloplacha.2016.10.002

McFadden, P. L., and McElhinny, M. W., 1988, The combined analysis of remagnetization circles and direct observations in palaeomagnetism: Earth and Planetary Science Letters, v. 87, n. 1–2, p. 161–172, https://doi.org/10.1016/0012-821X(88)90072-6

McQuarrie, N., and Wernicke, B. P., 2005, An animated tectonic reconstruction of southwestern North America since 36 Ma: Geosphere, v. 1. n. 3, p. 147–172, https://doi.org/10.1130/GES00016.1

Merdith, A. S., Collins, A. S., Williams, S. E., Pisarevsky, S., Foden, J. D., Archibald, D. B., Blades, M. L., Alessio, B. L., Armistead, S., Plavsa, D., Clark, C., and Müller, R. D., 2017, A full-plate global reconstruction of the Neoproterozoic: Gondwana Research, v. 50, p. 84–134, https://doi.org/10.1016/j.gr.2017.04.001

Miyata, T., 1990, Slump strain indicative of paleoslope in Cretaceous Izumi sedimentary basin along Median tectonic line, southwest Japan: Geology, v. 18, n. 5, p. 392–394, https://doi.org/10.1130/0091-7613(1990)018<0392:SSIOPI>2.3.CO;2

Monger, J., and Price, R., 2002, The Canadian Cordillera: Geology and tectonic evolution: CSEG Recorder, v. 27, p. 17–36.

Montes, C., Rodriguez-Corcho, A. F., Bayona, G., Hoyos, N., Zapata, S., and Cardona, A., 2019, Continental margin response to multiple arc-continent collisions: The northern Andes-Caribbean margin: Earth-Science Reviews, v. 198, p. 102903, https://doi.org/10.1016/j.earscirev.2019.102903

Mortimer, N., 2004, New Zealand's Geological Fundations: Gondwana Research, v. 7, n. 1, p.261–272, https://doi.org/10.1016/S1342-937X(05)70324-5

Mortimer, N., Rattenbury, M. S., King, P. R., Bland, K. J., Barrell, D. J. A., Bache, F., Begg, J. G., Campbell, H. J., Cox, S. C., Crampton, J. S., Edbrooke, S. W., Forsyth, P. J., Johnston, M. R., Jongens, R., Lee, J. M., Leonard, G. S., Raine, J. I., Skinner, D. N. B., Timm, C., Townsend, D. B., Tulloch, A. J., Turnbull, I. M., and Turnbull, R. E., 2014, High-level stratigraphic scheme for New Zealand rocks: New Zealand Journal of Geology and Geophysics, v. 57, n. 4, p. 402–419, https://doi.org/10.1080/00288306.2014.946062

Müller, R. D., Seton, M., Zahirovic, S., Williams, S. E., Matthews, K. J., Wright, N. M., Shephard, G. E., Maloney, K. T., Barnett-Moore, N., Hosseinpour, M., Bower, D. J., and Cannon, J., 2016, Ocean basin evolution and global-scale plate reorganization events since Pangea breakup: Annual Review of Earth and Planetary Sciences, v. 44, p. 107–138, https://doi.org/10.1146/annurev-earth-060115-012211

Müller, R. D., Cannon, J., Qin, X., Watson, R. J., Gurnis, M., Williams, S., Pfaffelmoser, T., Seton, M., Russell, S. H., and Zahirovic, S., 2018, GPlates: building a virtual Earth through deep time: Geochemistry, Geophysics, Geosystems, v. 19, n. 7, p. 2243–2261, https://doi.org/10.1029/2018GC007584

Müller, R. D., Zahirovic, S., Williams, S. E., Cannon, J., Seton, M., Bower, D. J., Tetley, M. G., Heine, C., Le Breton, E., Liu, S., Russel, S. H. J., Yang, T., Leonard, J., and Gurnis, M., 2019, A global plate model including lithospheric deformation along major rifts and orogens since the Triassic: Tectonics, v. 38, n. 6, p. 1884–1907, https://doi.org/10.1029/2018TC005462

Nance, R. D., Gutiérrez-Alonso, G., Keppie, J. D., Linnemann, U., Murphy, J. B., Quesada, C., Strachan, R. A., and Woodcock, N. H., 2010, Evolution of the Rheic Ocean: Gondwana Research, v. 17, n. 2–3, p. 194–222, https://doi.org/10.1016/j.gr.2009.08.001

Nance, R. D., Murphy, J. B., and Santosh, M., 2014, The supercontinent cycle: A retrospective essay: Gondwana Research, v. 25, p. 4–29, https://doi.org/10.1016/j.gr.2012.12.026

Noda, A., and Sato, D., 2018, Submarine slope–fan sedimentation in an ancient forearc related to contemporaneous magmatism: The Upper Cretaceous Izumi Group, southwestern Japan: Island Arc, v. 27, n. 2, p. e12240, https://doi.org/10.1111/iar.12240

Noda, A., and Toshimitsu, S., 2009, Backward stacking of submarine channel–fan successions controlled by strike-slip faulting: The Izumi Group (Cretaceous), southwest JapanSubmarine-fan successions controlled by strike-slip faulting: Lithosphere, v. 1, n. 1, p. 41–59, https://doi.org/10.1130/L19.1

Nokleberg, W. J., Parfenov, L. M., Monger, J. W. H., Norton, I. O., Khanchuk , A. I., Stone, D. B., Scotese, C. R., Scholl, D. W., and Fujita, K., 2000, Phanerozoic Tectonic Evolution of the Circum-North Pacific: U.S. Geological Survey Professional Papr 1626, https://pubs.usgs.gov/pp/2000/1626/

Oda, H., and Suzuki, H., 2000, Paleomagnetism of Triassic and Jurassic red bedded chert of the Inuyama area, central Japan: Journal of Geophysical Research: Solid Earth, v. 105, n. B11, p. 25743–25767, https://doi.org/10.1029/2000JB900267

Okada, A., 1973, On the quaternary faulting along the median tectonic line in the central part of Shikoku: Geographical Review of Japan, v. 45, n. 5, p. 295–322, https://doi.org/10.4157/grj.46.295

Oliver, P., 1994, The tectonic significance of paleomagnetic results from the Triassic and Jurassic Murihiku sedimentary rocks of the Kawhia region, North Island, New Zealand, *in* Van der Lingen, G. J., Swanson, K. M., and Muir, R. J., editors Evolution of the Tasman Sea basin: Rotterdam, The Netherlands, Balkema, Proceedings of the Tasman Sea conference, p. 67–82.

Ortega Rivera, A., 2003, Geochronological constraints on the tectonic history of the Peninsular Ranges batholith of Alta and Baja California: Tectonic implications for western México, *in* Johnson, S. E., Paterson, S. R., Fletcher, J. M., Girty, G. H., Kimbrough, D. L., and Martin-Barajas, A., editors, Tectonic evolution on north-western México and the southwestern USA: Boulder, Colorado, Geological Society of America Special Papers, v. 374, p. 297–335, https://doi.org/10.1130/0-8137-2374-4.297

Ota, A., and Isozaki, Y., 2006, Fusuline biotic turnover across the Guadalupian–Lopingian (Middle–Upper Permian) boundary in mid-oceanic carbonate buildups: Biostratigraphy of accreted limestone in Japan: Journal of Asian Earth Sciences, v. 26, n. 3–4, p. 353–368, https://doi.org/10.1016/j.jseaes.2005.04.001

Pessagno, E. A. Jr., Finch, W., and Abbott, P. L., 1979, Upper Triassic Radiolaria from the San Hipolito Formation, Baja California: Micropaleontology, v. 25, n. 2, p. 160–197, https://doi.org/10.2307/1485265

Pindell, J. L., and Dewey, J. F., 1982, Permo-Triassic reconstruction of western Pangea and the evolution of the Gulf of Mexico/Caribbean region: Tectonics, v. 1, n. 2, p. 179–211, https://doi.org/10.1029/TC001i002p00179

Pisarevsky, S. A., Elming, S.-Å., Pesonen, L. J., and Li, Z.-X., 2014, Mesoproterozoic paleogeography: Supercontinent and beyond: Precambrian Research, v. 244, p. 207–225, https://doi.org/10.1016/j.precamres.2013.05.014

Price, R., Mortimer, N., Smith, I., and Maas, R., 2015, Whole-rock geochemical reference data for Torlesse and Waipapa terranes, North Island, New Zealand: New Zealand Journal of Geology and Geophysics, v. 58, n. 3, p. 213–228, https://doi.org/10.1080/00288306.2015.1026832

Rangin, C., 1978, Speculative model of Mesozoic geodynamics, central Baja California to northeastern Sonora (Mexico), Mesozoic Paleogeography of the Western United States: Pacific Section S.E.P.M.

Retallack, G. J., 1987, Triassic vegetation and geography of the New Zealand portion of the Gondwana supercontinent, *in* McKenzie, G. D., editor, Gondwana Six: Stratigraphy, Sedimentology, and Paleontology: Geophysical Monograph Series, v. 41, https://doi.org/10.1029/GM041p0029

Riisager, P., Hall, S., Antretter, M., and Zhao, X., 2003, Paleomagnetic paleolatitude of Early Cretaceous Ontong Java Plateau basalts: Implications for Pacific apparent and true polar wander: Earth and Planetary Science Letters, v. 208, n. 3–4, p. 235–252, https://doi.org/10.1016/S0012-821X(03)00046-3

Rogers, R. D., Mann, P., and Emmet, P. A., 2007, Tectonic terranes of the Chortis block based on integration of regional aeromagnetic and geologic data, *in* Mann, P., editor, Geologic and Tectonic Development of the Caribbean Plate Boundary in Northern Central America: Geological Society of America Special Papers, v. 428, p. 65–88, https://doi.org/10.1130/2007.2428(04)

Sakashima, T., Terada, K., Takeshita, T., and Sano, Y., 2003, Large-scale displacement along the Median Tectonic Line, Japan: Evidence from SHRIMP zircon U–Pb dating of granites and gneisses from the South Kitakami and paleo-Ryoke belts: Journal of Asian Earth Sciences, v. 21, n. 9, p. 1019–1039, https://doi.org/10.1016/S1367-9120(02)00108-6

Sano, H., and Nakashima, K., 1997, Lowermost Triassic (Griesbachian) microbial bindstone-cementstone facies, southwest Japan: Facies, v. 36, p. 1–24, https://doi.org/10.1007/BF02536874

Sato, H., Kojima, Y., Murata, A., Ito, T., Kaneda, Y., Onishi, M., Iwasaki, T., Oho, Y., Ogino, S., Kano, K., Kawamura, T., Kurashimo, e., Koshiya, s., Takasu, A., Takeshita, T., Tsumura, N., Terabayashi, Y., Toyohara, F., Nakajima, T., Noda, K., Hashimoto, Y., Hasegawa, S., Hirata, N., Miyauchi, t., Miyata, T., Yamakita, S., Yoshida, T., Harder, S., Miller, K., Kapi, G., Ozawa, T., and Ikawa, T., 2005, Crustal structure of the outer zone in southwest Japan revealed by Shikoku and Seto-Inland-Sea seismic profiling in 2002: Bulletin of the Earthquake Research Institute, v. 80, p. 53–71.

Sato, H., Kato, N., Abe, S., Van Horne, A., and Takeda, T., 2015, Reactivation of an old plate interface as a strike-slip fault in a slip-partitioned system: Median Tectonic Line, SW Japan: Tectonophysics, v. 644–645, p. 58–67, https://doi.org/10.1016/j.tecto.2014.12.020

Sato, T., 1962, Études biostratigraphiques des ammonites du Jurassique du Japon: Mémoires de la Societé géologique de France NS, v. 94, p. 1–122.

Schellart, W., 2017, A geodynamic model of subduction evolution and slab detachment to explain Australian plate acceleration and deceleration during the latest Cretaceous–early Cenozoic: Lithosphere, v. 9, n. 6, p. 976–986, https://doi.org/10.1130/L675.1

Schepers, G., van Hinsbergen, D. J. J., Spakman, W., Kosters, M. E., Boschman, L. M., and McQuarrie, N., 2017, South-American plate advance and forced Andean trench retreat as drivers for transient flat subduction episodes: Nature Communications, v. 8, article number 15249, https://doi.org/10.1038/ncomms15249

Scotese, C. R., 2004, A continental drift flipbook: The Journal of Geology, v. 112, n. 6, p. 729–741, https://doi.org/10.1086/424867

Sedlock, R. L., 1988, Tectonic setting of blueschist and island-arc terranes of west-central Baja California, Mexico: Geology, v. 16, n. 7, p. 623–626, https://doi.org/10.1130/0091-7613(1988)016<0623:TSOBAI>2.3.CO;2

Sedlock, R. L., and Isozaki, Y., 1990, Lithology and Biostratigraphy of Franciscan-Like Chert and Associated Rocks in West-Central Baja-California, Mexico: GSA Bulletin, v. 102, n. 7, p. 852–864, https://doi.org/10.1130/0016-7606(1990)102<0852:LABOFL>2.3.CO;2

Seton, M., Mortimer, N., Williams, S., Quilty, P., Gans, P., Meffre, S., Micklethwaite, S., Zahirovic, S., Moore, J., and Matthews, K. J., 2016, Melanesian back-arc basin and arc development: Constraints from the eastern Coral Sea: Gondwana Research, v. 39, p. 77–95, https://doi.org/10.1016/j.gr.2016.06.011

Shibuya, H., and Sasajima, S., 1986, Paleomagnetism of red cherts: A case study in the Inuyama area, central Japan: Journal of Geophysical Research: Solid Earth, v. 91, n. B14, p. 14105–14116, https://doi.org/10.1029/JB091iB14p14105

Sigloch, K., and Mihalynuk, M. G., 2013, Intra-oceanic subduction shaped the assembly of Cordilleran North America: Nature, v. 496, p. 50–6, https://doi.org/10.1038/nature12019

Sigloch, K., McQuarrie, N., and Nolet, G., 2008, Two-stage subduction history under North America inferred from multiple-frequency tomography: Nature Geoscience, v. 1, p. 458–462, https://doi.org/10.1038/ngeo231

Spörli, K. B., and Grant-Mackie, J. A., 1976, Upper Jurassic fossils from the Waipapa Group of Tawharanui Peninsula, North Auckland, New Zealand: New Zealand Journal of Geology and Geophysics, v. 19, n. 1, p. 21–34, https://doi.org/10.1080/00288306.1976.10423547

Spörli, K. B., Aita, Y., and Gibson, G. W., 1989, Juxtaposition of Tethyan and Non-Tethyan Mesozoic radiolarian faunas in melanges, Waipapa Terrane, North-Island, New-Zealand: Geology, v. 17, n. 8, p. 753–756, https://doi.org/10.1130/0091-7613(1989)017<0753:JOTANT>2.3.CO;2

Stampfli, G. M., and Borel, G. D., 2002, A plate tectonic model for the Paleozoic and Mesozoic constrained by dynamic plate boundaries and restored synthetic oceanic isochrons: Earth and Planetary Science Letters, v. 196, n. 1–2, p. 17–33, https://doi.org/10.1016/S0012-821X(01)00588-X

Steiner, M. B., and Wallick, B. P., 1992, Jurassic to Paleocene paleolatitudes of the Pacific plate derived from the paleomagnetism of the sedimentary sequences at Sites 800, 801, and 802: Proceedings of the Ocean Drilling Program, Scientific Results, v. 129, p. 431–446, https://doi.org/10.2973/odp.proc.sr.129.136.1992

Sugiyama, Y., 1994, Neotectonics of southwest Japan due to the right-oblique subduction of the Philippine Sea plate: Geofísica Internacional, v. 33, n. 1, p. 53–76, https://doi.org/10.22201/igeof.00167169p.1994.33.1.540

Taira, A., Saito, Y., and Hashimoto, M., 1983, The role of oblique subduction and strike-slip tectonics in the evolution of Japan: Geodynamics of the Western Pacific-Indonesian Region, v. 11, p. 303–316, https://doi.org/10.1029/GD011p0303

Talavera-Mendoza, O., Ruiz, J., Gehrels, G. E., Valencia, V. A., and Centeno-García, E., 2007, Detrital zircon U/Pb geochronology of southern Guerrero and western Mixteca arc successions (southern Mexico): New insights for the tectonic evolution of southwestern North America during the late Mesozoic: GSA Bulletin, v. 119, n. 9–10, p. 1052–1065, https://doi.org/10.1130/B26016.1

Tarduno, J. A., McWilliams, M., Sliter, W. V., Cook, H. E., Blake, M. C. Jr., and Premoli-Silva, I., 1986, Southern hemisphere origin of the Cretaceous Laytonville limestone of California: Science, v. 231, n. 4744, p. 1425–1428, https://doi.org/10.1126/science.231.4744.1425

Tauxe, L., 2010, Essentials of Paleomagnetism: Oakland, California, University of California Press, 512 p., https://doi.org/10.1525/9780520946378

Tauxe, L., and Kent, D. V., 2004, A simplified statistical model for the geomagnetic field and the detection of shallow bias in paleomagnetic inclinations: was the ancient magnetic field dipolar? *in* Channell, J. E. T., Kent, D. V., Lowrie, W., and Meert, J. G., editors, Timescales of the Paleomagnetic Field: Geophysical Monograph Series, v. 145, p. 101–115, https://doi.org/10.1029/145GM08

Tauxe, L., and Watson, G. S., 1994, The Fold Test - an Eigen Analysis Approach: Earth and Planetary Science Letters, v. 122, n. 3–4, p. 331–341, https://doi.org/10.1016/0012-821X(94)90006-X

Tazawa, J.-I., 2001, Middle Permian brachiopod faunas of Japan and South Primorye, Far East Russia: Their palaeobiogeographic and tectonic implications: Geosciences Journal, v. 5, article number 19, https://doi.org/10.1007/BF02910170

Tazawa, J.-I., 2002, Late Paleozoic brachiopod faunas of the South Kitakami Belt, northeast Japan, and their paleobiogeographic and tectonic implications: Island Arc, v. 11, n. 4, p. 287–301, https://doi.org/10.1046/j.1440-1738.2002.00369.x

Tomurtogoo, O., Windley, B. F., Kröner, A., Badarch, G., and Liu, D. Y., 2005, Zircon age and occurrence of the Adaatsag ophiolite and Muron shear zone, central Mongolia: Constraints on the evolution of the Mongol–Okhotsk ocean, suture and orogen: Journal of the Geological Society, v. 162, n. 1, p. 125–134, https://doi.org/10.1144/0016-764903-146

Torsvik, T. H., 2003, Geology. The Rodinia jigsaw puzzle: Science, v. 300, n. 5624, p. 1379–81, https://doi.org/10.1126/science.1083469

Torsvik, T. H., and Van der Voo, R., 2002, Refining Gondwana and Pangea palaeogeography: Estimates of Phanerozoic non-dipole (octupole) fields: Geophysical Journal International, v. 151, n. 3, p. 771–794, https://doi.org/10.1046/j.1365-246X.2002.01799.x

Torsvik, T. H., Smethurst, M. A., Meert, J. G., Van der Voo, R., McKerrow, W. S., Brasier, M. D., Sturt, B. A., and Walderhaug, H. J., 1996, Continental break-up and collision in the Neoproterozoic and Palaeozoic—A tale of Baltica and Laurentia: Earth-Science Reviews, v. 40, n. 1–4, p. 229–258, https://doi.org/10.1016/0012-8252(96)00008-6

Torsvik, T. H., Müller, R. D., Van der Voo, R., Steinberger, B., and Gaina, C., 2008, Global plate motion frames: Toward a unified model: Reviews of Geophysics, v. 46, n. 3, https://doi.org/10.1029/2007RG000227

Torsvik, T. H., Steinberger, B., Gurnis, M., and Gaina, C., 2010, Plate tectonics and net lithosphere rotation over the past 150 My: Earth and Planetary Science Letters, v. 291, n. 1–4, p. 106–112, https://doi.org/10.1016/j.epsl.2009.12.055

Torsvik, T. H., Van der Voo, R., Preeden, U., Mac Niocaill, C., Steinberger, B., Doubrovine, P. V., van Hinsbergen, D. J. J., Domeier, M., Gaina, C., Tohver, E., Meert, J. G., McCausland, P. J. A., and Cocks, L. R. M., 2012, Phanerozoic polar wander, palaeogeography and dynamics: Earth-Science Reviews, v. 114, n. 3–4, p. 325–368, https://doi.org/10.1016/j.earscirev.2012.06.007

Torsvik, T. H., Steinberger, B., Shephard, G. E., Doubrovine, P. V., Gaina, C., Domeier, M., Conrad, C. P., and Sager, W. W., 2019, Pacific-Panthalassic reconstructions: Overview, errata and the way forward: Geochemistry, Geophysics, Geosystems, v. 20, n. 7, p. 3659–3689, https://doi.org/10.1029/2019GC008402

Tournon, J., 1994, The Santa Elena Peninsula: an ophiolitic nappe and a sedimentary volcanic relative autochthonous: Profil, v. 7, p. 87–96.

Tulloch, A. J., Kimbrough, D. L., Landis, C. A., Mortimer, N., and Johnston, M. R., 1999, Relationships between the Brook Street terrane and Median Tectonic Zone (Median batholith): Evidence from Jurassic conglomerates: New Zealand Journal of Geology and Geophysics, v. 42, n. 2, p. 279–293, https://doi.org/10.1080/00288306.1999.9514845

Ueda, H., 2003, Accretionary complex of remnant-arc origin: Greenstone-conglomerate-chert succession in the Oku-Niikappu area of the Idonnappu Zone, Hokkaido, Japan: The Journal of the Geological Society of Japan, v. 109, n. 9, p. XVII-XVIII, https://doi.org/10.5575/geosoc.109.XVII

Ueda, H., 2016, Hokkaido, *in* Moreno, T., Wallis, S., Kojima, T., and Gibbons, W., editors, The Geology of Japan: London, England, Geological Society, Geology of Series, p. 201–221.

Ueda, H., and Miyashita, S., 2003, Discovery of sheeted dikes in the Cretaceous accretionary complex of the Idonnappu Zone, Hokkaido, Japan: The Journal of the Geological Society of Japan, v. 109, n. 9, p. 559–562, https://doi.org/10.5575/geosoc.109.559

Ueda, H., and Miyashita, S., 2005, Tectonic accretion of a subducted intraoceanic remnant arc in Cretaceous Hokkaido, Japan, and implications for evolution of the Pacific northwest: Island Arc, v. 14, n. 4, p. 582–598, https://doi.org/10.1111/j.1440-1738.2005.00486.x

Uno, K., Furukawa, K., and Hada, S., 2011, Margin-parallel translation in the western Pacific: Paleomagnetic evidence from an allochthonous terrane in Japan: Earth and Planetary Science Letters, v. 303, n. 1–2, p. 153–161, https://doi.org/10.1016/j.epsl.2011.01.002

Vaes, B., van Hinsbergen, D. J. J., and Boschman, L. M., 2019, Reconstruction of subduction and back-arc spreading in the NW Pacific and Aleutian Basin: Clues to causes of Cretaceous and Eocene plate reorganizations: Tectonics, v. 38, n. 4, p. 1367–1413, https://doi.org/10.1029/2018TC005164

Vaes, B., Li, S., Langereis, C. G., and van Hinsbergen, D. J., 2021, Reliability of palaeomagnetic poles from sedimentary rocks: Geophysical Journal International, v. 225, b. 2, p. 1281–1303, https://doi.org/10.1093/gji/ggab016

van de Lagemaat, S. H. A., Boschman, L. M., Kamp, P. J. J., Langereis, C. G., and van Hinsbergen, D. J. J., 2018b, Post-remagnetisation vertical axis rotation and tilting of the Murihiku Terrane (North Island, New Zealand): New Zealand Journal of Geology and Geophysics, v. 61, n. 1, p. 9–25, https://doi.org/10.1080/00288306.2017.1400983

van de Lagemaat, S. H., van Hinsbergen, D. J. J., Boschman, L. M., Kamp, P. J. J., and Spakman, W., 2018a, Southwest Pacific absolute plate kinematic reconstruction reveals major Cenozoic Tonga-Kermadec slab dragging: Tectonics, v. 37, n. 8, p. 2647–2674, https://doi.org/10.1029/2017TC004901

van der Meer, D. G., Spakman, W., van Hinsbergen, D. J. J., Amaru, M. L., and Torsvik, T. H., 2010, Towards absolute plate motions constrained by lower-mantle slab remnants: Nature Geoscience, v. 3, p. 36–40, https://doi.org/10.1038/ngeo708

van der Meer, D. G., Torsvik, T. H., Spakman, W., van Hinsbergen, D. J. J., and Amaru, M. L., 2012, Intra-Panthalassa Ocean subduction zones revealed by fossil arcs and mantle structure: Nature Geoscience, v. 5, p. 215–219, https://doi.org/10.1038/ngeo1401

van der Meer, D. G., van Hinsbergen, D. J. J., and Spakman, W., 2018, Atlas of the Underworld: Slab remnants in the mantle, their sinking history, and a new outlook on lower mantle viscosity: Tectonophysics, v. 723, p. 309–448, https://doi.org/10.1016/j.tecto.2017.10.004

van Hinsbergen, D. J. J., and Schmid, S. M., 2012, Map view restoration of Aegean-West Anatolian accretion and extension since the Eocene: Tectonics, v. 31, n. 5, https://doi.org/10.1029/2012TC003132

van Hinsbergen, D. J. J., and Schouten, T. L. A., 2021, Deciphering paleogeography from orogenic architecture: Constructing orogens in a future supercontinent as thought experiment: American Journal of Science, v. 321, https://doi.org/10.2475/06.2021.02

van Hinsbergen, D. J. J., Lippert, P. C., Li, S., Huang, W., Advokaat, E. L., and Spakman, W., 2019, Reconstructing Greater India: Paleogeographic, kinematic, and geodynamic perspectives: Tectonophysics, v. 760, p. 69–94, https://doi.org/10.1016/j.tecto.2018.04.006

Viso, R. F., Larson, R. L., and Pockalny, R. A., 2005, Tectonic evolution of the Pacific–Phoenix–Farallon triple junction in the South Pacific Ocean: Earth and Planetary Science Letters, v. 233, n. 1–2, p. 179–194, https://doi.org/10.1016/j.epsl.2005.02.004

Wallick, B. P., and Steiner, M. B., 1992, Paleomagnetic and rock magnetic properties of Jurassic quiet zone basalts, hole 801C1: Proceedings of the Ocean Drilling Program, Scientific Results, v. 129, p. 455–470, https://doi.org/10.2973/odp.proc.sr.129.135.1992

Wessel, P., and Kroenke, L. W., 2009, Observations of geometry and ages constrain relative motion of Hawaii and Louisville plumes: Earth and Planetary Science Letters, v. 284, n. 3–4, p. 467–472, https://doi.org/10.1016/j.epsl.2009.05.012

Windley, B. F., Alexeiev, D., Xiao, W., Kröner, A., and Badarch, G., 2007, Tectonic models for accretion of the Central Asian Orogenic Belt: Journal of the Geological Society, London, v. 164, n. 1, p. 31–47, https://doi.org/10.1144/0016-76492006-022

Wright, N. M., Seton, M., Williams, S. E., and Müller, R. D., 2016, The Late Cretaceous to recent tectonic history of the Pacific Ocean basin: Earth-Science Reviews, v. 154, p. 138–173, https://doi.org/10.1016/j.earscirev.2015.11.015

Wu, J., Suppe, J., Lu, R., and Kanda, R., 2016, Philippine Sea and East Asian plate tectonics since 52 Ma constrained by new subducted slab reconstruction methods: Journal of Geophysical Research: Solid Earth, v. 121, n. 6, p. 4670–4741, https://doi.org/10.1002/2016JB012923

Xiao, W. J., Windley, B. F., Huang, B. C., Han, C. M., Yuan, C., Chen, H. L., Sun, M., Sun, S., and Li, J. L., 2009, End-Permian to mid-Triassic termination of the accretionary processes of the southern Altaids: Implications for the geodynamic evolution, Phanerozoic continental growth, and metallogeny of Central Asia: International Journal of Earth Sciences, v. 98, p. 1189–1217, https://doi.org/10.1007/s00531-008-0407-z

Xiao, W. J., Huang, B., Han, C., Sun, S., and Li, J., 2010a, A review of the western part of the Altaids: A key to understanding the architecture of accretionary orogens: Gondwana Research, v. 18, n. 2–3, p. 253–273, https://doi.org/10.1016/j.gr.2010.01.007

Xiao, W. J., Mao, Q. G., Windley, B. F., Han, C. M., Qu, J. F., Zhang, J. E., Ao, S. J., Guo, Q. Q., Cleven, N. R., Lin, S. F., Shan, Y. H., and Li, J. L., 2010b, Paleozoic multiple accretionary and collisional processes of the Beishan orogenic collage: American Journal of Science, v. 310, n. 10, p. 1553–1594, https://doi.org/10.2475/10.2010.12

Yamakita, S., and Otoh, S., 2000, Estimation of the amount of Late Cretaceous left-lateral strike-slip displacement along the Median Tectonic Line and its implications in juxtaposition of some geologic belts of Southwest Japan: Association for Geological Collaboration in Japan Monograph, v. 49, p. 93–104.

Yang, T., Ma, Y., Zhang, S., Bian, W., Yang, Z., Wu, H., Li, H., Chen, W., and Ding, J., 2015, New insights into the India–Asia collision process from Cretaceous paleomagnetic and geochronologic results in the Lhasa terrane: Gondwana Research, v. 28, n. 2, p. 625–641, https://doi.org/10.1016/j.gr.2014.06.010

Yao, A., 2000, Terrane arrangement of Southwest Japan in view of the Paleozoic-Mesozoic tectonics of East Asia: Association for Geological Collaboration in Japan Monograph, v. 49, p. 145–155.

Yao, A., Matsuda, T., and Isozaki, Y., 1980, Triassic and Jurassic radiolarians from the Inuyama area, central Japan: Osaka, Japan, Osaka City University, Journal of Geoscience, v. 23, article 4, p. 135–154,

Young, A., Flament, N., Maloney, K., Williams, S., Matthews, K., Zahirovic, S., and Müller, R. D., 2019, Global kinematics of tectonic plates and subduction zones since the late Paleozoic Era: Geoscience Frontiers, v. 10, n. 3, p. 989–1013, https://doi.org/10.1016/j.gsf.2018.05.011

Zahirovic, S., Seton, M., and Müller, R. D., 2014, The Cretaceous and Cenozoic tectonic evolution of Southeast Asia: Solid Earth, v. 5, p. 227–273, https://doi.org/10.5194/se-5-227-2014

Zijderveld, J. D. A., 2013, A.C. Demagnetization of rocks: Analysis of results, *in* Collinson, D. W., Crees, K. M., and Runcorn, S. K., editors, Methods in Paleomagnetism: Developments in Solid Earth Geophysics, v. 3, p. 254–286, https://doi.org/10.1016/B978-1-4832-2894-5.50049-5